INVESTIGATING NOVEL THERAPEUTIC TARGETS FOR THE TREATMENT OF FRAGILE X SYNDROME

By

Ferzin Sethna

A DISSERTATION

Submitted to
Michigan State University
in partial fulfillment of the requirements
for the degree of

Genetics—Doctor of Philosophy

2014

ABSTRACT

INVESTIGATING NOVEL THERAPEUTIC TARGETS FOR THE TREATMENT OF FRAGILE X SYNDROME

By

Ferzin Sethna

Fragile X syndrome (FXS) is the most common form of inherited mental retardation and a leading cause of autism. Most cases of FXS result from CGG repeat expansion in the 5' UTR of the FMR1 gene, which results in lack of expression of its protein product, FMRP. FMRP is an mRNA binding protein, which predominantly suppresses the translation of its targets. The absence of FMRP thus leads to excessive protein synthesis and altered synaptic signaling, which are believed to underlie the pathophysiology of FXS. There is currently no cure for FXS and often multiple drugs are administered to manage the symptoms. This highlights the importance of understanding the molecular mechanisms that are altered in FXS brains, in order to develop better therapeutic targets. My study identifies that translation of the brain-specific type-1 adenylyl cyclase (AC1) mRNA is controlled by FMRP and that AC1 protein is overexpressed in the absence of FMRP. Using genetic knockdown and pharmacological inhibition of AC1, I show that reducing AC1 activity can rescue several cellular and behavioral phenotypes in the *Fmr1* knockout mouse model. My research also reveals

calmodulin inhibitor can rectify several cellular and behavioral phenotypes in *Fmr1* KO mice. In summary this thesis describes the identification and validation of a novel therapeutic target and an FDA approved drug for treatment of FXS using the *Fmr1* KO mouse model.

ACKNOWLEDGEMENTS

I would like to thank my advisor Dr. Hongbing Wang for allowing me to work on this wonderful project. Thank you for all the ideas and discussions that helped shape my research. I would also like to thank my committee members, Dr. David Arnosti, Dr. Laura McCabe and Dr. Tony Nunez for the helpful discussions, ideas and support they provided during my PhD. The Genetics Program, Dept. of Physiology, Neuroscience Program, for funding and support extended throughout my PhD. career. I would like to thank: Wang lab members especially Dr. Fei Zhang who patiently taught me most of the techniques; Dr. Ming Zhang and our collaborators Dr. Eric Klann and Dr. Hanoc Kaphzan for providing electrophysiology data; Dr. Yue Feng and Dr. Wei Feng for performing the ribosome density gradient centrifugation experiment; Dr. Cara Westmark and Dr. James Malter for providing *Fmr1* knockout mice; Dr. Melinda Frame for help with microscopy. I sincerely thank Dr. A. J. Robison and Dr. Kenneth Moon for helping me set up the software for dendritic spine measurements. Thank you Dr. Xiao, Cindy, Mark and Feiye for always accommodating me to use various lab equipment. All staff members of the University Laboratory Animal Resources (ULAR), Diagnostic center for Population and Animal Health and Pharmacokinetics core (University of Michigan). I would like to thank the FRAXA research foundation for not only providing us a startup

grant but also providing me the opportunity to get to interact with very helpful colleagues working on Fragile X syndrome. These interactions were crucial to the development of my project ideas and experimental design, since our lab was just beginning research on Fragile X. I would also like to thank NIH (R01MH093445) for funding our research.

Thank you, Mrs. Kelley Peel for introducing me to two lovely children with Fragile X and giving me the opportunity to talk to their parents. This experience really put my research in the lab into real-life perspective. Thanks to my family and friends especially Mom and Beans for their unconditional love and support. Thank you Sudarshan- for everything, I don't know where to begin!

TABLE OF CONTENTS

LIST OF TABLES

LIST OF FIGURES

KEY TO SYMBOLS OR ABBREVIATIONS

AC1	Adenylyl cyclase 1
Adcy1	Adenylyl cyclase 1
AGS	Audiogenic seizure
Arc	Activity-regulated cytoskeleton-associated protein
CaM	Calmodulin
CCh	Carbamylcholine chloride
DHPG	Dihydroxyphenylglycine
DKO	Double knockout
Fmr1	Fragile X mental retardation 1
FMRP	Fragile X mental retardation 1 protein
FXS	Fragile X syndrome
Gq	Gq protein
KO	Knockout
LTD	Long- term depression
mAchR	Muscarinic acetylcholine receptor
MEK	Mitogen-activated kinase kinase

mGluR1/5	Metabotropic glutamate receptor 1/5
miRNA	microRNA
NB001	5-[[2-(6-Amino-9H-purin-9-yl)ethyl]amino]-1-pentanol
pERK1/2	Phospho extracellular-signal-regulated kinases 1/2
S6K	Ribosomal S6 kinase
tERK1/2	Total extracellular-signal-regulated kinases 1/2
TFP	Trifluoperazine- hydrochloride
U0126	1,4-Diamino-2,3-dicyano-1,4-*bis*[2-aminophenylthio]butadiene
UTR	Untranslated region
W13	*N*-(4-Aminobutyl)-5-chloro-2-naphthalenesulfonamide hydrochloride
WT	Wild-type

CHAPTER 1: INTRODUCTION

Adapted from Publication: Sethna, F., Moon, C., Wang, H., 2013. From FMRP Function to Potential Therapies for Fragile X Syndrome. *Neurochemical Research* [Epub ahead of print]

1.1 Fragile X Syndrome: A genetic disorder

Fragile X syndrome (FXS), is the most common form of inherited intellectual disability (or mental retardation) and a leading cause of autism (Santoro et al., 2012). The incidence of FXS in males is approximately 1 in 2,500–5,000 and in females is 1 in 4,000–6,000 (Bagni et al., 2012). The cytogenetic discovery of the ‘‘fragile site’’ on the X chromosome in patients (Krawczun et al., 1985) and the higher incidence in males strongly suggest that FXS is a genetic disease. Positional cloning definitively demonstrates the link between mutations in the fragile X mental retardation 1 (FMR1) gene, whose chromosome locus is at the Xq27.3 fragile site, and FXS (Pixxuti et al., 1991). Most FXS patients have a significant expansion of CGG trinucleotide repeats in the 5’ untranslated region (UTR) of the FMR1 gene. While healthy individuals have 5–45 CGG repeats (commonly 29–30 repeats), affected individuals with full mutation normally

have more than 200 repeats (Peprah, 2012). A few cases with missense mutations and deletions in the FMR1 gene have also been reported (De Boulle K et al., 2010).

Studies show that the high number of the CGG repeats may facilitate hypermethylation on the cytosine residues in the proximal regions of FMR1, including the promoter (i.e. about 250 bp to 1 kb upstream of the CGG repeats), leading to transcriptional silencing and consequently lack of protein expression (Pieretti et al., 1991; Sutcliffe et al., 1992). Other mechanisms posit that a full mutation in CGG repeats affects histone modification (including acetylation and methylation) and may in turn suppress the activity of the FMR1 promoter (Coffee et al., 2002).

1.2 Animal models of FXS

The development of valid animal models has been crucial for understanding FXS etiology, the function of FMRP and has been invaluable in the conception of potential therapeutics for FXS. The main animal models of FXS have been generated with mouse (Dutch-belgian et al., 1994), fruit fly (Morales et al., 2002), and zebrafish (den Broeder et al., 2009), in which the genetic ortholog of human FMR1 is deleted. In another mouse model, the wild type *Fmr1* allele was mutated to harbor an isoleucine to asparagine mutation (I304N, corresponding to the I367N mutation in a rare FXS patient) (De Boulle,

et al., 1993; Zang et al., 2009). It is important to note that the mouse model with an engineered expansion in CGG repeats does not show hypermethylation and lack of FMRP expression (Brouwer et al., 2007). Thus, animal models with perfect construct validity are not available. Stem cells from FXS patients show FMR1 silencing due to DNA hypermethylation upon differentiation (Eiges et al., 2007), and can be used for drug screening and preliminary examination of gene reactivation therapies (Chiurazzi et al., 1998, 1999).

Behavioral and physiological examinations have demonstrated that the current animal models show robust if not complete face validity of FXS. Some of the therapeutic strategies, which attenuate certain FXS-related symptoms in the animal models, have now been extended to human clinical trials, indicating reasonable predictive validity. FXS is characterized by mild to severe intellectual disability, susceptibility to seizures, hyperactivity, hypersensitivity to sensory stimuli, and autistic traits such as social anxiety, attention deficit, hand biting or flapping (repetitive behavior), and poor eye contact. Physical manifestations include long facial features with protruding ears, soft skin, connective tissue problems, and large testicles (macroorchidism). Many of these symptoms are recapitulated in the *Fmr1* knockout (KO) mouse (Table 1). *Fmr1* KO mice show cognitive deficits when examined by Morris water maze (Dobkin et al., 2000;

Baker et al., 2010)(but also see (Paradee et al., 1999)), passive avoidance (Qin et al., 2005; Dölen et al., 2007), contextual fear conditioning (Paradee et al., 1999)(but also see (Van Dam et al., 2000)), and object recognition (Bhattacharya et al., 2012). Susceptibility to seizures in *Fmr1* KO mice is implicated by wild- running and onset of seizure after receiving a high intensity sound (e.g. 125 dB at 1,800–6,300 Hz) (Musumeci et al., 2000; Chen and Toth, 2001). In addition to audiogenic seizures (AGS), *Fmr1* KO mice also show enhanced limbic epileptogenesis and mossy fiber sprouting following a kindling paradigm (Qiu et al., 2009). Furthermore, electrophysiological studies have identified prolonged epileptiform discharges in the *Fmr1* KO hippocampus (Chuang et al., 2005). *Fmr1* KO mice are hyperactive and have more locomotor movement in the open field test (Qin et al., 2002). They also show more entries to and spend more time in the center area of the open field arena (Qin et al., 2002; Yan et al., 2005), indicating less anxiety (in contrast to the human FXS phenotype). However, in a modified open field chamber surrounded with mirrored walls, *Fmr1* KO mice avoid the center area (Spencer et al., 2005). Interestingly, independent groups have found that *Fmr1* KO mice show more (Bilousova et al., 2009), normal (Nielsen et al., 2002), or less anxiety (Liu et al., 2011) in the elevated plus maze test. Hyperarousal and sensorimotor gating phenotypes have been examined by acoustic

startle responses and prepulse inhibition (PPI), respectively. While some studies show that low intensity white noise (at 80 dB) elicits higher startle responses and high intensity stimuli (at 120 dB) cause less startle in *Fmr1* KO mice (Nielsen et al., 2002), other studies demonstrate that deletion of the *Fmr1* gene in mice causes no change or lower startle response to different levels of auditory stimuli (Pietropaolo et al., 2011; Thomas et al., 2011). Reduced PPI (a symptom observed in human FXS patients) (Frankland et al., 2004) is seen in some investigations using *Fmr1* KO mice (de Vrij et al., 2008; Levenga et al., 2011), while other reports have described increased PPI (Chen and Toth, 2001; Nielsen et al., 2002; Frankland et al., 2004; Pietropaolo et al., 2011; Thomas et al., 2011). Autism-related symptoms are also detected in *Fmr1* mutant mice (Pietropaolo et al., 2011). *Fmr1* KO mice show less social dominance than wild type animals in the social dominance tube test (Spencer et al., 2005; Goebel-Goody et al., 2012). *Fmr1* mutants are less interested in social novelty and social interaction (Mines et al., 2010; Liu et al., 2011; Pietropaolo et al., 2011; Bhattacharya et al., 2012). Defective communication (tested by ultrasonic vocalization) (Wöhr and Scattoni, 2013) and repetitive behavior (tested by marble burying) (Thomas et al., 2009) are also detected in *Fmr1* KO mice (Rotschafer et al., 2012; Roy et al., 2012). FXS model mice harboring the I304N mutation exhibit hyperactivity, decreased acoustic startle response,

repetitive behavior, and audiogenic seizures (Zang et al., 2009). In addition to the neurological phenotypes, both *Fmr1* KO and I304N mutant mice show macroorchidism (Dutch-belgian et al., 1994; Zang et al., 2009). Furthermore, increased spine density and immature spines are observed from postmortem FXS brain samples (Irwin et al., 2001; Grossman et al., 2006), and such cellular abnormalities are detected in different brain regions of *Fmr1* KO mice as well as in cultured mutant hippocampal neurons (Grossman et al., 2006; Dölen et al., 2007; Hayashi et al., 2007; Bhattacharya et al., 2012).

In addition to vertebrate models, *Drosophila* (fruit fly) has been successfully used to study FXS. Flies with mutations in *dfmr1*, whose gene product shows similar function to that of human FMRP (Wan et al., 2000), show altered synaptic structure (Zhang et al., 2001), altered social interaction, impaired circadian rhythms (Dockendorff et al., 2002), and defective cognitive function (McBride et al., 2005). Additionally, *dfmr1* mutants have been used to validate therapeutic efficacy, understand signaling dysregulation in FXS, and screen potential pharmacological compounds for FXS therapy (McBride et al., 2005). Although these animal models do not recapitulate all FXS symptoms and inconsistent phenotypes have been reported, it is evident that the current animal models do show reasonable face validity. The inconsistent behavioral

phenotypes observed with *Fmr1* KO mice may be due to differences in the experimental protocol, age (Yun et al., 2006), animal handling (or environmental factors such as different housing facilities and stress (Qin et al., 2011)), and genetic background (Paradee et al., 1999; Baker et al., 2010; Pietropaolo et al., 2011). These inconsistent observations with animal models might reasonably reflect the fact that human FXS patients do not necessarily display a full spectrum of the symptoms. Importantly, differences in genetic background and environmental factors possibly contribute to the fact that FXS patients do not respond equally to behavioral and medical treatment (Berry-Kravis et al., 2008; Jacquemont et al., 2011).

1.3 Role of FMRP in mRNA metabolism

1.3.1 RNA binding activity of FMRP

FMRP is expressed in many tissues, but is most abundant in the brain and in the testis. In addition to its expression in the neuronal cell body, FMRP is also detected at dendrites and synapses (Berwine and Reenough, 1997). Sequence analysis of FMRP reveals several RNA binding domains, which mediate FMRP-RNA interaction (Nussbaum and Dreyfuss, 1993; Siomi et al., 1994), implicating its function in regulating RNA metabolism. Cellular fractionation experiments demonstrate that FMRP co-

sediments with actively translating polyribosomes (Corbin et al., 1997; Feng et al., 1997a, 1997b), further suggesting its role in regulating mRNA translation. Among the three canonical RNA binding domains, the two centrally localized hnRNP K-homology KH domains bind to the ‘‘kissing complex’’ tertiary motifs in RNA. The RGG (arginine-glycine-glycine) box is located close to the C terminus and binds to the G-quartet structures in RNA. The I367N missense mutation discovered in a human patient with severe FXS symptoms maps to the RNA binding pocket of the KH2 domain (Siomi et al., 1994). FMRP with the I367N mutation fails to bind to RNA (Siomi et al., 1994) and polyribosomes (Feng et al., 1997a). Mutant I304N-FMRP also does not show robust association with polyribosomes. This suggests that the loss of RNA-binding/translation-regulating function of FMRP may be causal for the phenotypes in FXS. RNA selection experiments in vitro have revealed that the KH2 domain of FMRP binds to an RNA complex called loop–loop pseudoknot or ‘‘kissing complex’’. This binding activity is abolished in I304N-FMRP (Darnell et al., 2005). Further, RNA containing the ‘‘kissing complex’’ but not G-quartet decreases the association of FMRP with polyribosomes (Darnell et al., 2005), suggesting that the ‘‘kissing complex’’ mimics the site that FMRP uses to regulate translation of its target mRNA. However, it is important to note that the kissing complex structure has not been yet convincingly identified in endogenous

mRNAs. The C-terminal RGG box has been found to bind to G-quadruplex RNA secondary structures in vitro (Darnell et al., 2001). Several FMRP target mRNAs (such as Fmr1, Map1b, and Sema3f) possess predicted G-quadruplex structures, and in vitro biochemical examinations have confirmed their binding to FMRP (Santoro et al., 2012). A new structure SoSLIP (Sod1 stem loops) in Sod1 (superoxide dismutase 1) mRNA may also interact with FMRP via the RGG domain (Bechara et al., 2009). In addition to the RNA binding domains, FMRP possesses two other regions (i.e. nuclear localization signal and nuclear export signal) that enable it to shuttle between the cytoplasm and the nucleus (Eberhart et al., 1996). It is postulated that FMRP may pick up its mRNA targets in the nucleus and transport them to the dendrites, where local protein synthesis is regulated in an activity-dependent manner. It is shown that some protein–protein interaction domains may also exist to mediate FMRP association with proteins involved in translational regulation (Napoli et al., 2008) and the RNA- induced silencing complex (RISC) (Jin et al., 2004).

1.3.2 RNA targets of FMRP

It is estimated that FMRP binds to roughly 4 % of the mRNAs in the brain (Santoro et al., 2012). An earlier genome-wide microarray study identified 432 FMRP-interacting mRNAs (Brown et al., 2001). A recent study using UV cross-linking to covalently link FMRP to mRNA followed by stringent coimmunoprecipitation and high throughput sequencing identified 842 mRNA targets of FMRP in postnatal 11–25 day mouse brain. This study found that many of the targets were involved in synaptic function, cell signalling, neural development, and autism. Further, most of the FMRP binding sites were in the coding region but not in the 5' or 3' UTR of the mRNA targets and no specific sequence or structural feature was identified as preferred FMRP-binding motifs (Darnell et al., 2011). Another recent study used 4-thiouridine (4SU) photoactivatable ribonucleoside-enhanced crosslinking and immunoprecipitation (PAR-CLIP) in HEK293 cells expressing HA-tagged FMRP. Complementary DNA libraries were generated and sequenced. By analyzing the resulting reads, the study identified around 6,000 mRNAs that were bound to FMRP. More than 95 % of the binding sites were either in the coding region or the 3' UTR. Unlike the previous study, this study identified only few more binding sites in the coding region than in the 3' UTR. Further, two RNA-recognition elements (RRE), ACUK and WGGA (where K is G or U and W is A

or U), were found to occur in more than 50 % of the binding sites (Ascano et al., 2012). Consistent with the study by Darnell et al. (Darnell et al., 2011), many of the identified FMRP targets were also involved in autism spectrum disorder and synaptic signaling. It remains unclear whether these FMRP targets are functionally regulated by FMRP and contribute to cellular and behavioral abnormalities in FXS. Among all the identified FMRP targets, only a handful of them are verified by independent methods and functional studies (see Table 2). Interestingly, FMRP also interacts with non-coding microRNAs (miRNAs) (Jin et al., 2004; Edbauer et al., 2010). Among them, miR-125a and 125b can cooperate with FMRP to regulate the translation of validated FMRP targets PSD-95 and NR2A, respectively (Edbauer et al., 2010; Muddashetty et al., 2011). Further, overexpression of miR-125b results in longer and thinner dendritic spines (Edbauer et al., 2010), which is a cellular phenotype of FXS (Grossman et al., 2006). A functional significance of FMRP-miRNA interaction is that FMRP may regulate translation through coordination with miRNAs that bind to the 3' UTR of FMRP target mRNAs.

1.3.3 FMRP regulates mRNA metabolism

The existence of RNA binding domains in FMRP suggests its function in regulating RNA metabolism. Although some studies have demonstrated that FMRP regulates mRNA transport (Dictenberg et al., 2008) and stability (Zalfa et al., 2007), it is well accepted that FMRP mainly suppresses the translation of its target mRNAs. In addition to mRNAs, FMRP also interacts with proteins such as CYFIP1 that regulate translation (Napoli et al., 2008). FMRP has been found to co-sediment with actively translating polyribosomes particularly in synaptic preparations (Corbin et al., 1997; Feng et al., 1997a). In *Fmr1* KO neurons, FMRP targets such as MAP1B (Lu et al., 2004) and PSD-95 (Muddashetty et al., 2011) mRNAs are more enriched in the actively translating polyribosomes rather than in the translationally quiescent messenger ribonucleoprotein (mRNP) complexes. Consequently, the expression of many FMRP targets is up-regulated in the absence of FMRP (see Table 2). Thus FMRP is believed to control local protein synthesis at synapses by acting as a translational repressor and the loss of such translation control leads to many of the defects seen in FXS. In a rare case, FMRP binding to Sod1 mRNA positively regulates its translation (Bechara et al., 2009). It is important to point out that the protein levels of many FMRP targets remain unchanged or even reduced in *Fmr1* KO mice (see Table 2). To fully understand how the

expression level of FMRP targets is controlled, investigations on compensatory mechanisms and secondary effects are needed. Considering that FMRP interacts with the translation machinery and some of the FMRP targets (such as S6K1, PI3 K, PIKE, and ERK1/2) can indirectly stimulate translation (Figure 1), it is understandable that the basal level of global protein synthesis is increased in *Fmr1* KO mouse brains and in cell cultures derived from FXS patients (Dölen et al., 2007; Gross et al., 2010; Osterweil et al., 2010). In addition to its involvement in the cap-dependent initiation and elongation steps (et al., 2011), FMRP may also impede translation through coordination with miRNAs that bind to both FMRP and the 3' UTR of FMRP targets. The interaction between FMRP and components of the RISC (such as AGO1/2 and Dicer) may provide another layer of control on RNA metabolism. For example, the expression of FMRP target NR2A is regulated through the coordination of FMRP and miR-125, and knockdown of AGO1 increases NR2A expression (Edbauer et al., 2010). As the basal translation is elevated in FXS, activity-dependent upregulation of translation is dampened in *Fmr1* KO neurons. As opposed to wild type neurons, *Fmr1* KO neurons do not show increased translation following the activation of mGluR1/5 (Todd et al., 2003; Hou et al., 2006; Muddashetty et al., 2011), NMDAR (Lee et al., 2011), and upon membrane depolarization (Weiler et al., 2004). Consequently, certain aspects of

mGluR1/5- and NMDAR-dependent synaptic plasticity (such as long-term depression and long-term potentiation) are altered in *Fmr1* KO mice (Bear et al., 2004; Lauterborn et al., 2007).

1.4 Role of FMRP in regulating synaptic function

1.4.1 Exaggerated mGluR1/5-LTD in *Fmr1* KO mice

Synaptic protein synthesis and spine development are altered in FXS, thus it is hypothesized that FMRP regulates synaptic function and plasticity. Huber et al. (Huber et al., 2002) showed that synaptic long-term depression (LTD) triggered by mGluR1/5 agonist DHPG is enhanced at the CA1 synapses in the hippocampus of *Fmr1* KO mice. This seminal study builds the foundation of the ‘‘mGluR theory’’, which highlights that mGluR1/5 signaling is exaggerated in FXS, and explains how FMRP function is connected to mGluR1/5-mediated synaptic responses (Bear et al., 2004). Multiple lines of evidence support the functional link between FMRP and mGluR1/5-LTD. First, mGluR1/5-LTD depends on new protein synthesis. The upregulation of protein translation following mGluR1/5 activation may be related to the dynamic changes in FMRP due to mGluR1/5 induced signal transduction. The activation of mGluR1/5 triggers rapid increase in FMRP translation (Berwine and Reenough, 1997) but it is

followed by FMRP degradation and de-phosphorylation, which may cause de-repression on the translation of certain synaptic mRNA (Hou et al., 2006; Nalavadi et al., 2012; Niere et al., 2012). Indeed, the translation of several FMRP targets is up-regulated following DHPG stimulation (see Table 2 and Figure 1). Second, the expression of mGluR1/5-LTD requires AMPA receptor internalization (Waung et al., 2008). DHPG-stimulated receptor internalization depends on the translation of certain ‘‘LTD’’ proteins such as Arc and STEP (Figure 1). In the absence of FMRP, the translation of these ‘‘LTD’’ proteins is not suppressed. The elevated expression of such ‘‘LTD’’ proteins in *Fmr1* KO neurons consequently facilitates AMPAR internalization (Nakamoto et al., 2007), leading to enhanced synaptic depression (LTD). It is evident that other mGluR1/5-mediated synaptic functions are also regulated by FMRP. The activation of mGluR1/5 stimulates spine growth (Vanderklish and Edelman, 2002) and there are more immature spines in FXS neurons (Irwin et al., 2001). Collectively, mGluR1/5-mediated synaptic function and cellular changes are regulated by FMRP and are exaggerated in FXS.

1.4.2 Effects of mGluR inhibition on FXS

Based on the mGluR theory, it is postulated that dampening mGluR1/5 activity may be therapeutic for FXS. Indeed, administration of mGluR5 antagonists to animal models of FXS has shown promising therapeutic effects. Specifically, administration of mGluR5 antagonist MPEP attenuates elevated protein translation (Gross et al., 2010; Osterweil et al., 2010), enhanced AMPAR internalization (Nakamoto et al., 2007), abnormal spine morphology, PPI (de Vrij et al., 2008) (but also see (Thomas et al., 2012)), AGS, hyperactivity (Yan et al., 2005), and repetitive behavior (Thomas et al., 2012) in *Fmr1* KO mice. The use of fenobam, a potent negative allosteric modulator of mGluR5, promisingly attenuates spine abnormality (de Vrij et al., 2008) and impairments in procedural memory and avoidance discrimination (Vinueza Veloz et al., 2012). Genetic approaches have further demonstrated the therapeutic role of mGluR1/5 in FXS. Double mutant mice (heterozygous for mGluR5 and hemizygous for *Fmr1*) show normal basal translation, spine density, no significant AGS, and normal fear memory extinction. However, macroorchidism is not rescued (Dölen et al., 2007). Intriguingly, a more recent study found that the mGluR5/ *Fmr1* double mutants still show AGS, repetitive behavior, and abnormalities in anxiety and memory (Thomas et al., 2011). Encouraged by the effects of mGluR5 inhibition, an open label single dose fenobam trial

has been performed with 12 adult patients. While there is mild improvement in PPI, no significant effect is observed for CPT (continuous performance test) (Berry-Kravis et al., 2009). New compounds that negatively regulate mGluR5 have been developed and tested in clinical trials. AFQ056 (Novartis) was found to rescue abnormal spine morphology and PPI, phenotypes in *Fmr1* KO mice (Levenga et al., 2011; Gantois et al., 2013). In a phase II double blind placebo-controlled crossover trial with AFQ056 on 30 adult males for 28 days, administration of AFQ056 resulted in improvement of maladaptive behaviors only in a selective subpopulation of FXS patients with full promoter methylation (Jacquemont et al., 2011). Clinical trials with STX107 (Seaside therapeutics) also had mostly negative results, a result of which both companies decided to discontinue further drug development.

1.4.3 mGluR-Independent mechanisms

Inhibition of mGluR1/5 rescues some but not all FXS- related symptoms (Thomas et al., 2011) and shows therapeutic effects on a sub-population of FXS patients (Jacquemont et al., 2011). This suggests the existence of mGluR-independent mechanisms. Similar to mGluR1/5, activation of another group of Gq-coupled receptors, such as Gq-coupled muscarinic acetylcholine receptors (Gq-mAchR), also triggers

AMPAR internalization and translation-dependent LTD. Gq-mAchR-LTD is significantly exaggerated in *Fmr1* KO mice (Volk et al., 2007). Treating *Fmr1* KO mice with an inhibitor of M1 (one subtype of Gq-mAchR) dampens AGS (Veeraragavan et al., 2011). It remains to be determined whether simultaneous blocking of mGluR1/5 and Gq-mAchR offers more robust correction of FXS traits. Several lines of evidence have demonstrated that alteration of other G-protein coupled receptors are connected to FXS. For example, genetic or pharmacological inhibition of the Gi-coupled muscarinic M4 receptor rescues limited abnormal behaviors in *Fmr1* KO mice (Veeraragavan, S, Bui N, Perkins J, Yuva-Paylor L, 2011; Veeraragavan et al., 2012). Dopaminergic D1 receptor-mediated AMPAR surface expression and signaling in prefrontal cortex requires FMRP and D1 receptor agonist SKF81297 attenuates hyperactivity in *Fmr1* KO mice (Wang et al., 2008).

1.5 Effects of manipulating FMRP targets on FXS

As the basal level of translation is elevated in *Fmr1* KO neurons, it is generally accepted that FMRP suppresses the translation of its target mRNAs. Thus, it is postulated that the elevated expression of certain ‘‘key’’ FMRP targets may be causal for FXS, and dampening such ‘‘key’’ targets may be therapeutic. However, this

therapeutic approach is still in its infancy. Only a handful of studies show that suppressing FMRP targets attenuates cellular abnormalities (Park et al., 2008; Lee et al., 2011) and certain (but not all) behavioral phenotypes of FXS (Bilousova et al., 2009; Westmark et al., 2011; Goebel-Goody et al., 2012). Most of the verified FMRP targets are involved in synaptic plasticity, neurotransmission, and neuronal signalling. Some targets have a connection to neurological and psychiatric disorders. The therapeutic value of FMRP targets is investigated using a combination of genetic and pharmacological approaches. Arc (activity-regulated cytoskeleton-associated protein), an FMRP target, is associated with the synaptic cytoskeleton network and regulates AMPA receptor (e.g. GluR1) trafficking (Figure 1) (Park et al., 2008; Waung et al., 2008). The basal level of Arc expression is elevated in *Fmr1* KO neurons (Niere et al., 2012) and its translation is rapidly stimulated by the activation of mGluR1/5 and is required for mGluR1/5-LTD (Park et al., 2008; Waung et al., 2008). Genetic deletion of Arc in wild type and *Fmr1* KO mice results loss of mGluR1/5-LTD (Park et al., 2008). Another FMRP target, APP (amyloid beta precursor protein) (Westmark and Malter, 2007) is also a structural protein that regulates synaptic function as well as neurodegeneration (Korte et al., 2012). While overexpression of APP in *Fmr1* KO mice increases seizure susceptibility (Westmark et al., 2008), reduction of APP in *Fmr1* KO

mice rescues multiple FXS symptoms including AGS, higher density of immature spines, and the enhanced mGluR1/5-LTD (Westmark et al., 2011). These studies identify a link between FXS and Alzheimer's disease (AD), and suggest that therapies developed for AD to reduce APP level may be used to treat FXS. The expression level of another FMRP target, STEP (striatal-enriched tyrosine phosphatase) (Figure 1), is elevated in *Fmr1* KO neurons and genetic reduction of STEP rescues some FXS phenotypes (Goebel-Goody et al., 2012). A number of FMRP targets are functionally involved in the PI3K (phosphoinositide 3-kinase) and MAPK (mitogen-activated protein kinase) pathways (see Table 2 and Figure 1), which positively regulate ribosomal function and translation in an activity-dependent manner. The activity of both PI3K and MAPK is required for LTD. PI3K activity and the expression of its catalytic subunit p110β are elevated (Gross et al., 2010; Sharma et al., 2010) in *Fmr1* KO neurons. Inhibition of PI3K by LY294002 suppresses the cellular phenotypes of FXS including exaggerated basal translation, GluR1 internalization, and spine density (Gross et al., 2010). Increased expression of an up-stream activator of PI3K (i.e. PIKE or PI3 K enhancer) and increased activity of a down- stream effector of PI3K (i.e. mTOR or mammalian target of rapamycin) are observed in the hippocampus of *Fmr1* KO mice. Furthermore, activity of an up-stream suppressor of PI3K (i.e. PTEN or phosphatase and tensin

homolog) is decreased in the hippocampus of *Fmr1* KO mice (Sharma et al., 2010). However, inhibition of mTOR with rapamycin only suppresses mGluR1/5-LTD in wild type (Hou and Klann, 2004) but not *Fmr1* KO mice (Sharma et al., 2010). Treating *Fmr1* KO mice with rapamycin does not suppress the elevated basal translation, but does dampen AGS (Osterweil et al., 2010). ERK1/2 (extracellular signal-regulated kinase 1/2), a component of the MAPK pathway, is an FMRP target. The activity rather than the expression level of ERK1/2 is elevated in *Fmr1* KO mice. Pharmacological inhibition of ERK1/2 reduces AGS, elevated protein translation, and prolonged epileptiform discharges in *Fmr1* KO mice (Chuang et al., 2005; Osterweil et al., 2010). Osterweil et al. (Osterweil et al., 2013) reported similar therapeutic effects in *Fmr1* KO mouse by using lovastatin, (a clinically approved cholesterol-lowering drug) to suppress ERK1/2 activity. Although studies on the therapeutic function of ERK1/2 and PI3K have shown some degree of controversy (Gross et al., 2010; Osterweil et al., 2010), the two signaling pathways may converge and co-regulate the activity of some FMRP targets. S6K1 (ribosomal protein S6 kinase 1) is involved in ribosome biogenesis and regulates protein translation; its activity can be up regulated by ERK1/2- and PI3K-mediated phosphorylation at different residues (Figure 1) (Zhou et al., 2010). Although the expression level of S6K1 is normal in *Fmr1* KO neurons, phospho-S6K1 is elevated

(Sharma et al., 2010). Genetic deletion of S6K1 in *Fmr1* KO mice rescues the enhanced mGluR1/5-LTD, abnormal spine morphology, and deficits in recognition memory and social interaction. However, some FXS-related phenotypes such as hyperactivity and repetitive behavior are not corrected (Bhattacharya et al., 2012). GSK3B is another FMRP target whose activity can be down regulated by PI3K (Rayasam et al., 2009) and ERK1/2-mediated phosphorylation (Markou et al., 2008). Since PI3K and ERK1/2 activity are elevated in *Fmr1* KO mice, the phosphorylation of both GSK3A and GSK3B is decreased in FXS (Min et al., 2009a). Thus GSK3 activity is abnormally higher in *Fmr1* KO neurons. Treating *Fmr1* KO mice with GSK3 inhibitors lithium and SB- 216763 attenuates AGS, hyperactivity, defective cognitive function, deficits in social interaction, defective neurogenesis, and abnormal spine morphology (Min et al., 2009a; Yuskaitis et al., 2010; Liu et al., 2011; Guo et al., 2012). An open label study with 15 FXS males treated with lithium showed that lithium improves social and maladaptive behavior as well as auditory memory. However, 7 individuals had side effects of polydipsia and polyuria (Berry-Kravis et al., 2008). Different subunits of GABA-A receptors are down regulated in *Fmr1* KO mice (El Idrissi et al., 2005; D'Hulst et al., 2006; Curia et al., 2009). It is not surprising that GABA-A receptor agonists and positive allosteric modulators (such as diazepam and ganaxolone), which are clinically used as

anticonvulsants, attenuate AGS (Heulens et al., 2012). Another GABA system modulator, gaboxadol, reduces hyperactivity and PPI in *Fmr1* KO mice (Olmos-Serrano et al., 2011). Although GABA-B receptor mRNA is identified as an FMRP target by high-throughput screening (Darnell et al., 2011), its expression level in FXS is not known. However, its functional relevance is demonstrated by the fact that GABA-B agonists baclofen and arbaclofen (STX209) rescue AGS in *Fmr1* KO mice. Further, arbaclofen treatment reduces the enhanced basal translation, AMPA receptor internalization, and spine density in *Fmr1* KO mice (Henderson et al., 2012). The expression of NMDAR subunits (i.e. NR1 and NR2B) is increased in the neocortex and hippocampus of *Fmr1* KO mice (Schutt et al., 2009), but also see (Krueger et al., 2011). FMRP also suppresses the translation of NR2A (Edbauer et al., 2010). Thus, there is possibly a combination of excessive NMDAR function and deficient GABA function. Based on this hypothesis, acamprosate, which acts as an NMDAR antagonist and GABA-A agonist, was used in an open-label clinical study. Young FXS patients receiving acamprosate show significant improvement in social behavior and reduction in hyperactivity (Erickson et al., 2013). Minocycline, an FDA-approved broad-spectrum tetracycline antibiotic, shows some promising therapeutic effects in human FXS patients. In a pilot open label study on 50 FXS individuals, minocycline treatment improved cognition, language and

behavior (Utari et al., 2010). In another open label study, 20 FXS individuals treated with minocycline showed improvement in irritability and other global behavior tests (Paribello et al., 2010). A double blind, placebo-controlled, crossover trial with minocycline treatment in FXS children resulted in improvements in anxiety and mood-related behavior (Leigh et al., 2013). Treating *Fmr1* KO neurons and mice with minocycline corrects abnormal spine morphology, anxiety phenotype, defective ultrasonic vocalization, AGS, and hyperactivity (Bilousova et al., 2009; Rotschafer et al., 2012). Possible mechanisms include minocycline- mediated inhibition of ribosome function or MMP9 (matrix metallopeptidase 9), an FMRP target whose expression level is elevated in FXS (Bilousova et al., 2009; Dziembowska et al., 2013).

1.6 Connecting the mGluR theory and FMRP targets

The mGluR theory and FMRP-mediated translation have been fundamental to the development of therapeutic approaches for FXS. It is not clear how the dysregulated translation of FMRP targets contributes to elevated mGluR1/5 signalling in FXS. A recent study reported that the expression of mGluR5 itself, whose mRNA is identified as an FMRP target through high through-put screening (Darnell et al., 2011), is elevated in the prefrontal cortex of FXS patients (Lohith et al., 2013). However, another study has

shown that the expression level of mGluR5 is not changed in the forebrain and cerebellum of *Fmr1* KO mice (Giuffrida et al., 2005). As a major downstream effector of mGluR1/5 signalling, ERK1/2 shows higher activity in *Fmr1* KO neurons but its total expression level is not changed (Osterweil et al., 2013). Thus, the changes in ERK1/2 may represent an outcome of the elevated mGluR1/5 signaling rather than having a causal role on the enhanced mGluR5 function. Investigation on the molecules in the PI3K cascade has found that the expression levels of both PIKE and the p110β subunit of PI3K are elevated in the absence of FMRP (Gross et al., 2010; Sharma et al., 2010). Considering that PI3K activation can be triggered by mGluR1/5 stimulation, the enhanced expression of these FMRP-targets may contribute to the elevated basal mGluR1/5 activity in FXS.

1.7 Concluding remarks

Since the positional cloning of the FMR1 gene, there have been tremendous advances in understanding the function of FMRP, which have led to rational designs of therapeutic approaches. While new agents are being examined in animal models and clinical trials, successful repurposing of the available drugs such as memantine, acamprosate, minocycline, fenobam, baclofen, lithium, and lovastatin could benefit FXS

patients without involving the lengthy drug development process. As FMRP regulates many aspects of neuronal function, simultaneous manipulation of multiple FMRP targets and/or signaling pathways should also deserve significant consideration. Although the prevailing theory posits that FMRP suppresses translation and mGluR1/5 signalling, significant involvement of FMRP in up-regulating protein synthesis and mGluR1/5-independent synaptic functions has also been identified. How these newly discovered functions of FMRP are relevant to FXS etiology remains to be determined.

APPENDIX

Table 1: Human FXS traits that are recapitulated in *Fmr1* knockout mice.

FXS symptoms in human	**FXS-related behavior in Fmr1 KO mice**
Intellectual disability	Defective spatial learning and memory (Dobkin et al., 2000; Baker et al., 2010) Defective passive avoidance memory (Qin et al., 2002, 2005) Defective contextual memory (Paradee et al., 1999) Defective recognition memory (Bhattacharya et al., 2012)
Susceptibility to seizures	Audiogenic seizure (Musumeci et al., 2000; Chen and Toth, 2001) Enhanced limbic epileptogenesis (Qiu et al., 2009) Prolonged epileptiform discharges (Chuang et al., 2005)
Hyperactivity	Increased locomotor movement In open field test (Qin et al., 2002; Liu et al., 2011)
Hyperarousal	Higher acoustic startle responses to low intensity stimuli (Nielsen et al., 2002)
Abnormal sensorimotor gating (reduced PPI)	Variable phenotypes in PPI (Chen and Toth, 2001; Nielsen et al., 2002; Frankland et al., 2004; de Vrij et al., 2008; Levenga et al., 2011; Pietropaolo et al., 2011; Thomas et al., 2011)
Social anxiety Defective social interaction	Deficits in social dominance (Spencer et al., 2005; Goebel-Goody et al., 2012) Decreased interests in social novelty and social interaction (Yuskaitis et al., 2010; Liu et al., 2011; Pietropaolo et al., 2011; Bhattacharya et al., 2012) Defective communication (tested by ultrasonic vocalization) (Roy et al., 2012)
Perseveration/repetitive behavior	Increased marble burying (Zang et al., 2009; Rotschafer et al., 2012)
Macroorchidism	Enlarged testes (Dutch-belgian et al., 1994; Zang et al., 2009)
Higher density of immature spine	Higher density of immature spine (Grossman et al., 2006; Dölen et al., 2007; Hayashi et al., 2007; de Vrij et al., 2008; Bhattacharya et al., 2012)

Table 2: FMRP targets that may be functionally involved in FMRP-regulated translation and FXS-related phenotypes

Gene symbol	**Protein name**	**Validation method**	**Changes in FXS**	**Response to mGluR1/5 stimulation**	**Therapeutic effects**	**Inhibitors**
Agap2	PIKE	HT (Darnell et al., 2011)	↑protein (Sharma et al., 2010)			
App	APP	HT (Darnell et al., 2011; Ascano et al., 2012), CoIP (Westmark and Malter, 2007)	↑protein (Westmark et al., 2011)	↑translation (Westmark and Malter, 2007)	AGS, hyperactivity, spines, mGluR-LTD (Westmark et al., 2011)	
Arc	Arc	HT (Darnell et al., 2011; Ascano et al., 2012), CoIP (Zalfa et al., 2003)	↑protein (Zalfa et al., 2003) ↓ protein (Krueger et al., 2011)	↑translation (Park et al., 2008; Waung et al., 2008)	mGluR-LTD (Park et al., 2008)	
Camk2a	CaMKII α	HT(Darnell et al., 2011), CoIP (Zalfa et al., 2003; Muddashetty et al., 2007)	↑protein (Zalfa et al., 2003; Hou et al., 2006)	↑translation (Hou et al., 2006; Kao et al., 2010; Osterweil et al., 2010)		KN62, KN93
Cyfip2	CYFIP2	HT (Darnell et al., 2011; Ascano et al., 2012)	↑protein (Hoeffer et al., 2012)			

Table 2 (cont'd)

Dlg4	PSD-95	HT(Darnell et al., 2011), miR-125a (Muddashetty et al., 2011), G-quadruplex (Todd et al., 2003)	↑protein (Todd et al., 2003) ↓protein degradation (Tsai et al., 2012) ↓ protein (Krueger et al., 2011)	↑translation (Todd et al., 2003; Muddashetty et al., 2011)		
EF1a	EF1α	CoIP (Sung et al., 2003)	↑protein (Sung et al., 2003)	↑translation (Huang et al., 2005)		
Fmr1	FMRP	In vitro (Schaeffer et al., 2001)	↓ or lack of expression	↑translation followed by degradation (Berwine and Reenough, 1997; Hou et al., 2006; Nalavadi et al., 2012; Niere et al., 2012)		
Gabbr1	GABA-B1	HT (Darnell et al., 2011)			Protein synthesis, AMPAR internalization, abnormal spines, AGS (Pacey et al., 2009; Henderson et al., 2012)	STX209, baclofen
Gabrd	GABA-Aδ	In vitro (Miyashiro et al., 2003)	↓protein (Curia et al., 2009)		AGS(Heulens et al., 2012), hyperactivity and PPI(Olmos-Serrano et al., 2011)	Acampros-ate, alphaxalone, gaboxadol, diazepam

Table 2 (cont'd)

Gria1	AMPA-1	HT, Co-IP (Muddashetty et al., 2007)	↑protein (Muddashetty et al., 2007; Schutt et al., 2009) no change (Giuffrida et al., 2005)	↑translation (Muddashetty et al., 2007)		
Grin1	NR1	HT(Darnell et al., 2011), CoIP (Schutt et al., 2009)	↑protein (Schutt et al., 2009) no change (Giuffrida et al., 2005) ↓ protein (Krueger et al., 2011)		Some clinical efficacy in human patients (Erickson et al., 2009, 2013)	Memantine, Acampros-ate
Grin2a	NR2A	miR-125b (Edbauer et al., 2010)	no change (Giuffrida et al., 2005) ↓ protein (Krueger et al., 2011)		Some clinical efficacy in human patients (Erickson et al., 2009, 2013)	Memantine, Acampros-ate
Grin2b	NR2B	HT(Darnell et al., 2011), CoIP (Schutt et al., 2009)	↑protein (Schutt et al., 2009) no change (Giuffrida et al., 2005) ↓ protein (Krueger et al., 2011)		Some clinical efficacy in human patients (Erickson et al., 2009, 2013)	Memantine, Acampros-ate

Table 2 (cont'd)

Gsk3b	GSK3β	HT (Darnell et al., 2011; Ascano et al., 2012)	↑activity (Min et al., 2009a)		AGS, hyperactivity, passive avoidance memory, contextual, and cued fear memory, social preference and social anxiety, defective neurogenesis, spine abnormality (Min et al., 2009b; Mines et al., 2010; Yuskaitis et al., 2010; Liu et al., 2011; Guo et al., 2012)	Lithium, SB216763
Hcn1	HCN1		↑protein (Brager D. Akhavan A, 2012)			
Homer 1	Homer1	HT (Ascano et al., 2012)		Unchanged (Ronesi et al., 2012)	Restored mGluR5 signaling, AGS, anxiety phenotype in open field (Ronesi et al., 2012)	
Kcnc1	Kv3.1; Kv3.2	In vitro (Darnell et al., 2001)	↑protein (Strumbos et al., 2010)			
Kcnd2	Kv4.2	HT(Darnell et al., 2011), in vitro (Lee et al., 2011)	↑protein(Lee et al., 2011), ↓ protein (Gross et al., 2011)		LTP (Lee et al., 2011)	Heteropoda-toxin HpTx2
Map1b	MAP1B	HT (Darnell et al., 2011; Ascano et al., 2012) In vitro (Lu et al., 2004; Menon et al., 2008)	↑protein (Zalfa et al., 2003; Lu et al., 2004; Hou et al., 2006)	↑translation (Hou et al., 2006; Chen and Shen, 2013)		

Table 2 (cont'd)

Mapk1	MAPK1 or ERK2	HT (Darnell et al., 2011; Ascano et al., 2012)	↑phosphorylation (Hou et al., 2006; Osterweil et al., 2013)	↑activation (Hou et al., 2006; Osterweil et al., 2010)	Protein synthesis, AGS (Osterweil et al., 2010, 2013)	U0126, SL 327, lovastatin
Mmp9	MMP9		↑protein (Bilousova et al., 2009; Dziembowska et al., 2013)		Spine abnormality, anxiety phenotype in elevate plus maze, AGS, hyperactivity, communication (Bilousova et al., 2009; Rotschafer et al., 2012)	Minocycline
Mtor	mTOR	HT (Darnell et al., 2011; Ascano et al., 2012)	↑phosphory-lation ↑activity (Sharma et al., 2010)	↑activation (Sharma et al., 2010)	AGS (Osterweil et al., 2010)	Rapamycin
Pak1	PAK1	HT (Darnell et al., 2011; Ascano et al., 2012)			Spine abnormality, LTP, hyperactivity, repetitive behavior, anxiety, trace fear conditioning, AGS (Hayashi et al., 2007; Dolan et al., 2013)	FRAX486
Pik3cb	PI3K P110β catalytic subunit	HT (Ascano et al., 2012)	↑protein ↑activity (Gross et al., 2010; Sharma et al., 2010)	↑translation ↑activation (Gross et al., 2010)	Protein synthesis, spine abnormality, AMPA receptor internalization (Gross et al., 2010)	LY294002 Wortmannin
Pten	PTEN	HT (Darnell et al., 2011; Ascano et al., 2012)	↓phosphory-lation (Sharma et al., 2010)			
Ptpn5	STEP	HT (Darnell et al., 2011)	↑protein (Goebel-Goody et al., 2012)	↑translation (Zhang et al., 2008)	AGS, social interaction, social anxiety (Goebel-Goody et al., 2012)	

Table 2 (cont'd)

Rgs5	RGS5	In vitro (Miyashiro et al., 2003)				
Rps6kb1	S6K1	HT (Ascano et al., 2012)	↑phosphory-lation (Bhattacharya et al., 2012)	↑activation (Sharma et al., 2010)	Protein synthesis, mGluR-LTD, dendritic spines, novel object recognition, social interaction (Bhattacharya et al., 2012)	
Sapap3/4	SAPAP3/4		↑protein (Schutt et al., 2009) ↓protein (Krueger et al., 2011)			
Shank1	SHANK1	HT(Darnell et al., 2011; Ascano et al., 2012), 3'UTR (Schutt et al., 2009)	↑protein (Schutt et al., 2009)	↑translation (Schutt et al., 2009)		
Shank3	SHANK3	HT (Darnell et al., 2011)	↑protein (Schutt et al., 2009)			
Sod1	SOD1	In vitro (Bechara et al., 2009)	↓protein (Bechara et al., 2009)			
Tsc2	TSC2	HT (Darnell et al., 2011; Ascano et al., 2012)			mGluR-LTD, memory deficit (Auerbach et al., 2011)	

Table 2 (cont'd)

Key: HT: high throughput screening; CoIP: coimmunoprecipitation; AGS: audiogenic seizure; PPI: prepulse inhibition; ↑: increase; ↓: decrease. Therapeutic effects are observed in *Fmr1* KO mice when the corresponding FMRP target is genetically reduced or pharmacologically inhibited.

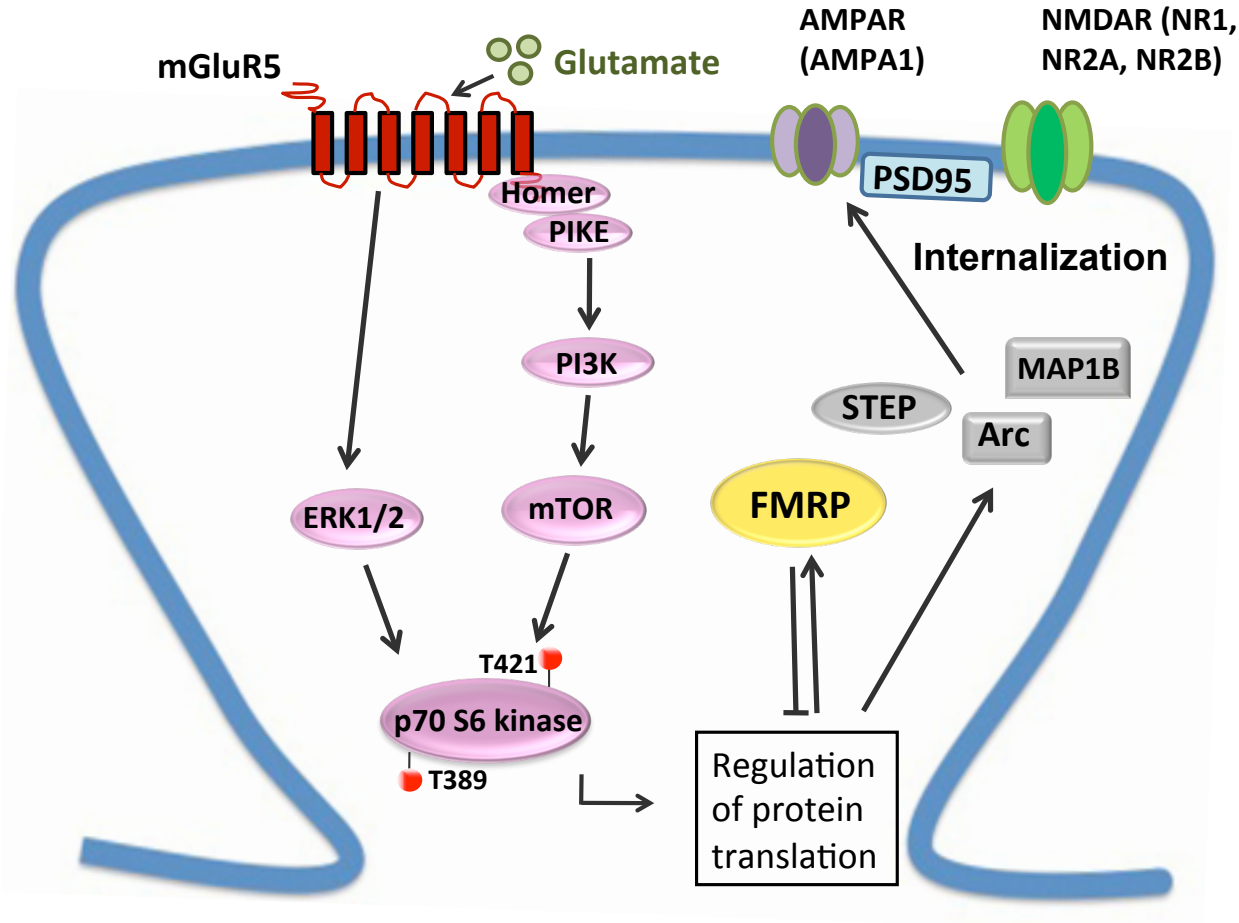

Figure 1: FMRP mRNA targets whose proteins are activated/translated upon mGluR5 stimulation.

REFERENCES

REFERENCES

Ascano, M., Mukherjee, N., Bandaru, P., Miller, J.B., Nusbaum, J.D., Corcoran, D.L., et al. (2012). FMRP targets distinct mRNA sequence elements to regulate protein expression. Nature *492*: 382–6.

Auerbach, B.D., Osterweil, E.K., and Bear, M.F. (2011). Mutations causing syndromic autism define an axis of synaptic pathophysiology. Nature *480*: 63–8.

Bagni, C., Tassone, F., Neri, G., and Hagerman, R. (2012). Fragile X syndrome : causes , diagnosis , mechanisms , and therapeutics. J. Clin. Invest. *122*:

Baker, K.B., Wray, S.P., Ritter, R., Mason, S., and Savelieva, K. V (2010). Male and female Fmr1 knockout mice on C57 albino background exhibit spatial learning and memory impairments. 562–574.

Bear, M.F., Huber, K.M., and Warren, S.T. (2004). The mGluR theory of fragile X mental retardation. Trends Neurosci. *27*: 370–7.

Bechara, E.G., Didiot, M.C., Melko, M., Davidovic, L., Bensaid, M., Martin, P., et al. (2009). A novel function for fragile X mental retardation protein in translational activation. PLoS Biol. *7*: e16.

Berry-Kravis, E., Hessl, D., Coffey, S., Hervey, C., Schneider, a, Yuhas, J., et al. (2009). A pilot open label, single dose trial of fenobam in adults with fragile X syndrome. J. Med. Genet. *46*: 266–71.

Berry-Kravis, E., Sumis, A., Hervey, C., Nelson, M., Porges, S.W., Weng, N., et al. (2008). Open-label treatment trial of lithium to target the underlying defect in fragile X syndrome. J. Dev. Behav. Pediatr. *29*: 293–302.

Berwine, J.A.E., and Reenough, W.I.T.G. (1997). Fragile X mental retardation protein is translated near synapses. *94*: 5395–5400.

Bhattacharya, a, Kaphzan, H., Alvarez-Dieppa, a C., Murphy, J.P., Pierre, P., and Klann, E. (2012). Genetic Removal of p70 S6 Kinase 1 Corrects Molecular, Synaptic, and Behavioral Phenotypes in Fragile X Syndrome Mice. Neuron *76*: 325–337.

Bilousova, T. V, Dansie, L., Ngo, M., Aye, J., Charles, J.R., Ethell, D.W., et al. (2009). Minocycline promotes dendritic spine maturation and improves behavioural performance in the fragile X mouse model. J. Med. Genet. *46*: 94–102.

Boulle K, Verkerk AJ, Reyniers E, Vits L, Hendrickx J, Van Roy B, Van Den Bos F, de Graaf E, Oostra BA, W.P. De (1993). A point mutation in the FMR-1 gene associated with fragile X mental retardation. Nat. Genet. *3(1)*: 31–35.

Brager D. Akhavan A, J.D. (2012). Impaired dendritic expression and plasticity of h-channels in the fmr1(-/y) mouse model of fragile X syndrome. Cell Rep *1*: 225–233.

Broeder, M.J. den, Linde, H. van der, Brouwer, J.R., Oostra, B. a, Willemsen, R., and Ketting, R.F. (2009). Generation and characterization of FMR1 knockout zebrafish. PLoS One *4*: e7910.

Brouwer, J.R., Mientjes, E.J., Bakker, C.E., Nieuwenhuizen, I.M., Severijnen, L. a, Linde, H.C. Van der, et al. (2007). Elevated Fmr1 mRNA levels and reduced protein expression in a mouse model with an unmethylated Fragile X full mutation. Exp. Cell Res. *313*: 244–53.

Brown, V., Jin, P., Ceman, S., Darnell, J.C., O'Donnell, W.T., Tenenbaum, S. a, et al. (2001). Microarray Identification of FMRP-Associated Brain mRNAs and Altered mRNA Translational Profiles in Fragile X Syndrome. Cell *107*: 477–487.

Chen, L., and Toth, M. (2001). Fragile X mice develop sensory hyperreactivity to auditory stimuli. Neuroscience *103*: 1043–50.

Chen, Y.-L., and Shen, C.-K.J. (2013). Modulation of mGluR-Dependent MAP1B Translation and AMPA Receptor Endocytosis by MicroRNA miR-146a-5p. J. Neurosci. *33*: 9013–9020.

Chiurazzi, P., Pomponi, M.G., Pietrobono, R., Bakker, C.E., Neri, G., and Oostra, B. a (1999). Synergistic effect of histone hyperacetylation and DNA demethylation in the reactivation of the FMR1 gene. Hum. Mol. Genet. *8*: 2317–23.

Chiurazzi, P., Pomponi, M.G., Willemsen, R., Oostra, B. a, and Neri, G. (1998). In vitro reactivation of the FMR1 gene involved in fragile X syndrome. Hum. Mol. Genet. *7*: 109–13.

Chuang, S.-C., Zhao, W., Bauchwitz, R., Yan, Q., Bianchi, R., and Wong, R.K.S. (2005). Prolonged epileptiform discharges induced by altered group I metabotropic glutamate receptor-mediated synaptic responses in hippocampal slices of a fragile X mouse model. J. Neurosci. *25*: 8048–55.

Coffee, B., Ikeda, M., Budimirovic, D.B., Hjelm, L.N., Kaufmann, W.E., and Warren, S.T. (2008). Mosaic FMR1 deletion causes fragile X syndrome and can lead to molecular misdiagnosis: a case report and review of the literature. Am. J. Med. Genet. A *146A*: 1358–67.

Coffee, B., Zhang, F., Ceman, S., Warren, S.T., and Reines, D. (2002). Histone modifications depict an aberrantly heterochromatinized FMR1 gene in fragile x syndrome. Am. J. Hum. Genet. *71*: 923–32.

Collins, S.C., Bray, S.M., Suhl, J. a, Cutler, D.J., Coffee, B., Zwick, M.E., et al. (2010). Identification of novel FMR1 variants by massively parallel sequencing in developmentally delayed males. Am. J. Med. Genet. A *152A*: 2512–20.

Corbin, F., Bouillon, M., Fortin, a, Morin, S., Rousseau, F., and Khandjian, E.W. (1997). The fragile X mental retardation protein is associated with poly(A)+ mRNA in actively translating polyribosomes. Hum. Mol. Genet. *6*: 1465–72.

Curia, G., Papouin, T., Séguéla, P., and Avoli, M. (2009). Downregulation of tonic GABAergic inhibition in a mouse model of fragile X syndrome. Cereb. Cortex *19*: 1515–20.

D'Hulst, C., Geest, N. De, Reeve, S.P., Dam, D. Van, Deyn, P.P. De, Hassan, B. a, et al. (2006). Decreased expression of the GABAA receptor in fragile X syndrome. Brain Res. *1121*: 238–45.

Dam, D. Van, D'Hooge, R., Hauben, E., Reyniers, E., Gantois, I., Bakker, C.E., et al. (2000). Spatial learning, contextual fear conditioning and conditioned emotional response in Fmr1 knockout mice. Behav. Brain Res. *117*: 127–36.

Darnell, J.C., Driesche, S.J. Van, Zhang, C., Hung, K.Y.S., Mele, A., Fraser, C.E., et al. (2011). FMRP stalls ribosomal translocation on mRNAs linked to synaptic function and autism. Cell *146*: 247–61.

Darnell, J.C., Fraser, C.E., Mostovetsky, O., Stefani, G., Jones, T. a, Eddy, S.R., et al. (2005). Kissing complex RNAs mediate interaction between the Fragile-X mental retardation protein KH2 domain and brain polyribosomes. Genes Dev. *19*: 903–18.

Darnell, J.C., Jensen, K.B., Jin, P., Brown, V., Warren, S.T., and Darnell, R.B. (2001). Fragile X mental retardation protein targets G quartet mRNAs important for neuronal function. Cell *107*: 489–99.

Dictenberg, J.B., Swanger, S. a, Antar, L.N., Singer, R.H., and Bassell, G.J. (2008). A direct role for FMRP in activity-dependent dendritic mRNA transport links filopodial-spine morphogenesis to fragile X syndrome. Dev. Cell *14*: 926–39.

Dobkin, C., Rabe, A., Dumas, R., Idrissi, A.E.L., Haubenstock, H., and Brown, W.T.E.D. (2000). Fmr 1 knockout mouse has a distinctive strain-specific learning impairment. *100*: 423–429.

Dockendorff, T.C., Su, H.S., McBride, S.M.J., Yang, Z., Choi, C.H., Siwicki, K.K., et al. (2002). Drosophila lacking dfmr1 activity show defects in circadian output and fail to maintain courtship interest. Neuron *34*: 973–84.

Dolan, B.M., Duron, S.G., Campbell, D. a, Vollrath, B., Shankaranarayana Rao, B.S., Ko, H.-Y., et al. (2013). Rescue of fragile X syndrome phenotypes in Fmr1 KO mice by the small-molecule PAK inhibitor FRAX486. Proc. Natl. Acad. Sci. U. S. A. *110*: 5671–6.

Dölen, G., Osterweil, E., Rao, B.S.S., Smith, G.B., Auerbach, B.D., Chattarji, S., et al. (2007). Correction of fragile X syndrome in mice. Neuron *56*: 955–62.

Dutch-belgian, T., Helm, R. Van Der, Oerlemans, F., Hoogeveen, T., and Oostra, B.A. (1994). Fmrl Knockout M ice : A Model to Study Fragile X Mental Retardation. *78*: 23–33.

Dziembowska, M., Pretto, D.I., Janusz, A., Kaczmarek, L., Leigh, M.J., Gabriel, N., et al. (2013). High MMP-9 activity levels in fragile X syndrome are lowered by minocycline. Am. J. Med. Genet. A *161A*: 1897–903.

Eberhart, D.E., Malter, H.E., Feng, Y., and Warren, S.T. (1996). The fragile X mental retardation protein is a ribonucleoprotein containing both nuclear localization and nuclear export signals. Hum. Mol. Genet. *5*: 1083–91.

Edbauer, D., Neilson, J.R., Foster, K. a, Wang, C.-F., Seeburg, D.P., Batterton, M.N., et al. (2010). Regulation of synaptic structure and function by FMRP-associated microRNAs miR-125b and miR-132. Neuron *65*: 373–84.

Eiges, R., Urbach, A., Malcov, M., Frumkin, T., Schwartz, T., Amit, A., et al. (2007). Developmental study of fragile X syndrome using human embryonic stem cells derived from preimplantation genetically diagnosed embryos. Cell Stem Cell *1*: 568–77.

Erickson, C. a, Mullett, J.E., and McDougle, C.J. (2009). Open-label memantine in fragile X syndrome. J. Autism Dev. Disord. *39*: 1629–35.

Erickson, C. a, Wink, L.K., Ray, B., Early, M.C., Stiegelmeyer, E., Mathieu-Frasier, L., et al. (2013). Impact of acamprosate on behavior and brain-derived neurotrophic factor: an open-label study in youth with fragile X syndrome. Psychopharmacology (Berl). 75–84.

Feng, Y., Absher, D., Eberhart, D.E., Brown, V., Malter, H.E., and Warren, S.T. (1997a). FMRP associates with polyribosomes as an mRNP, and the I304N mutation of severe fragile X syndrome abolishes this association. Mol. Cell *1*: 109–18.

Feng, Y., Gutekunst, C. a, Eberhart, D.E., Yi, H., Warren, S.T., and Hersch, S.M. (1997b). Fragile X mental retardation protein: nucleocytoplasmic shuttling and association with somatodendritic ribosomes. J. Neurosci. *17*: 1539–47.

Frankland, P.W., Wang, Y., Rosner, B., Shimizu, T., Balleine, B.W., Dykens, E.M., et al. (2004). Sensorimotor gating abnormalities in young males with fragile X syndrome and Fmr1-knockout mice. Mol. Psychiatry *9*: 417–25.

Gantois, I., Pop, A.S., Esch, C.E.F. de, Buijsen, R. a M., Pooters, T., Gomez-Mancilla, B., et al. (2013). Chronic administration of AFQ056/Mavoglurant restores social behaviour in Fmr1 knockout mice. Behav. Brain Res. *239*: 72–9.

Giuffrida, R., Musumeci, S., D'Antoni, S., Bonaccorso, C.M., Giuffrida-Stella, A.M., Oostra, B. a, et al. (2005). A reduced number of metabotropic glutamate subtype 5 receptors are associated with constitutive homer proteins in a mouse model of fragile X syndrome. J. Neurosci. *25*: 8908–16.

Goebel-Goody, S.M., Wilson-Wallis, E.D., Royston, S., Tagliatela, S.M., Naegele, J.R., and Lombroso, P.J. (2012). Genetic manipulation of STEP reverses behavioral abnormalities in a fragile X syndrome mouse model. Genes. Brain. Behav. *11*: 586–600.

Gross, C., Nakamoto, M., Yao, X., Chan, C.B., Yim, S.Y., Ye, K., et al. (2010). Excess phosphoinositide 3-kinase subunit synthesis and activity as a novel therapeutic target in fragile x syndrome. J Neurosci *30*: 10624–10638.

Gross, C., Yao, X., Pong, D.L., Jeromin, A., and Bassell, G.J. (2011). Fragile X mental retardation protein regulates protein expression and mRNA translation of the potassium channel Kv4.2. J. Neurosci. *31*: 5693–8.

Grossman, A.W., Aldridge, G.M., Weiler, I.J., and Greenough, W.T. (2006). Local protein synthesis and spine morphogenesis: Fragile X syndrome and beyond. J. Neurosci. *26*: 7151–5.

Guo, W., Murthy, A.C., Zhang, L., Johnson, E.B., Schaller, E.G., Allan, A.M., et al. (2012). Inhibition of GSK3β improves hippocampus-dependent learning and rescues neurogenesis in a mouse model of fragile X syndrome. Hum. Mol. Genet. *21*: 681–91.

Hayashi, M.L., Rao, B.S.S., Seo, J.-S., Choi, H.-S., Dolan, B.M., Choi, S.-Y., et al. (2007). Inhibition of p21-activated kinase rescues symptoms of fragile X syndrome in mice. Proc. Natl. Acad. Sci. U. S. A. *104*: 11489–94.

Henderson, C., Wijetunge, L., Kinoshita, M.N., Shumway, M., Hammond, R.S., Postma, F.R., et al. (2012). Reversal of Disease-Related Pathologies in the Fragile X Mouse Model by Selective Activation of GABA B Receptors with Arbaclofen. *4*: 1–11.

Heulens, I., D'Hulst, C., Dam, D. Van, Deyn, P.P. De, and Kooy, R.F. (2012). Pharmacological treatment of fragile X syndrome with GABAergic drugs in a knockout mouse model. Behav. Brain Res. *229*: 244–9.

Hoeffer, C. a, Sanchez, E., Hagerman, R.J., Mu, Y., Nguyen, D. V, Wong, H., et al. (2012). Altered mTOR signaling and enhanced CYFIP2 expression levels in subjects with fragile X syndrome. Genes. Brain. Behav. *11*: 332–41.

Hou, L., Antion, M.D., Hu, D., Spencer, C.M., Paylor, R., and Klann, E. (2006). Dynamic translational and proteasomal regulation of fragile X mental retardation protein controls mGluR-dependent long-term depression. Neuron *51*: 441–54.

Hou, L., and Klann, E. (2004). Activation of the phosphoinositide 3-kinase-Akt-mammalian target of rapamycin signaling pathway is required for metabotropic glutamate receptor-dependent long-term depression. J. Neurosci. *24*: 6352–61.

Huang, F., Chotiner, J.K., and Steward, O. (2005). The mRNA for elongation factor 1alpha is localized in dendrites and translated in response to treatments that induce long-term depression. J. Neurosci. *25*: 7199–209.

Huber, K.M., Gallagher, S.M., Warren, S.T., and Bear, M.F. (2002). Altered synaptic plasticity in a mouse model of fragile X mental retardation. Proc. Natl. Acad. Sci. U. S. A. *99*: 7746–7750.

Idrissi, A. El, Ding, X.-H., Scalia, J., Trenkner, E., Brown, W.T., and Dobkin, C. (2005). Decreased GABA(A) receptor expression in the seizure-prone fragile X mouse. Neurosci. Lett. *377*: 141–6.

Irwin, S. a, Patel, B., Idupulapati, M., Harris, J.B., Crisostomo, R. a, Larsen, B.P., et al. (2001). Abnormal dendritic spine characteristics in the temporal and visual cortices of patients with fragile-X syndrome: a quantitative examination. Am. J. Med. Genet. *98*: 161–7.

Jacquemont, S., Curie, A., Portes, V. des, Torrioli, M.G., Berry-Kravis, E., Hagerman, R.J., et al. (2011). Epigenetic modification of the FMR1 gene in fragile X syndrome is associated with differential response to the mGluR5 antagonist AFQ056. Sci. Transl. Med. *3*: 64ra1.

Jin, P., Zarnescu, D.C., Ceman, S., Nakamoto, M., Mowrey, J., Jongens, T. a, et al. (2004). Biochemical and genetic interaction between the fragile X mental retardation protein and the microRNA pathway. Nat. Neurosci. *7*: 113–7.

Kao, D.-I., Aldridge, G.M., Weiler, I.J., and Greenough, W.T. (2010). Altered mRNA transport, docking, and protein translation in neurons lacking fragile X mental retardation protein. Proc. Natl. Acad. Sci. U. S. A. *107*: 15601–6.

Korte, M., Herrmann, U., Zhang, X., and Draguhn, A. (2012). The role of APP and APLP for synaptic transmission, plasticity, and network function: lessons from genetic mouse models. Exp. Brain Res. *217*: 435–40.

Krawczun, M.S., Jenkins, E.C., and Brown, W.T. (1985). Analysis of the fragile-X chromosome: localization and detection of the fragile site in high resolution preparations. Hum. Genet. *69*: 209–11.

Krueger, D.D., Osterweil, E.K., Chen, S.P., Tye, L.D., and Bear, M.F. (2011). Cognitive dysfunction and prefrontal synaptic abnormalities in a mouse model of fragile X syndrome. Proc. Natl. Acad. Sci. U. S. A. *108*: 2587–92.

Lauterborn, J.C., Rex, C.S., Kramár, E., Chen, L.Y., Pandyarajan, V., Lynch, G., et al. (2007). Brain-derived neurotrophic factor rescues synaptic plasticity in a mouse model of fragile X syndrome. J. Neurosci. *27*: 10685–94.

Lee, H.Y., Ge, W.-P., Huang, W., He, Y., Wang, G.X., Rowson-Baldwin, A., et al. (2011). Bidirectional regulation of dendritic voltage-gated potassium channels by the fragile X mental retardation protein. Neuron *72*: 630–42.

Leigh, M.J.S., Nguyen, D. V, Mu, Y., Winarni, T.I., Schneider, A., Chechi, T., et al. (2013). A randomized double-blind, placebo-controlled trial of minocycline in children and adolescents with fragile x syndrome. J. Dev. Behav. Pediatr. *34*: 147–155.

Levenga, J., Hayashi, S., Vrij, F.M.S. de, Koekkoek, S.K., Linde, H.C. van der, Nieuwenhuizen, I., et al. (2011). AFQ056, a new mGluR5 antagonist for treatment of fragile X syndrome. Neurobiol. Dis. *42*: 311–7.

Liu, Z.-H., Chuang, D.-M., and Smith, C.B. (2011). Lithium ameliorates phenotypic deficits in a mouse model of fragile X syndrome. Int. J. Neuropsychopharmacol. *14*: 618–30.

Lohith, T.G., Osterweil, E.K., Fujita, M., Jenko, K.J., Bear, M.F., and Innis, R.B. (2013). Is metabotropic glutamate receptor 5 upregulated in prefrontal cortex in fragile X syndrome? Mol. Autism *4*: 15.

Lu, R., Wang, H., Liang, Z., Ku, L., O'donnell, W.T., Li, W., et al. (2004). The fragile X protein controls microtubule-associated protein 1B translation and microtubule stability in brain neuron development. Proc. Natl. Acad. Sci. U. S. A. *101*: 15201–6.

Markou, T., Cullingford, T.E., Giraldo, A., Weiss, S.C., Alsafi, A., Fuller, S.J., et al. (2008). Glycogen synthase kinases 3alpha and 3beta in cardiac myocytes: regulation and consequences of their inhibition. Cell. Signal. *20*: 206–18.

McBride, S.M.J., Choi, C.H., Wang, Y., Liebelt, D., Braunstein, E., Ferreiro, D., et al. (2005). Pharmacological rescue of synaptic plasticity, courtship behavior, and mushroom body defects in a Drosophila model of fragile X syndrome. Neuron *45*: 753–64.

Menon, L., Mader, S.A., Mihailescu, M., and Mader, S.A.N.N. (2008). Fragile X mental retardation protein interactions with the microtubule associated protein 1B RNA Fragile X mental retardation protein interactions with the microtubule associated protein 1B RNA. 1644–1655.

Min, W.W., Yuskaitis, C.J., Yan, Q., Sikorski, C., Chen, S., Jope, R.S., et al. (2009). Elevated glycogen synthase kinase-3 activity in Fragile X mice: key metabolic regulator with evidence for treatment potential. Neuropharmacology *56*: 463–72.

Mines, M. a, Yuskaitis, C.J., King, M.K., Beurel, E., and Jope, R.S. (2010). GSK3 influences social preference and anxiety-related behaviors during social interaction in a mouse model of fragile X syndrome and autism. PLoS One *5*: e9706.

Miyashiro, K.Y., Beckel-Mitchener, A., Purk, T.P., Becker, K.G., Barret, T., Liu, L., et al. (2003). RNA cargoes associating with FMRP reveal deficits in cellular functioning in Fmr1 null mice. Neuron *37*: 417–431.

Morales, J., Hiesinger, P.R., Schroeder, A.J., Kume, K., Verstreken, P., Jackson, F.R., et al. (2002). Drosophila fragile X protein, DFXR, regulates neuronal morphology and function in the brain. Neuron *34*: 961–72.

Muddashetty, R.S., Kelić, S., Gross, C., Xu, M., and Bassell, G.J. (2007). Dysregulated metabotropic glutamate receptor-dependent translation of AMPA receptor and postsynaptic density-95 mRNAs at synapses in a mouse model of fragile X syndrome. J. Neurosci. Off. J. Soc. Neurosci. *27*: 5338–48.

Muddashetty, R.S., Nalavadi, V.C., Gross, C., Yao, X., Xing, L., Laur, O., et al. (2011). Reversible Inhibition of PSD-95 mRNA Translation by miR-125a, FMRP Phosphorylation, and mGluR Signaling. Mol Cell *42*: 673–688.

Musumeci, S. a, Bosco, P., Calabrese, G., Bakker, C., Sarro, G.B. De, Elia, M., et al. (2000). Audiogenic seizures susceptibility in transgenic mice with fragile X syndrome. Epilepsia *41*: 19–23.

Nakamoto, M., Nalavadi, V., Epstein, M.P., Narayanan, U., Bassell, G.J., and Warren, S.T. (2007). Fragile X mental retardation protein deficiency leads to excessive mGluR5-dependent internalization of AMPA receptors. Proc. Natl. Acad. Sci. U. S. A. *104*: 15537–15542.

Nalavadi, V.C., Muddashetty, R.S., Gross, C., and Bassell, G.J. (2012). Dephosphorylation-induced ubiquitination and degradation of FMRP in dendrites: a role in immediate early mGluR-stimulated translation. J. Neurosci. *32*: 2582–7.

Napoli, I., Mercaldo, V., Boyl, P.P., Eleuteri, B., Zalfa, F., Rubeis, S. De, et al. (2008). The fragile X syndrome protein represses activity-dependent translation through CYFIP1, a new 4E-BP. Cell *134*: 1042–54.

Nielsen, D.M., Derber, W.J., McClellan, D. a, and Crnic, L.S. (2002). Alterations in the auditory startle response in Fmr1 targeted mutant mouse models of fragile X syndrome. Brain Res. *927*: 8–17.

Niere, F., Wilkerson, J.R., and Huber, K.M. (2012). Evidence for a fragile X mental retardation protein-mediated translational switch in metabotropic glutamate receptor-triggered Arc translation and long-term depression. J. Neurosci. *32*: 5924–36.

Nussbaum, R.L., and Dreyfuss, G. (1993). The Protein Product of the Fragile X Gene , FMRI , Has Characteristics of an RNA-Binding Protein. *74*: 291–298.

Olmos-Serrano, J.L., Corbin, J.G., and Burns, M.P. (2011). The GABA(A) receptor agonist THIP ameliorates specific behavioral deficits in the mouse model of fragile X syndrome. Dev. Neurosci. *33*: 395–403.

Osterweil, E.K., Chuang, S.-C., Chubykin, A. a, Sidorov, M., Bianchi, R., Wong, R.K.S., et al. (2013). Lovastatin corrects excess protein synthesis and prevents epileptogenesis in a mouse model of fragile X syndrome. Neuron *77*: 243–50.

Osterweil, E.K., Krueger, D.D., Reinhold, K., and Bear, M.F. (2010). Hypersensitivity to mGluR5 and ERK1/2 leads to excessive protein synthesis in the hippocampus of a mouse model of fragile X syndrome. J. Neurosci. *30*: 15616–27.

Pacey, L.K.K., Heximer, S.P., and Hampson, D.R. (2009). Increased GABA B Receptor-Mediated Signaling Reduces the Susceptibility of Fragile X Knockout Mice to Audiogenic Seizures. *76*: 18–24.

Paradee, W., Melikian, H.E., Rasmussen, D.L., Kenneson, a, Conn, P.J., and Warren, S.T. (1999). Fragile X mouse: strain effects of knockout phenotype and evidence suggesting deficient amygdala function. Neuroscience *94*: 185–92.

Paribello, C., Tao, L., Folino, A., Berry-Kravis, E., Tranfaglia, M., Ethell, I.M., et al. (2010). Open-label add-on treatment trial of minocycline in fragile X syndrome. BMC Neurol. *10*: 91.

Park, S., Park, J.M., Kim, S., Kim, J.-A., Shepherd, J.D., Smith-Hicks, C.L., et al. (2008). Elongation factor 2 and fragile X mental retardation protein control the dynamic translation of Arc/Arg3.1 essential for mGluR-LTD. Neuron *59*: 70–83.

Peprah, E. (2012). Fragile X syndrome: the FMR1 CGG repeat distribution among world populations. Ann. Hum. Genet. *76*: 178–91.

Pieretti, M., Zhang, F., Fu, Y., Warren, S.T., Oostra, B.A., Caskey, C.T., et al. (1991). Absence of Expression in Fragile X Syndrome of the HIM-7 Gene. Cell *66*: 817–822.

Pietropaolo, S., Guilleminot, A., Martin, B., D'Amato, F.R., and Crusio, W.E. (2011). Genetic-background modulation of core and variable autistic-like symptoms in Fmr1 knock-out mice. PLoS One *6*: e17073.

Pixxuti, A., Refner, O., Richards, S., Victoria, M.F., Zhang, F., Eussen, B.E., et al. (1991). Identification of a gene (FMR-1) containing a CGG repeat coincident with a breakpoint cluster region exhibiting length variation in fragile X syndrome. Cell *65*: 905–914.

Qin, M., Kang, J., and Smith, C.B. (2002). Increased rates of cerebral glucose metabolism in a mouse model of fragile X mental retardation. Proc. Natl. Acad. Sci. U. S. A. *99*: 15758–63.

Qin, M., Kang, J., and Smith, C.B. (2005). A null mutation for Fmr1 in female mice: effects on regional cerebral metabolic rate for glucose and relationship to behavior. Neuroscience *135*: 999–1009.

Qin, M., Xia, Z., Huang, T., and Smith, C.B. (2011). Effects of chronic immobilization stress on anxiety-like behavior and basolateral amygdala morphology in Fmr1 knockout mice. Neuroscience *194*: 282–90.

Qiu, L.-F., Lu, T.-J., Hu, X.-L., Yi, Y.-H., Liao, W.-P., and Xiong, Z.-Q. (2009). Limbic epileptogenesis in a mouse model of fragile X syndrome. Cereb. Cortex *19*: 1504–14.

Rayasam, G.V., Tulasi, V.K., Sodhi, R., Davis, J.A., and Ray, A. (2009). Glycogen synthase kinase 3: more than a namesake. Br. J. Pharmacol. *156*: 885–98.

Ronesi, J. a, Collins, K. a, Hays, S. a, Tsai, N.-P., Guo, W., Birnbaum, S.G., et al. (2012). Disrupted Homer scaffolds mediate abnormal mGluR5 function in a mouse model of fragile X syndrome. Nat. Neurosci. *15*: 431–40, S1.

Rotschafer, S.E., Trujillo, M.S., Dansie, L.E., Ethell, I.M., and Razak, K. a (2012). Minocycline treatment reverses ultrasonic vocalization production deficit in a mouse model of Fragile X Syndrome. Brain Res. *1439*: 7–14.

Roy, S., Watkins, N., and Heck, D. (2012). Comprehensive analysis of ultrasonic vocalizations in a mouse model of fragile X syndrome reveals limited, call type specific deficits. PLoS One *7*: e44816.

Santoro, M.R., Bray, S.M., and Warren, S.T. (2012). Molecular mechanisms of fragile X syndrome: a twenty-year perspective. Annu. Rev. Pathol. *7*: 219–45.

Schaeffer, C., Bardoni, B., Mandel, J.L., Ehresmann, B., Ehresmann, C., and Moine, H. (2001). The fragile X mental retardation protein binds specifically to its mRNA via a purine quartet motif. EMBO J. *20*: 4803–13.

Schutt, J., Falley, K., Richter, D., Kreienkamp, H.J., and Kindler, S. (2009). Fragile X mental retardation protein regulates the levels of scaffold proteins and glutamate receptors in postsynaptic densities. J Biol Chem *284*: 25479–25487.

Sharma, A., Hoeffer, C. a, Takayasu, Y., Miyawaki, T., McBride, S.M., Klann, E., et al. (2010). Dysregulation of mTOR signaling in fragile X syndrome. J. Neurosci. *30*: 694–702.

Siomi, H., Choi, M., Siomi, M.C., Nussbaum, R.L., and Dreyfuss, G. (1994). Essential role for KH domains in RNA binding: impaired RNA binding by a mutation in the KH domain of FMR1 that causes fragile X syndrome. Cell *77*: 33–9.

Spencer, C.M., Alekseyenko, O., Serysheva, E., Yuva-Paylor, L. a, and Paylor, R. (2005). Altered anxiety-related and social behaviors in the Fmr1 knockout mouse model of fragile X syndrome. Genes. Brain. Behav. *4*: 420–30.

Strumbos, J.G., Brown, M.R., Kronengold, J., Polley, D.B., and Kaczmarek, L.K. (2010). Fragile X mental retardation protein is required for rapid experience-dependent regulation of the potassium channel Kv3.1b. J. Neurosci. *30*: 10263–71.

Sung, Y.J., Dolzhanskaya, N., Nolin, S.L., Brown, T., Currie, J.R., and Denman, R.B. (2003). The fragile X mental retardation protein FMRP binds elongation factor 1A mRNA and negatively regulates its' translation in vivo. J Biol Chem *278*: 15669–15678.

Sutcliffe, J.S., Nelson, D.L., Zhang, F., Pieretti, M., Caskey, C.T., Saxe, D., et al. (1992). DNA methylation represses FMR-1 transcription in fragile X syndrome. Hum. Mol. Genet. *1*: 397–400.

Thomas, A., Burant, A., Bui, N., Graham, D., Yuva-Paylor, L. a, and Paylor, R. (2009). Marble burying reflects a repetitive and perseverative behavior more than novelty-induced anxiety. Psychopharmacology (Berl). *204*: 361–73.

Thomas, A.M., Bui, N., Graham, D., Perkins, J.R., Yuva-Paylor, L. a, and Paylor, R. (2011). Genetic reduction of group 1 metabotropic glutamate receptors alters select behaviors in a mouse model for fragile X syndrome. Behav. Brain Res. *223*: 310–21.

Thomas, A.M., Bui, N., Perkins, J.R., Yuva-Paylor, L. a, and Paylor, R. (2012). Group I metabotropic glutamate receptor antagonists alter select behaviors in a mouse model for fragile X syndrome. Psychopharmacology (Berl). *219*: 47–58.

Todd, P.K., Mack, K.J., and Malter, J.S. (2003). The fragile X mental retardation protein is required for type-I metabotropic glutamate receptor-dependent translation of PSD-95. Proc. Natl. Acad. Sci. U. S. A. *100*: 14374–8.

Tsai, N.-P., Wilkerson, J.R., Guo, W., Maksimova, M. a, DeMartino, G.N., Cowan, C.W., et al. (2012). Multiple autism-linked genes mediate synapse elimination via proteasomal degradation of a synaptic scaffold PSD-95. Cell *151*: 1581–94.

Utari, A., Chonchaiya, W., Rivera, S.M., Schneider, A., Hagerman, R.J., Faradz, S.M.H., et al. (2010). Side effects of minocycline treatment in patients with fragile X syndrome and exploration of outcome measures. Am. J. Intellect. Dev. Disabil. *115*: 433–43.

Vanderklish, P.W., and Edelman, G.M. (2002). Dendritic spines elongate after stimulation of group 1 metabotropic glutamate receptors in cultured hippocampal neurons. Proc. Natl. Acad. Sci. U. S. A. *99*: 1639–44.

Veeraragavan, S., Bui, N., Perkins, J.R., Yuva-Paylor, L. a, Carpenter, R.L., and Paylor, R. (2011). Modulation of behavioral phenotypes by a muscarinic M1 antagonist in a mouse model of fragile X syndrome. Psychopharmacology (Berl). *217*: 143–51.

Veeraragavan, S., Graham, D., Bui, N., Yuva-Paylor, L. a, Wess, J., and Paylor, R. (2012). Genetic reduction of muscarinic M4 receptor modulates analgesic response and acoustic startle response in a mouse model of fragile X syndrome (FXS). Behav. Brain Res. *228*: 1–8.

Veeraragavan, S, Bui N, Perkins J, Yuva-Paylor L, P.R. (2011). The modulation of fragile X behaviors by the muscarinic M4 antagonist, tropicamide. Behav. Neurosci. *125*: 783–790.

Vinueza Veloz, M.F., Buijsen, R. a M., Willemsen, R., Cupido, a, Bosman, L.W.J., Koekkoek, S.K.E., et al. (2012). The effect of an mGluR5 inhibitor on procedural memory and avoidance discrimination impairments in Fmr1 KO mice. Genes. Brain. Behav. *11*: 325–31.

Volk, L.J., Pfeiffer, B.E., Gibson, J.R., and Huber, K.M. (2007). Multiple Gq-coupled receptors converge on a common protein synthesis-dependent long-term depression that is affected in fragile X syndrome mental retardation. J. Neurosci. *27*: 11624–34.

Vrij, F.M.S. de, Levenga, J., Linde, H.C. van der, Koekkoek, S.K., Zeeuw, C.I. De, Nelson, D.L., et al. (2008). Rescue of behavioral phenotype and neuronal protrusion morphology in Fmr1 KO mice. Neurobiol. Dis. *31*: 127–32.

Wan, L., Dockendorff, T.C., Jongens, T.A., Wan, L., Dockendorff, T.C., and Jongens, T.A. (2000). Characterization of dFMR1 , a Drosophila melanogaster Homolog of the Fragile X Mental Retardation Protein Homolog of the Fragile X Mental Retardation Protein.

Wang, H., Wu, L.-J., Kim, S.S., Lee, F.J.S., Gong, B., Toyoda, H., et al. (2008). FMRP acts as a key messenger for dopamine modulation in the forebrain. Neuron *59*: 634–47.

Waung, M.W., Pfeiffer, B.E., Nosyreva, E.D., Ronesi, J. a, and Huber, K.M. (2008). Rapid translation of Arc/Arg3.1 selectively mediates mGluR-dependent LTD through persistent increases in AMPAR endocytosis rate. Neuron *59*: 84–97.

Weiler, I.J., Spangler, C.C., Klintsova, A.Y., Grossman, A.W., Kim, S.H., Bertaina-Anglade, V., et al. (2004). Fragile X mental retardation protein is necessary for neurotransmitter-activated protein translation at synapses. Proc. Natl. Acad. Sci. U. S. A. *101*: 17504–9.

Westmark, C.J., and Malter, J.S. (2007). FMRP mediates mGluR5-dependent translation of amyloid precursor protein. PLoS Biol. *5*: e52.

Westmark, C.J., Westmark, P.R., Beard, A.M., Hildebrandt, S.M., and Malter, J.S. (2008). Seizure susceptibility and mortality in mice that over-express amyloid precursor protein. Int. J. Clin. Exp. Pathol. *1*: 157–68.

Westmark, C.J., Westmark, P.R., O'Riordan, K.J., Ray, B.C., Hervey, C.M., Salamat, M.S., et al. (2011). Reversal of fragile X phenotypes by manipulation of AβPP/Aβ levels in Fmr1KO mice. PLoS One *6*: e26549.

Wöhr, M., and Scattoni, M.L. (2013). Behavioural methods used in rodent models of autism spectrum disorders: current standards and new developments. Behav. Brain Res. *251*: 5–17.

Yan, Q.J., Rammal, M., Tranfaglia, M., and Bauchwitz, R.P. (2005). Suppression of two major Fragile X Syndrome mouse model phenotypes by the mGluR5 antagonist MPEP. Neuropharmacology *49*: 1053–66.

Yun, S.-W., Platholi, J., Flaherty, M.S., Fu, W., Kottmann, A.H., and Toth, M. (2006). Fmrp is required for the establishment of the startle response during the critical period of auditory development. Brain Res. *1110*: 159–65.

Yuskaitis, C.J., Mines, M. a, King, M.K., Sweatt, J.D., Miller, C. a, and Jope, R.S. (2010). Lithium ameliorates altered glycogen synthase kinase-3 and behavior in a mouse model of fragile X syndrome. Biochem. Pharmacol. *79*: 632–46.

Zalfa, F., Eleuteri, B., Dickson, K.S., Mercaldo, V., Rubeis, S. De, Penta, A. di, et al. (2007). A new function for the fragile X mental retardation protein in regulation of PSD-95 mRNA stability. Nat. Neurosci. *10*: 578–87.

Zalfa, F., Giorgi, M., Primerano, B., Moro, A., Penta, A. Di, Reis, S., et al. (2003). The fragile X syndrome protein FMRP associates with BC1 RNA and regulates the translation of specific mRNAs at synapses. Cell *112*: 317–27.

Zang, J.B., Nosyreva, E.D., Spencer, C.M., Volk, L.J., Musunuru, K., Zhong, R., et al. (2009). A mouse model of the human Fragile X syndrome I304N mutation. PLoS Genet. *5*: e1000758.

Zhang, Y., Venkitaramani, D. V, Gladding, C.M., Zhang, Y., Kurup, P., Molnar, E., et al. (2008). The tyrosine phosphatase STEP mediates AMPA receptor endocytosis after metabotropic glutamate receptor stimulation. J. Neurosci. *28*: 10561–6.

Zhang, Y.Q., Bailey, a M., Matthies, H.J., Renden, R.B., Smith, M. a, Speese, S.D., et al. (2001). Drosophila fragile X-related gene regulates the MAP1B homolog Futsch to control synaptic structure and function. Cell *107*: 591–603.

Zhou, X., Lin, D.S., Zheng, F., Sutton, M. a, and Wang, H. (2010). Intracellular calcium and calmodulin link brain-derived neurotrophic factor to p70S6 kinase phosphorylation and dendritic protein synthesis. J. Neurosci. Res. *88*: 1420–32.

CHAPTER 2: TYPE I ADENYLYL CYCLASE AS A POTENTIAL THERAPEUTIC TARGET FOR FRAGILE X SYNDROME

2.1 ABSTRACT

Fragile X syndrome (FXS) is the most common cause of inherited mental retardation and autism. It is caused by silencing of the FMR1 gene, which encodes the fragile X mental retardation protein (FMRP). The loss of FMRP, a translational repressor, leads to excessive translation of its mRNA targets, which results in altered synaptic signaling and the various phenotypes of FXS. Here we identify type 1 adenylyl cyclase (AC1), which is neurospecifically expressed, as an mRNA target whose translation is controlled by FMRP. Our results show that AC1 mRNA translation is upregulated in the absence of FMRP and is responsive to mGluR5 stimulation only in the presence of FMRP. Further using a genetic double knockout and acute inhibition of AC1 by NB001, our study demonstrates the rescue of several cellular and behavioral phenotypes in the Fmr1 knockout mouse model. Our study thus identifies AC1, a novel mRNA target whose translation is controlled by FMRP as a potential therapeutic target for FXS.

2.2 Introduction

FXS is the most common inherited form of mental retardation and a leading cause of autism (Santoro et al., 2012). It is caused by a trinucleotide repeat expansion in the *FMR1* (Fragile X mental retardation 1) gene, which causes transcriptional silencing of the gene resulting in reduced expression of its protein FMRP (Pixxuti et al., 1991). FMRP is an mRNA binding protein that selectively binds to mRNA and suppresses their translation (Darnell et al., 2001, 2011a). In the absence of FMRP the translation of these mRNAs is enhanced, leading to exaggerated protein synthesis (Zalfa et al., 2003; Westmark and Malter, 2007; Gross et al., 2010). A seminal study by Huber et al showed that the protein-synthesis dependent mGluR5 induced LTD is enhanced in *Fmr1* knockout (KO) mice (Huber et al., 2002). This led to the development of the "mGluR theory of FXS" which posits that many of the cellular, synaptic and behavioral phenotypes of FXS are due to exaggerated mGluR signaling (Bear et al., 2004). Subsequent studies have shown that genetic as well as pharmacological reduction of mGluR5 activity can rescue several abnormal phenotypes in the *Fmr1* KO mouse model (Yan et al., 2005; Dölen et al., 2007; de Vrij et al., 2008). Another valuable approach to identify new therapeutic targets for FXS has been to study the mRNA that is regulated by FMRP and mGluR signaling (Krueger and Bear, 2011). Indeed the

dysregulated translation of FMRP mRNA targets is vital to the phenotypes of FXS (Darnell and Klann, 2013; Sethna et al., 2013). Here we observed that the neurospecific, Ca^{2+}/Calmodulin stimulated type 1 adenylyl cyclase (AC1) mRNA is a top FMRP binding target in three high-throughput studies (Brown et al., 2001; Darnell et al., 2011b; Ascano et al., 2012). Since AC1 is stimulated by Ca^{2+} and calmodulin which are downstream to the Gq-coupled signaling associated with mGluR5, we hypothesized that AC1 mRNA translation would be regulated by FMRP and be responsive to mGluR5 signaling. We further hypothesized that if AC1 expression was elevated in *Fmr1* KO mice, several phenotypic abnormalities in these mice would be corrected by genetic or pharmacological inhibition of AC1.

2.3 Materials and Methods

2.3.1 Animals

WT C57BL/6 mice were obtained from Jackson Labs. *Fmr1* KO C57BL/6 mice were obtained from Dr. C. Westmark and were crossed into the lab WT C57BL/6 strain for at least 5 generations. AC1 KO C57BL/6 mice were previously reported (Wu et al., 1995). DKO mice were generated by crossing *Fmr*1 KO males with AC1 KO females, followed by crossing of the female progeny with AC1 KO males. This cross-yielded some DKO

males and AC1-/-, *Fmr1*+/- females. Brother-sister crossing of the above progeny generated DKO females. Animals were housed in the university laboratory animal research facility and all the manipulations were in compliance with the guidelines of Institutional Animal Care and Use Committee at Michigan State University. The mice had ad libitum access to water and food and were housed under 12 h dark/light cycles.

2.3.2 Biochemical analyses

WT and *Fmr1* KO primary hippocampal neurons were established as described in (Zhou et al., 2010) and grown to DIV14 for western blotting and RNA extraction. Neurons were treated with 100mM DHPG (RS)-3,5-Dihydroxyphenylglycine, Tocris Cat #0342) for various time points before they were lysed in Buffer H (50 mM b-glycerophosphate, 1.5 mM EGTA, 0.1 mM Na3VO4, 1 mM DTT). The concentration of protein in the extracts was determined by Bradford assay and 20ug protein was loaded on the 4-20% SDS-PAGE gel (Invitrogen) and transferred to nitrocellulose membranes. The membranes were probed with anti-Adcy1 antibody (Sigma Cat #SAB4500146) at diluted in 5% BSA at 1:1000 and anti-b-actin antibody (Sigma Cat #A1978). Western blot signal intensities were quantitated using ImageJ (NIH, MD, USA). Protein samples from brain tissues were processed similarly. DIV8 Fmr1 KO hippocampal neurons were used for luciferase assays. Neurons were transfected using Lipofectamine 2000 (Life Technologies Cat

#11668027) 48 hours before determining luciferase activity using the dual glow luciferase assay protocol (Promega Cat #E2920). WT FMRP PC-Flag 2.17 and pLuci3 plasmids were kindly provided by Dr. Yue Feng (Emory University). Adcy1 3' UTR constructs were cloned into the pLuci3 vector between the KpnI and EcoRI sites. miRIDIAN microRNA mouse mmu-miR-100-5p-hairpin inhibitor was purchased from Thermo Scientific (Cat # IH-310567-07-0005) and transfected using Lipofectamine 2000 along with the other plasmids. Protein synthesis was determined by SuNSET method (Schmidt et al., 2009; Bhattacharya et al., 2012). DIV 8 WT and Fmr1 KO hippocampal neurons were pre-treated with various doses of NB001 (5-{[2-(6-Amino-9H-purin-9-yl)ethyl]amino}-1-pentanol) from Toronto Research Chemicals Inc. (Cat # A628913) for 30-min before treating with 5 ug/ml puromycin (Sigma, Cat #P8833) for 30 min. Cells were lysed processed for western blotting as described above. The membranes were probed with anti-puromycin antibody (KeraFAST, Cat # EQ0001, 1:1000). b-actin was used as the loading control. ImageJ was used to measure the combined signal intensity of proteins with molecular weights ranging from 15 to 250 kDa.

2.3.3 Drugs and treatments

NB001 was dissolved in water to give a 25mM stock solution. The stock was diluted in saline and i.p. injected into mice at 1mg/kg body weight. In all cases except for open

field, the drug was administered 1-hour before testing or before training for passive avoidance. The drug was administered 30-min before introducing the mouse to the open field chamber. Control mice were treated similarly but injected with saline.

2.3.4 Behavioral testing

Open field test. 2 month old male mice were placed in the center of a chamber measuring 28cm X 28 cm with 34 cm high walls and were allowed to move freely for 2-hours. Ambulatory movement time, ambulatory movement distance, number of center entries and the time spent in different areas of the chamber were determined at every 10-min interval during the 2-hour testing period by the TruScan Photo Beam Activity System (Coulbourn Instruments, Whitehall, PA).

Light-dark test. 3-4 month old male mice were placed in the dark half of the chamber (Coulbourn Instruments) and the trap door was opened after 1-min. The mice were allowed to move freely between the two chambers for 5-min. The time spent in each chamber and the number of crossings into the lit side was recorded.

Passive avoidance. 3-4 month old male mice were introduced into the lit half of the chamber (Coulbourn Instruments) and allowed to explore it for 1-min before the trap door was opened. The trap door was closed as soon as the mouse entered the dark chamber. A foot shock (0.7mA for 2s) was immediately delivered. The mouse was

removed from the dark chamber and returned to its home cage 30-seconds after the foot shock was administered. The mice were tested 24- hours after training. During testing, the mouse was put in the lit chamber and crossover latency to the dark chamber was measured. The cutoff for crossover latency was set at 600-seconds.

Audiogenic seizure testing. 21-24 day old male and female mice were placed in a box of dimensions 30 cm X 17 cm and 12 cm high walls with a flat plastic lid. A personal alarm (from Streetwise, item # SWPDAL) was taped to the lid of the box and wired to a DC power supply to keep the sound amplitude constant. The mouse was allowed to acclimatize to the box for 5-min following which a 120 dB sound was emitted from the alarm for 2-min. The number of mice undergoing seizure within the 2-min period was counted. Audiogenic seizure was classified into different stages: wild-running, clonic/tonic seizure and death (as classified in Dolen et al., 2007)

Marble burying test. 2-3 month old male mice were placed in a 27 cm X 15 cm box with 12cm high walls and 7.6 cm depth of bedding for 1 hour prior to the test. The mouse was then briefly removed from the testing box and 15 marbles were evenly arranged in a 5 X 3 pattern on the surface of the bedding. The mouse was reintroduced into its testing box and was allowed to bury marbles for 10-min. At the end of the testing period,

the mouse was removed from the box and the number of marbles that were fully buried, partially buried and left on the surface was counted.

Social interaction test. 2-3 month old male mice were placed in a 3-chambered social interaction box (cmX cmX cm) and allowed to explore freely for 5-min. If a mouse displayed a strong preference for one side during this time, it was omitted from the study. The test mouse was placed in the center chamber and the entryways to the side chambers were blocked. A novel male WT mouse was introduced in a confined space in either of the side chambers. The entryways were then opened and the activity of the test mouse was recorded. Time spent in each of the chambers, number of entries between the chambers and time spent sniffing the novel mouse versus the empty enclosure in the opposite chamber was recorded.

2.3.5 Dendritic spine analysis

2 month old mouse brains were processed according to manufacture instructions using Fd Rapid GolgiStain Kit (FD NeuroTechnologies. Inc. Cat # PK401). 150um thick sections were cut using vibratome and images were collected using the 100X objective on an Olympus FluoView 1000 microscope. Spines starting from 50um from the cell body up to 100um were analyzed along the apical dendrites of CA1 and primary visual

cortex pyramidal neurons. Spines were classified as stubby, thin and mushroom shaped using NeuronStudio Version 0.9.92 software.

2.3.6 NB001 toxicology studies

2-3 month old male mice were dosed by oral gavage or intraperitoneally twice daily with either vehicle or 100 mg/kg NB001 over 2 weeks. Clinical observations were performed twice daily and body weights will be collected at various days of the dosing. Mice were euthanized on the day following the dosing period and blood was collected for clinical pathology (Diagnostic Center for Population and Animal Health, Michigan State University). The liver and kidney were collected at necropsy and tissues were fixed in 10% buffered formalin (INVIVO facility at Michigan State University). H&E staining was performed on the tissues and tissue morphology was observed.

2.3.7 NB001 pharmacokinetic studies

20 mg/kg NB001 was given by IP injection. Mice were euthanized at various time points and 0.5-0.8 ml of blood was drawn from a cardiac puncture into a 1 ml syringe, which was pretreated with NaHeparin. The blood was collected into 1.5 mL microfuge tubes coated with NaHeparin and put on ice immediately. Samples were centrifuged at 15,000 rpm for 15 min. Blood plasma was collected from the upper layer, leaving the blood cells behind in the microfuge tube. The plasma was frozen at -80ºC for later analysis. Brains

were taken out and weighed out immediately. Brains were frozen at -80ºC for later preparation and analysis. The samples were subjected to LC/MS/MS with Turbo-IonsprayTM Interface used in the positive ion-mode. LC/MS/MS experiment specifications- column：5 cm x 4.6 mm I.D., packed with 5.0 μm C18 (XBridge, Waters), mobile phase A- 0.1% formic acid in purified water, mobile phase B- 0.1% formic acid in acetonitrile, flow rate 1ml/min, injection volume-5ul, run time 6.5 min (Pharmacokinetics Core at University of Michigan). Mouse liver microsome stability assay was performed at the Pharmacokinetics Core at University of Michigan.

2.3.8 Statistical analysis

One-way ANOVA followed by post hoc LSD (least significant difference) test or Student's t-test was used to compare multiple groups. Student t-test was used to compare two groups. Two-way ANOVA followed by Student's t test or LSD test was used to compare different groups in the luciferase assay as well as behavior studies using NB001 and the SUnSET assay. Chi-square test was used to analyze AGS data. One-way and Two-way repeated measures ANOVA was used for open field data with DKO and NB001 respectively. Data were expressed as the mean ± SEM. Differences with p values < 0.05 were considered significant. SPSS 11.5 for Windows (IBM) was used for all data analysis.

2.4 Results

2.4.1 AC1 mRNA translation is elevated in the *Fmr1* KO hippocampus

The translation of several mRNA targets of FMRP is dysregulated in the *Fmr1* KO mouse brain (Table 2). Since AC1 mRNA was identified as a top FMRP binding target in three highthroughput studies, I investigated whether AC1 mRNA translation was altered in the brains of *Fmr1* KO mice. Hippocampal lysates from *Fmr1* KO mice showed higher expression of AC1 protein ($p < 0.05$), whereas protein levels were similar in cortical lysates (Figure 2A). Since the AC1 mRNA levels in the *Fmr1* KO lysates were similar to WT (Figure 2B), we tested whether AC1 mRNA was undergoing increased active translation in the absence of FMRP. Using linear sucrose gradient fractionation, we observed that AC1 mRNA was more abundant in the actively translating polyribosome fractions in the *Fmr1* KO hippocampal lysate than in WT lysate (Figure 2C and D, $p < 0.05$) (Dr. Wei Feng and Dr. Yue Feng). These results show that the basal level of AC1 protein is overabundant in the *Fmr1* KO hippocampus due to excessive translation of AC1 mRNA in the absence of FMRP.

To test whether mGluR5 stimulation led to translation of AC1, I treated DIV14 hippocampal neurons with 100μM DHPG. Rapid increase in AC1 protein levels, was observed in WT (Figure 3A $p < 0.05$) but not *Fmr1* KO neurons (Figure 3C). As a control

for the health of the neurons and the efficacy of DHPG, I measured the phosphorylation of ERK1/2, which is known to be phosphorylated upon DHPG stimulation. DHPG caused a significant upregulation in ERK1/2 phosphorylation in both WT and *Fmr1* KO neurons (Figure 3B and D, $p < 0.05$). Interestingly, different studies show that ERK1/2 may or may not be phosphorylated in *Fmr1* KO hippocampal slices upon DHPG stimulation (Prince, T et al., 2007, Ronesi J and Huber K, 2008). My study with DIV14 hippocampal neurons shows that ERK1/2 is phosphorylated upon DHPG treatment in *Fmr1* KO neurons but not as significantly as in WT neurons (Figure 3B and D). Together, these data show that mGluR5 stimulation and FMRP regulate AC1 protein expression.

2.4.2 FMRP regulates AC1 translation by microRNA mediated mechanisms

To investigate how FMRP could regulate AC1 mRNA translation, I looked at FMRP-mediated microRNA (miRNA) mechanisms. FMRP is known to interact with proteins of the miRNA pathway and also interacts with specific miRNA (Jin et al., 2004). Using TargetScanMouse (Release 6.2: June 2012), I searched whether known FMRP binding miRNA had target sites on the mouse AC1 3' UTR. I narrowed down five prospective miRNA sites in the 3' UTR (Figure 4A). For further investigation, a firefly-luciferase reporter construct with either the proximal part (UTR1) or the distal part

(UTR2) of the 3' UTR was expressed in cultured *Fmr1* KO hippocampal neurons (Figure 4A). I observed FMRP dependent reduction in luciferase expression specifically in the UTR2 containing neurons (Figure 4B, $p < 0.05$). Since UTR2 contained three prospective miRNA sites, I transfected *Fmr1* KO neurons with luciferase-UTR2 constructs with 21bp deletions in each of the miRNA sites (refer to Figure 4A). While deletion of the other two miRNA binding sites had no FMRP dependent effect, deletion of the miR100 site abolished the ability of FMRP to reduce luciferase expression (Figure 4C). To further confirm the involvement of miR100 in FMRP dependent translation of the luciferase-UTR2 reporter, I co-transfected *Fmr1* KO neurons with anti-miR100 to inhibit miR100 activity. Inhibiting miR100 led to a dramatic increase in the reporter expression only in the presence of FMRP (Figure 4D, $p < 0.01$). Further, anti-miR100 could not increase reporter expression when co-transfected with FMRP and a luciferase-UTR2 construct with a deletion in the miR100 binding site (Figure 4D). Together these data show that FMRP suppresses translation of AC1 via its 3' UTR, further, an intact miR100 binding site and miR100 activity is required for this inhibitory effect.

2.4.3 Rescue of several FXS phenotypes in DKO mice

Since AC1 expression was enhanced in *Fmr1* KO mice, we wanted to test whether dampening AC1 activity would be of therapeutic value for fragile X syndrome.

As the major mouse model for studying FXS, the *Fmr1* KO mouse recapitulates many of the symptoms seen in human fragile X patients (Sethna et al., 2013). I dampened AC1 activity in the *Fmr1* KO mouse by generating AC1, *Fmr1* double-knockout mice (DKO). I first tested audiogenic seizure (AGS) in *Fmr1* KO mice which when exposed to a loud sound experience seizure (Chen and Toth, 2001). When exposed to a 120dB sound, *Fmr1* KO mice showed the various stages of AGS whereas WT and AC1 KO mice showed no seizure (Table 3). DKO mice showed greatly reduced seizure occurrence and there were no seizure- associated deaths in these mice (Table 3, $p < 0.05$). I observed repetitive/hyperactive behavior in *Fmr1* KO mice in the marble- burying test, where *Fmr1* KO buried more marbles than WT mice (Figure 5A, $p < 0.001$). This behavior was restored to WT levels in the DKO mice, while AC1 KO showed normal marble burying behavior (Figure 5A). I further tested for repetitive/hyperactive behavior using the light-dark test. *Fmr1* KO mice made more transitions between the light and dark chambers (Figure 5B, $p < 0.001$) while time spent in the light chamber was similar to WT (Figure 5C). This behavior was rescued in the DKO mice while the AC1 mutation had no effect on this behavior (Figure 5B and C). When tested for hyperactivity with the open-field test, both *Fmr1* KO and AC1 KO mice displayed higher ambulatory distance (Figure 6A, $p < 0.001$) and more entries (Figure 6B, $p < 0.001$) into the center area than

WT mice and this seemed to have an additive effect on the DKO mice whose ambulatory distance and center entries was higher than AC1 and *Fmr1* KO mice (Figure 6A and B, $p < 0.001$). I then examined whether the social interaction deficits in *Fmr1* KO mice would be corrected in the DKO mice. As expected (Mines et al., 2010), *Fmr1* KO mice spent less time sniffing the novel mouse in the social interaction test when compared to the WT (Figure 6C, $p < 0.001$) and this behavior was completely rescued in the DKO mice (Figure 6C) while AC1 KO showed a normal phenotype. All the genotypes spent considerably more time sniffing the novel mouse rather than the empty enclosure (Figure 6D, $p < 0.05$). To test for cognitive deficits, I trained the mice with passive avoidance training. While all the groups showed similar crossover latency during training, *Fmr1* KO mice had a significantly lower crossover latency compared to WT when tested 24 hours later (Figure 7, $p < 0.005$). AC1 KO mice showed a slight decrease in crossover latency but this was not statistically significant compared to WT mice while the DKO mice were similar to *Fmr1* KO (Figure 7), that is, there was no rescue in this behavior. Dendritic spine abnormalities are a robust phenotype seen in *Fmr1* KO mice. Here I observed significantly higher total spine density on the apical dendrites of *Fmr1* KO pyramidal neurons in the CA1 area of the hippocampus (Figure 8A and B, $p < 0.05$). This phenotype was corrected in the DKO neurons, while there

was no difference between AC1 KO and WT spine densities (Figure 8A and B). Together, these results demonstrate that genetic knockout of AC1 in the *Fmr1* KO mouse rescues several well-characterized behavioral deficits and the dendritic spine abnormality in FXS model mice.

2.4.4 Pharmacological rescue of FXS phenotypes by an AC1 inhibitor

Encouraged by the above results we tested whether acute suppression of AC1 activity by the newly discovered antagonist NB001 (Wang et al., 2011) could rectify behavioral and cellular abnormalities in the *Fmr1* KO mouse. *Fmr1* KO mice receiving 1mg/kg NB001 intraperitoneally, 60-minutes before exposure to a 120dB sound, experienced significantly fewer occurrences of AGS (Table 4, $p < 0.05$) when compared to vehicle (saline) injected *Fmr1* KO mice. WT mice injected with vehicle or NB001 did not show AGS (Table 4). Acute injection 1mg/kg NB001 also restored marble burying behavior in *Fmr1* KO mice to WT levels, although it seems to have a mild but not statistically significant effect on decreasing the number of marbles buried in WT injected mice (Figure 9A). *Fmr1* KO mice injected with NB001 (1mg/kg) showed reduced hyperactive/repetitive transitions between the light-dark chambers, which was equivalent to the number seen in vehicle injected WT mice (Figure 9B). NB001 did not have an effect on WT mice in this test. Surprisingly, NB001 (1mg/kg) injected WT mice

did not show increased activity in the open field test in contrast to that seen in AC1 KO mice (Figure 10A and B). Concurrently, NB001 (1mg/kg) administration prior to testing reduced the higher *Fmr1* KO ambulatory activity to WT levels (Figure 10A and B, $p < 0.001$). Collectively, these results show that acute intraperitoneal administration of 1mg/kg NB001 rescues the repetitive/hyperactive phenotype observed in *Fmr1* KO mice. In the social interaction test, *Fmr1* KO mice injected with 1mg/kg NB001, 60-minutes before testing, spent significantly more time sniffing the novel mouse, almost comparable to WT vehicle injected levels (Figure 10C, $p < 0.005$). When administered before passive avoidance training, 1mg/kg NB001 surprisingly rescued the memory deficit observed in *Fmr1* KO mice (Figure 11). Interestingly, WT mice injected with NB001 showed very mild but not statistically significant memory impairment in the passive avoidance test (Figure 11). Since enhanced basal protein synthesis is thought to underlie much of the pathophysiology of FXS and its correction to normal levels is a potential strategy to treat FXS (Darnell and Klann, 2013), I studied whether NB001 treatment could normalize this abnormality in *Fmr1* KO hippocampal neurons. Upon labeling newly synthesized proteins with puromycin using the SUnSET method (Schmidt et al., 2009; Bhattacharya et al., 2012), I observed increased basal protein synthesis in DIV 8 *Fmr1* KO neurons as compared to WT neurons (Figure 12A and B, $p < 0.05$).

Fmr1 KO neurons treated with various doses of NB001 30-minutes prior to the start of the assay showed protein levels similar to WT neurons, whereas, NB001 had no effect on WT basal protein synthesis (Figure 12B). These results together demonstrate that acute administration of NB001 can correct several behavioral deficits as well as excessive protein synthesis in the *Fmr1* KO mouse.

2.4.5 NB001 toxicity and pharmacokinetics

In our study, NB001 showed promising therapeutic value in ameliorating FXS phenotypes, however, since it is a newly discovered drug, its toxicity has not been studied. Here we performed some basic toxicology tests in WT male mice by chronically administering 100mg/kg- a dose ten-times higher than needed for therapeutic efficacy in mice; twice daily through oral gavage or intraperitoneally for 14 days. Neither oral nor intraperitoneal NB001 administration affected body weight (Figure 13A), heart/lung, kidney and liver weight (Figure 13B) (Diagnostic center for Population and Animal Health) as well as kidney and liver histopathology (Figure 13C). The drug also had no effect on blood levels of various electrolytes and other proteins (Table 5) (data provided by Diagnostic center for Population and Animal Health). Together these studies show that NB001 may be a relatively safe drug when tested in mice. Further we show that NB001 is very stable in the mouse liver microsome assay (Figure 14A) and can cross

the blood-brain barrier to enter the brain (Figure 14B) (Pharmacokinetics core, University of Michigan).

2.5 Discussion

Here I validate that Ca2+/Calmodulin dependent type 1 adenylyl cyclase translation is controlled by FMRP via miR100 binding to its 3' UTR. Further we observe that AC1 protein is over abundant in the hippocampus of FXS mice due to increased translation of its mRNA and is expressed rapidly upon mGluR5 stimulation only in the presence of FMRP. This is consistent with numerous studies, which show that proteins regulated by FMRP have increased basal levels in the FXS mouse and are therefore not responsive to mGluR stimulation (Westmark and Malter, 2007; Park et al., 2008; Goebel-Goody et al., 2012). It is interesting to note that cyclic AMP (cAMP) levels are lower in patients with FXS (Kelley et al., 2007), this may be a compensatory mechanism to counteract the higher mGluR signaling in the absence of FMRP. Since AC1 is expressed only in the central nervous system (CNS), it provides a unique pharmacological target to treat CNS disorders without its effects on peripheral organs (Wang and Storm, 2003). AC1 KO mice have normal growth, longevity, motor coordination and have no detectable anatomical or morphological differences in their

brains except for lacking barrel patterning in the sensory-motor cortex (Abdel-Majid et al., 1998). AC1 KO mice also show normal physiological functions of acute pain, have normal long-lasting LTP, normal long-term memory for several forms of fear memory, and perform normally in the Morris water maze (Wang and Storm, 2003). In the current study, AC1 KO mice exhibit behavior comparable to WT mice except in the open field test where they show hyperactivity. Using a battery of behavioral tests that are key phenotypes of FXS mice, I show that knocking out AC1 in the *Fmr1* KO mice rescue several phenotypes. DKO mice have markedly fewer occurrences of AGS and no AGS induced deaths. Autism-like symptoms such as repetitive/hyperactive behavior and social deficit that are seen in *Fmr1* KO mice are corrected in the DKO mice. Further, pharmacological inhibition of AC1 using NB001 also corrected these phenotypes, in addition to correcting the learning deficit in *Fmr1* KO mice. Interestingly, differences in behavior between the DKO mice and NB001 injected *Fmr1* KO mice were seen in the open field test and the passive avoidance test. These differences may be attributed to one or more of several reasons why a genetic knockdown and pharmacological inhibition of the same target may produce varying phenotypes (Knight and Shokat, 2007). It is unlikely that NB001 inhibited other ACs in our study because we used a low dose and the specificity of NB001 for AC1 is at least ten times higher than for other ACs

(Wang et al., 2011). My study also shows that NB001 can reduce the enhanced basal protein levels in *Fmr1* KO neurons, a cellular phenotype that is thought to be critical to the pathophysiology of FXS (Darnell and Klann, 2013). Since the abnormal dendritic spine phenotype was corrected in DKO mice, it would be interesting to measure the spine phenotype upon prolonged exposure to NB001. Finally, our study demonstrates that prolonged administration of a 100 fold higher dose of NB001 did not have measurable toxic effects on mice. Very importantly, NB001 could pass through the blood brain barrier and be detected in the brain following i.p. injection. This together with the observation that NB001 did not produce any measurable behavior deficits and had no toxic effects makes it an attractive drug target to pursue for future studies. While there has been much success in identifying drug targets for FXS in a preclinical setting, there is limited success in clinical trials, resulting in the recent withdrawal of two promising drugs (STX209 and AFQ056). This highlights the importance of continuing to investigate deeper into the molecular mechanisms underlying FXS and identifying new therapeutic targets. In conclusion, our study identifies AC1 as a novel and promising therapeutic target for FXS.

APPENDIX

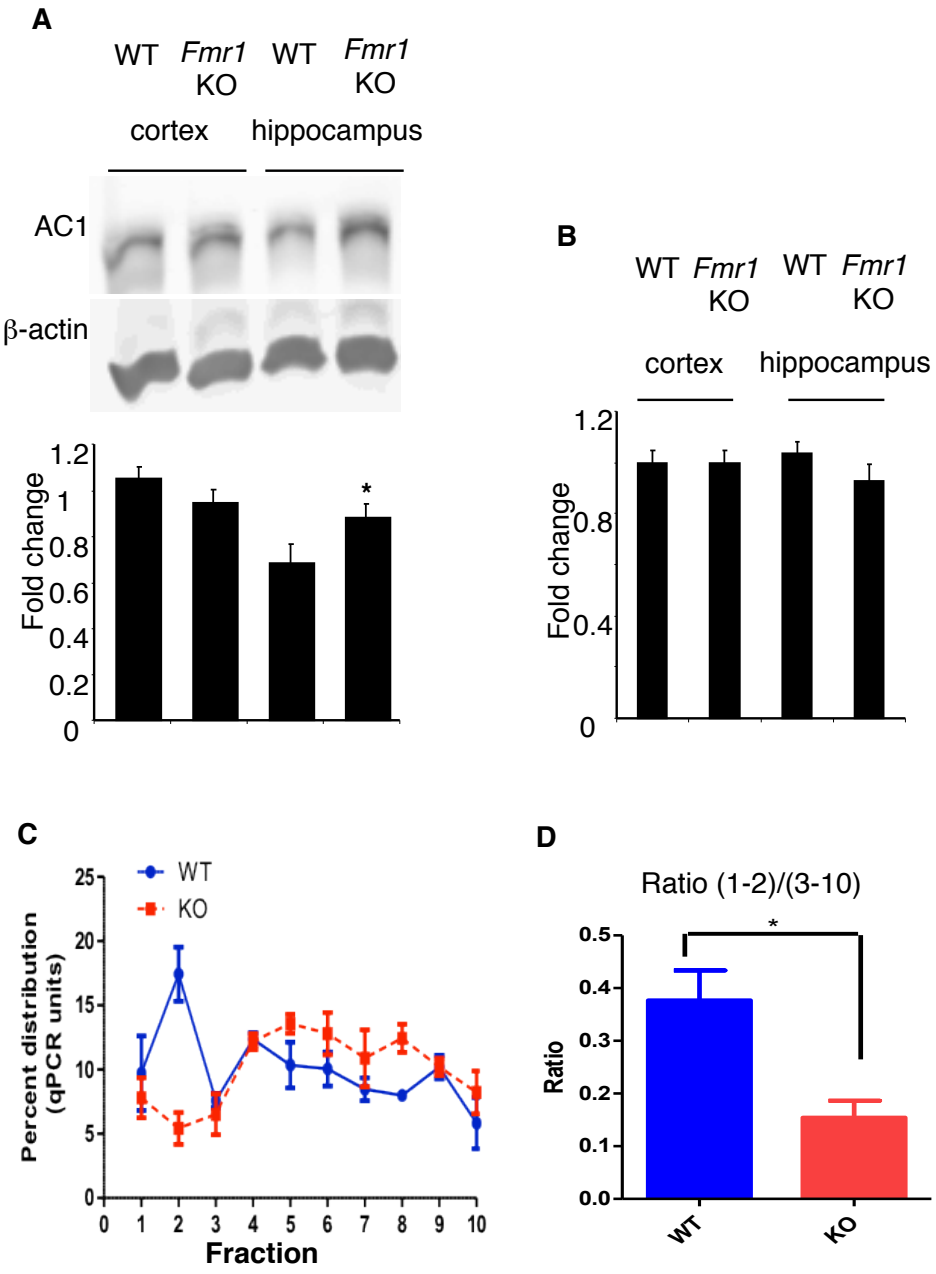

Figure 2: FMRP represses AC1 translation. (A) Western blot of AC1 protein from cortex and hippocampus of 21 day old WT and *Fmr1* KO mice (n=6 per group), representative image top panel, quantification bottom. AC1 protein levels are normalized to β-actin and expressed as relative level to the WT cortex group. * indicates

Figure 2 (cont'd)

$p < 0.05$ between WT and indicated group determined by Student's t-test. (B) AC1 mRNA quantitated by qPCR from cortical and hippocampal RNA preparations from 21 day old WT and *Fmr1* KO mice. AC1 values normalized to GAPDH and expressed as levels relative to the WT cortex group, (n=6 per group) (C) Percent distribution of AC1 mRNA determined by qPCR using ribosome fractions obtained from linear sucrose gradient centrifugation of hippocampal lysates from WT (n=3) and *Fmr1* KO (n=3) mice**.** (D) Ratio of AC1 mRNA in fractions 1-2 and fractions 3-10 in WT and *Fmr1* KO hippocampal lysates. * indicates $p < 0.05$ between WT and indicated group determined by Student's t-test.

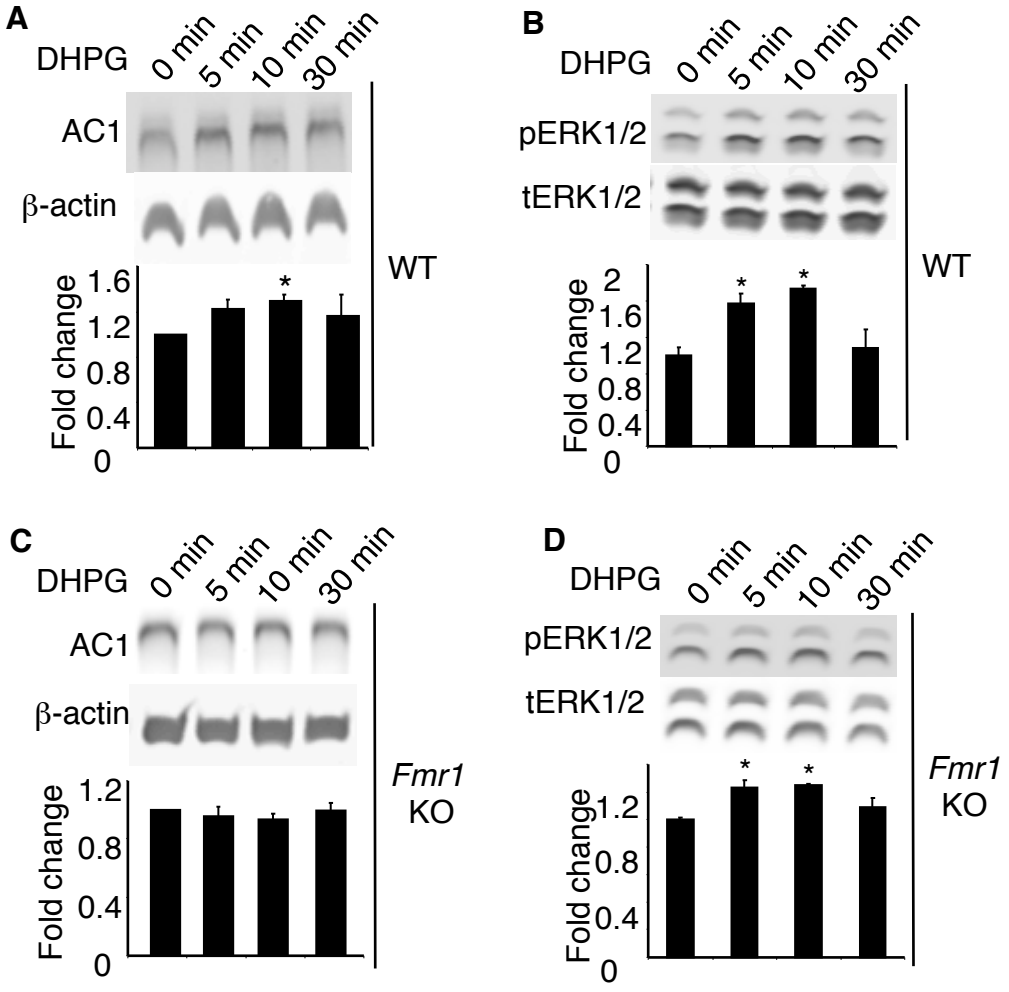

Figure 3: Rapid translation of AC1 upon mGluR5 activation in the presence of FMRP. (A- D) Western blot of AC1 (A,C) and phospho-ERK1/2 (B,D) from DIV14 WT and *Fmr1* KO hippocampal neurons (n=6 per group) treated with 100μM DHPG for various time points, representative image top panel, quantification bottom. AC1 protein levels are normalized to β-actin and pERK1/2 levels are normalized to total-ERK1/2. All

Figure 3 (cont'd)

values are represented relative to the 0 min time point. * indicates $p < 0.05$ between control and indicated group determined by one-way ANOVA and LSD test.

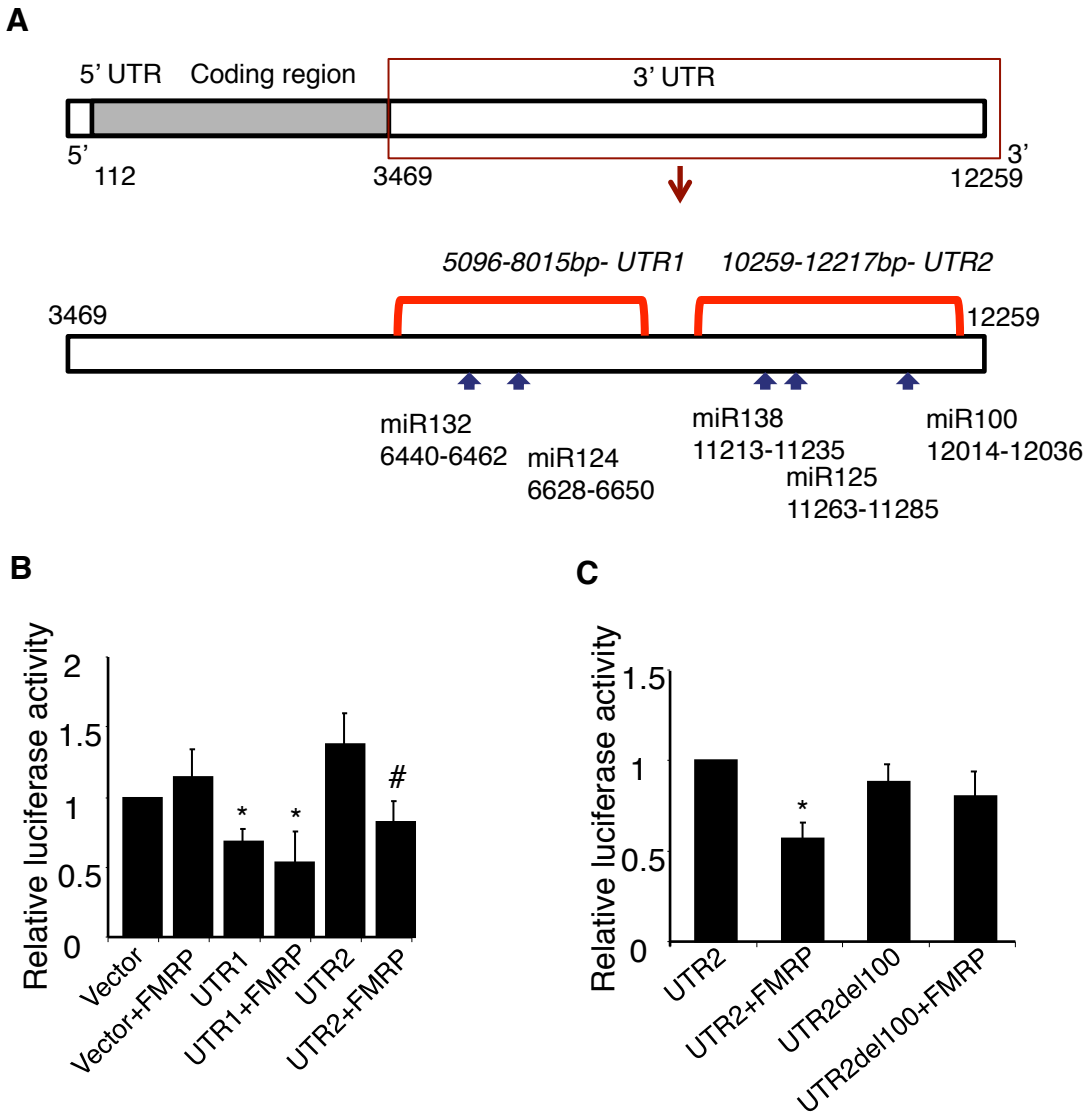

Figure 4: FMRP controls AC1 translation by microRNA-mediated mechanisms. (A) Schematic representation of AC1 (*Adcy1*) mRNA 3'UTR. Top. Mouse *Adcy1* mRNA, numbers below represent base-pairs (bp) from the 5' end. Bottom. 3' UTR of *Adcy1* starting at 3469 to 12259 bp. The UTR1 fragment from 5096 to 8015 bp has an miR132 binding site from 6440 to 6462 bp and an miR124 binding site from 6628 to 6650 bp.

Figure 4 (cont'd)

D

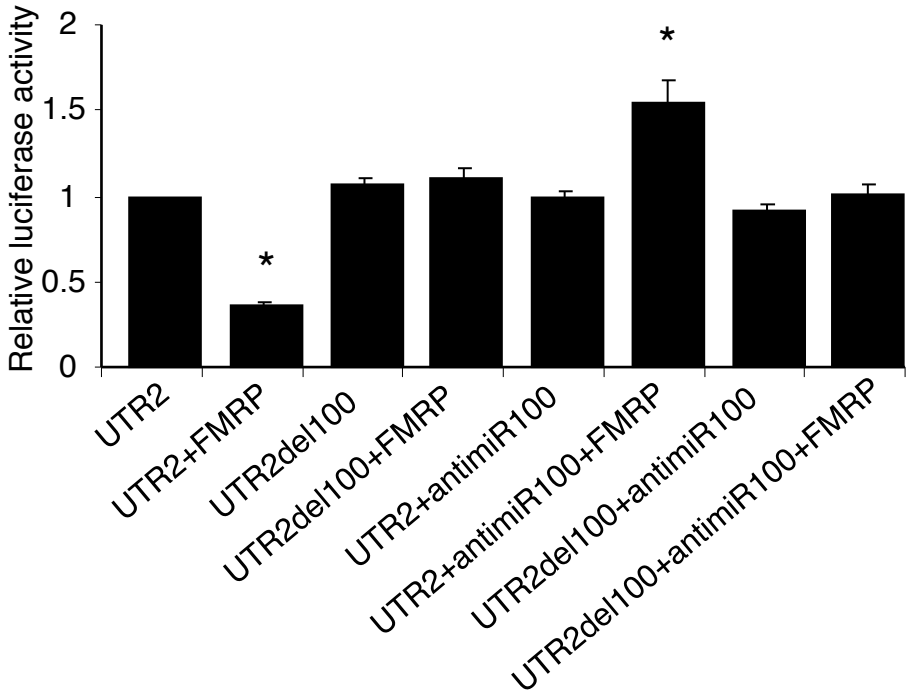

The UTR2 fragment from 10259 to 12217 bp has one miR138 binding site from 11213 to 11235 bp, one miR125 site from 11263 to 11285 bp and an miR100 site from 12014 to 12036 bp. (B) Relative firefly/renilla luciferase activity from DIV8 *Fmr1* KO hippocampal neurons transfected with UTR1 or UTR2 constructs with or without FMRP (n=6 per group). Luciferase activity represented relative to the Vector group. * indicates $p < 0.05$ between control and indicated group, # indicates $p < 0.05$ between UTR2 and indicated group determined by two-way ANOVA followed by LSD test. (C) Relative luciferase activity in DIV8 *Fmr1* KO hippocampal neurons transfected with UTR2 or

Figure 4 (cont'd)

UTR2del100 constructs with or without FMRP (n=6 per group). Values expressed relative to UTR2. * indicates $p < 0.05$ between UTR2 and indicated group determined by two-way ANOVA and Student's t-test. (D) Relative luciferase activity in DIV8 *Fmr1* KO hippocampal neurons transfected with UTR2 or UTR2del100 constructs along with antimiR100 with or without FMRP (n=6 per group). Values normalized to the UTR2 group. * indicates $p < 0.05$ between UTR2 and indicated group, # indicates $p < 0.05$ between UTR2+antimiR100 and indicated group determined by two-way ANOVA and LSD test.

Table 3: Rescue of audiogenic seizure in DKO mice

	n	% Wild running	% Clonic/ Tonic seizure	% Death
WT	10	0	0	0
Fmr1 KO	27	68.5	62.6	13.7
AC1 KO	10	0	0	0
DKO	27	3.7	0	0

Table 3: Audiogenic seizure (AGS) measured in 21-24 day WT, *Fmr1* KO, AC1 KO and DKO mice. Percent of mice experiencing different stages of AGS- wild running, clonic/tonic seizure and death was recorded. Chi-square test confirmed $p < 0.05$ between *Fmr1* KO and DKO groups.

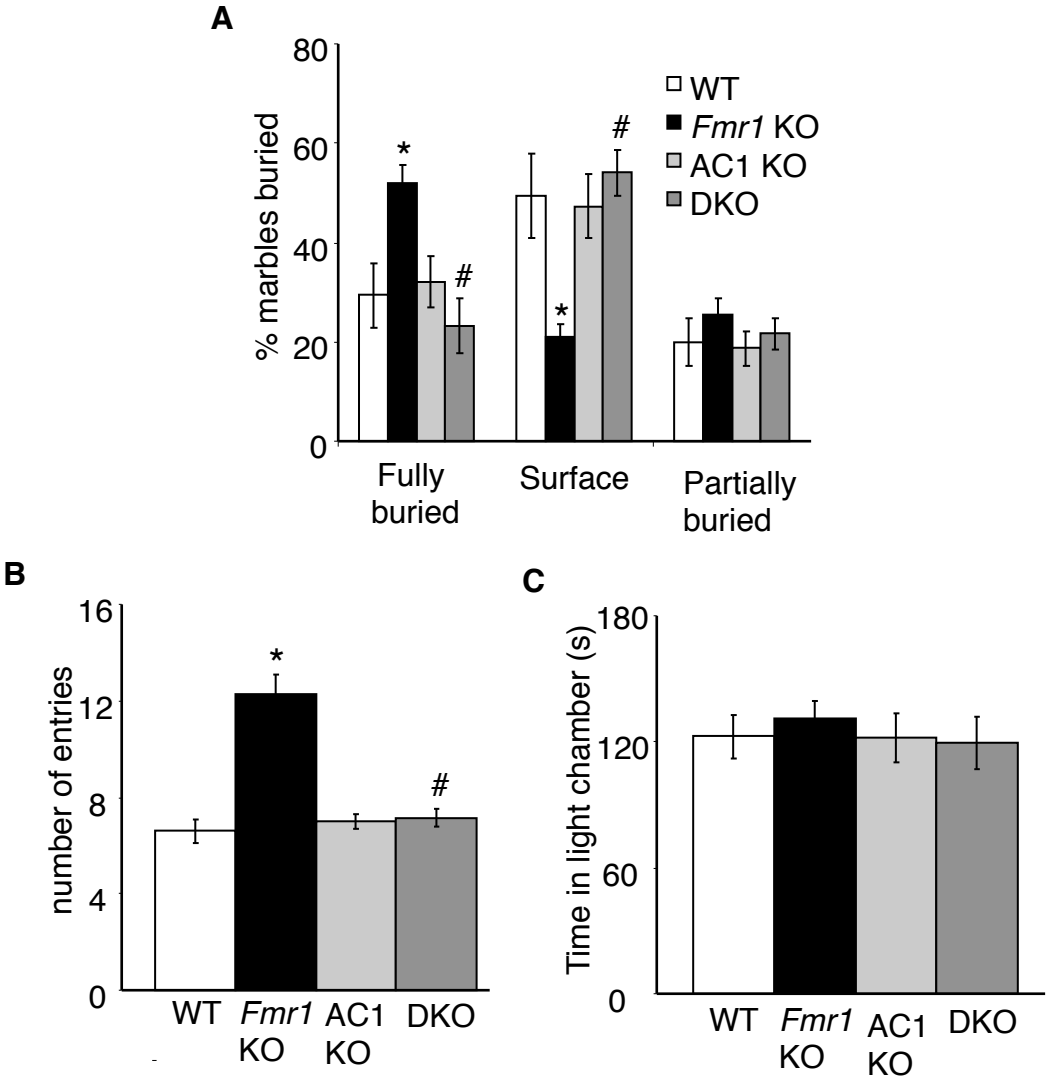

Figure 5: Rescue of hyperactive/repetitive phenotypes in DKO mice. (A) Marble burying test was performed in 2-3 month old WT (n=10), *Fmr1* KO (n=15), AC1 KO (n=10) and DKO (n=17) mice. % marbles buried fully or partially was measured. (B, C) Light-dark activity test was performed in in 2-3 month old WT (n=12), *Fmr1* KO (n=12), AC1 KO (n=12) and DKO (n=9) mice. Number of entries into the light-chamber was

Figure 5 (cont'd)

measured (B). Time spent in the light chamber was measured (C). One-way ANOVA followed by LSD test was used to compute p-values. * indicates $p < 0.001$ between WT and indicated group, # indicates $p < 0.001$ between *Fmr1* KO and indicated group.

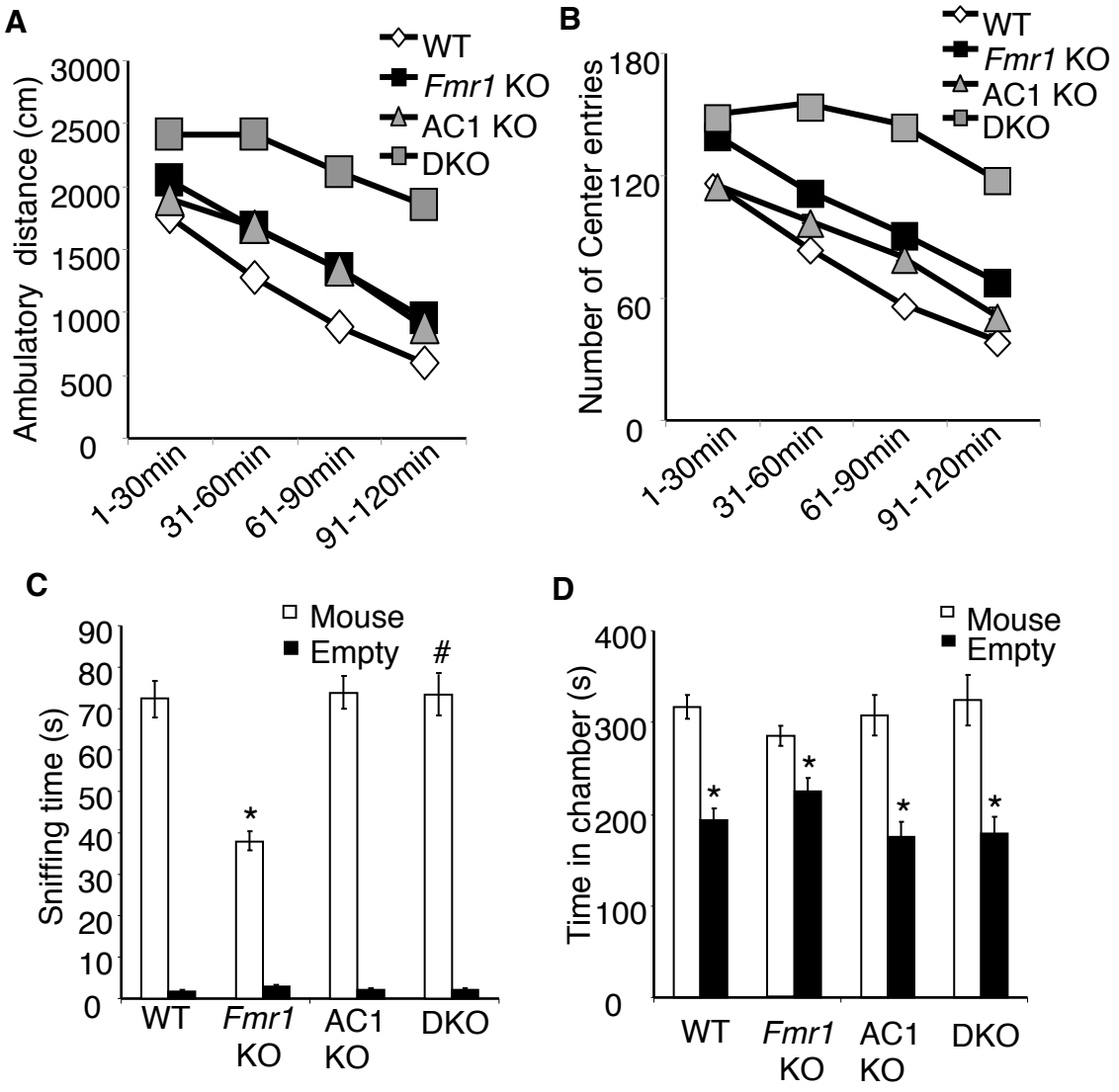

Figure 6: Rescue of social behavior but not open-field hyperactivity in DKO mice.

(A,B) Ambulatory distance (A) and number of entries into the central area (C) in an open field was measured in 2-3 month old WT (n=9), *Fmr1* KO (n=11), AC1 KO (n=12) and DKO (n=12) mice. Repeated measures ANOVA and LSD test was used to determine $p<0.05$ between WT and *Fmr1* KO, WT and AC1 KO and WT and DKO

Figure 6 (cont'd)

groups. (C,D) Sniffing time (C) and time spent in different chambers (D) during the social interaction test was measured in 2-3 month old WT (n=11), *Fmr1* KO (n=11), AC1 KO (n=10) and DKO (n=10) mice. * $p < 0.001$ between WT and indicated group, # $p < 0.001$ between *Fmr1* KO and indicated group (C) measured by One-way ANOVA and LSD test. * indicates $p < 0.05$ between chamber with mouse and empty chamber (D) measured by Student's t-test.

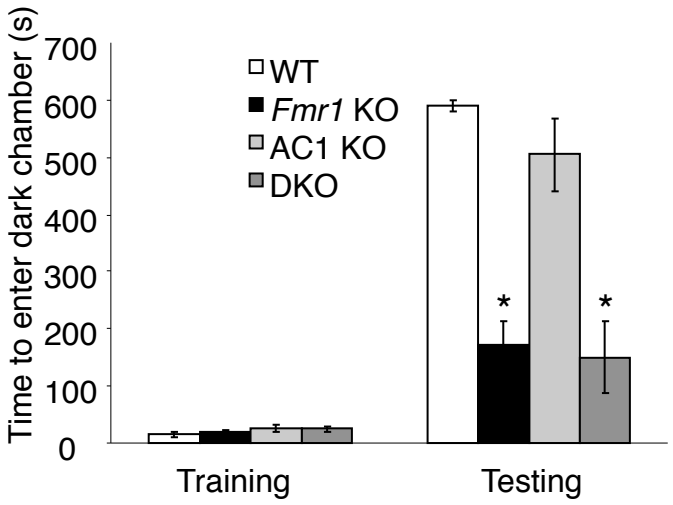

Figure 7: Impaired cognitive function in DKO mice. Passive avoidance testing was performed in 2-3 month old WT (n=10), *Fmr1* KO (n=10), AC1 KO (n=11) and DKO (n=12) mice. Latency to enter the dark chamber was measured 24 hours after shocking the mice. * $p < 0.005$ between WT and indicated group. One-way ANOVA and LSD test was used to measure the p-value.

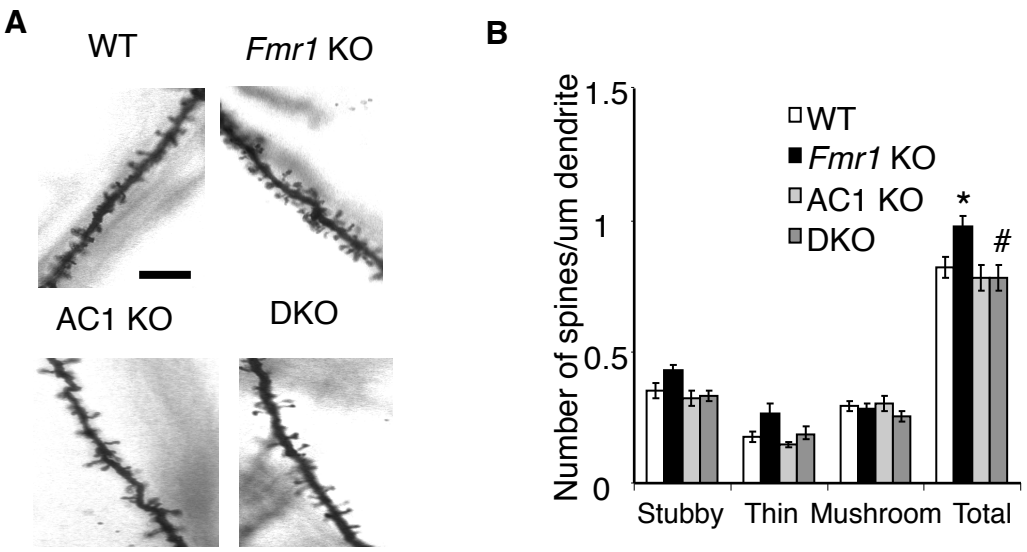

Figure 8: Rescue of dendritic spine phenotype in DKO mice. (A) Representative image of Golgi staining of dendritic spines in the apical dendrites from the CA1 area. Scale bar: 8μm (B) Classification and quantification of dendritic spines n ~ 450 spines per genotype. * $p < 0.05$ between WT and indicated group, # $p < 0.05$ between *Fmr1* KO and indicated group measured by One-way ANOVA and LSD test.

Table 4: NB001 rescues audiogenic seizure in *Fmr1* KO mice

	n	% Wild running	% Clonic/ Tonic seizure	% Death
WT vehicle	8	0	0	0
Fmr1 KO vehicle	17	71.4	64.2	21.4
WT NB001	6	0	0	0
Fmr1 KO NB001	17	35.2	5.8	5.8

Table 4: Audiogenic seizure was measured in 21-24 day WT and *Fmr1* KO mice injected with vehicle (saline). Percent mice experiencing wild-running, clonic/tonic seizure and death were reported. $p < 0.05$ between *Fmr1* KO vehicle and *Fmr1* KO NB001 groups computed by Chi-square test.

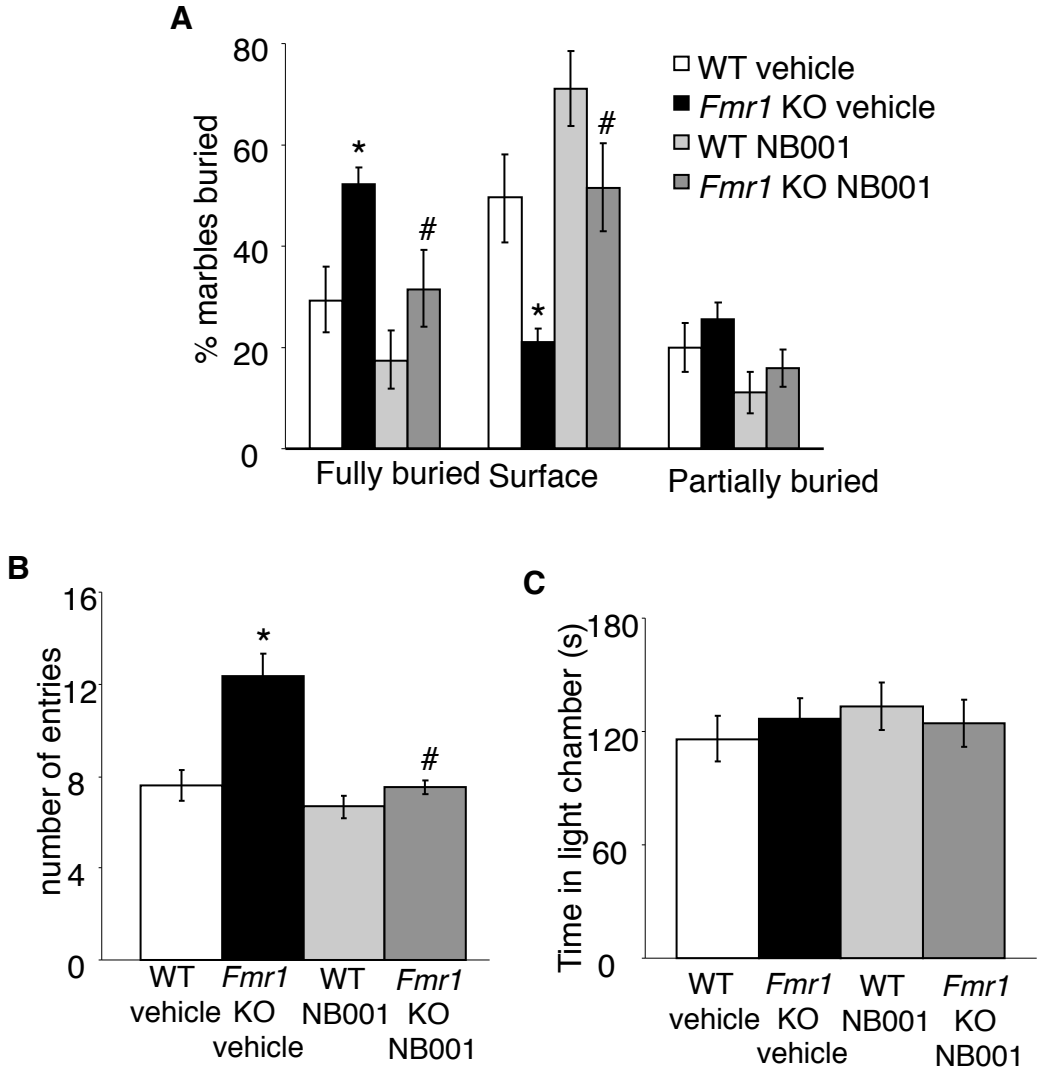

Figure 9: NB001 rescues hyperactive/repetitive phenotypes in *Fmr1* KO mice. (A) Marble burying test was performed in 2-3 month old WT and *Fmr1* KO mice injected with vehicle (WT=9, *Fmr1* KO=12) or 1mg/kg NB001 (WT=9, *Fmr1* KO=9). % marbles buried fully or partially was measured. (B,C) Light-dark activity test was performed in 2-3 month old WT and *Fmr1* KO mice injected with vehicle (WT=11, *Fmr1* KO=13) or

Figure 9 (cont'd)

1mg/kg NB001 (WT=10, *Fmr1* KO=15). Number of entries into the light-chamber was measured (B). Time spent in the light chamber was recorded (C). * $p < 0.001$ between WT and indicated group, # $p < 0.001$ between *Fmr1* KO and indicated group. p -values measured by Two-way ANOVA and Student's t-test.

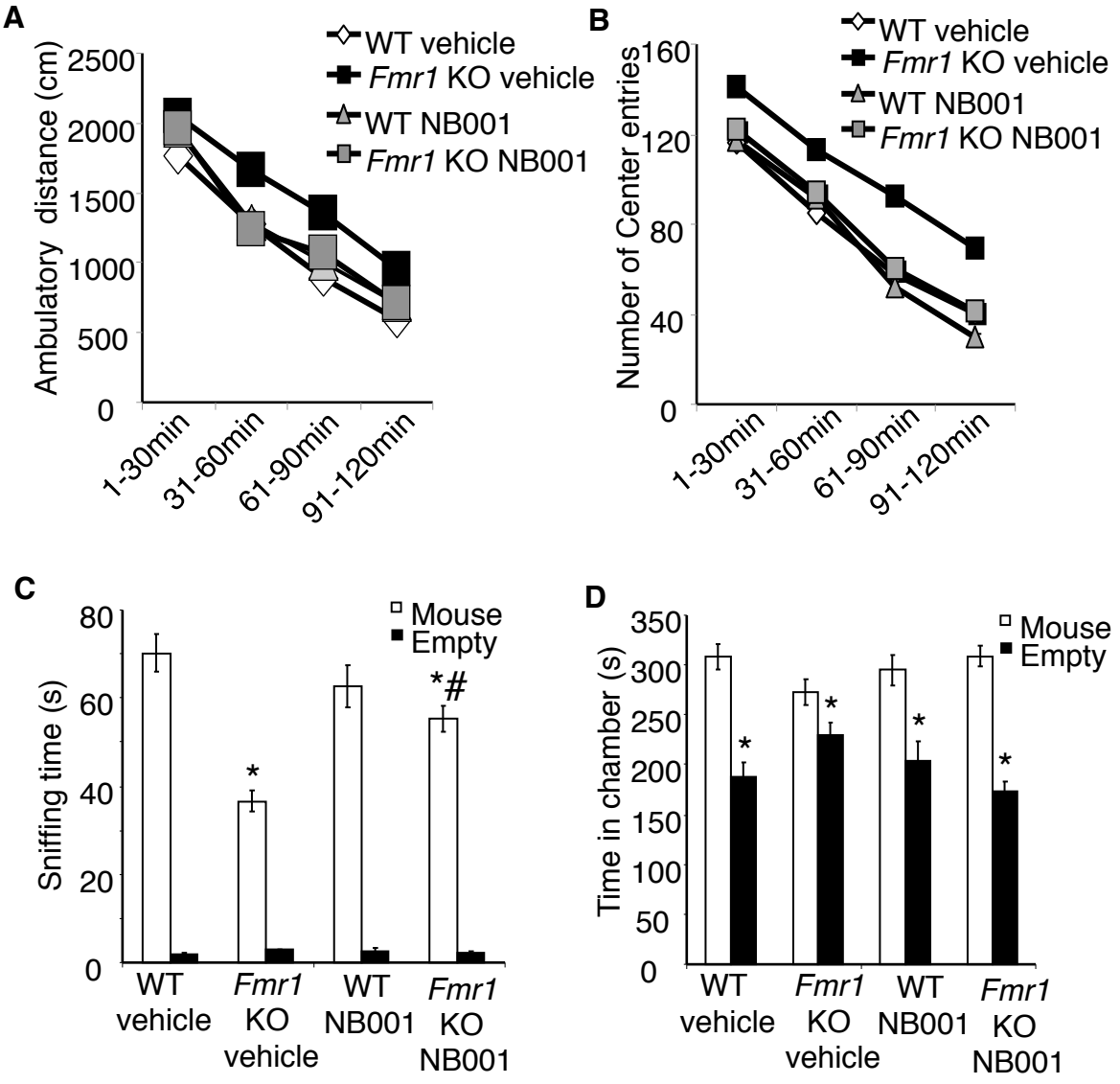

Figure 10: NB001 rescues open-field hyperactivity and social deficit in *Fmr1* KO mice. (A, B) Ambulatory distance (A) and number of entries into the center area (B) in an open field was measured in 2-3 month old WT and *Fmr1* KO mice injected with vehicle (WT=10, *Fmr1* KO=10) or 1mg/kg NB001 (WT=10, *Fmr1* KO=10). Repeated

Figure 10 (cont'd)

measures ANOVA was used to determine significance between WT: *Fmr1* KO and *Fmr1* KO: DKO groups. (C,D) Sniffing time during the social interaction test was measured in 2-3 month old WT and *Fmr1* mice injected with vehicle (WT=12, *Fmr1* KO=12) or 1mg/kg NB001 (WT=10, *Fmr1* KO=12). Two-way ANOVA and Student's t-test was used to compute p values. * $p < 0.005$ between WT and indicated group, # $p < 0.005$ between *Fmr1* KO and indicated group (C). * $p < 0.05$ between chamber with mouse and empty chamber (D).

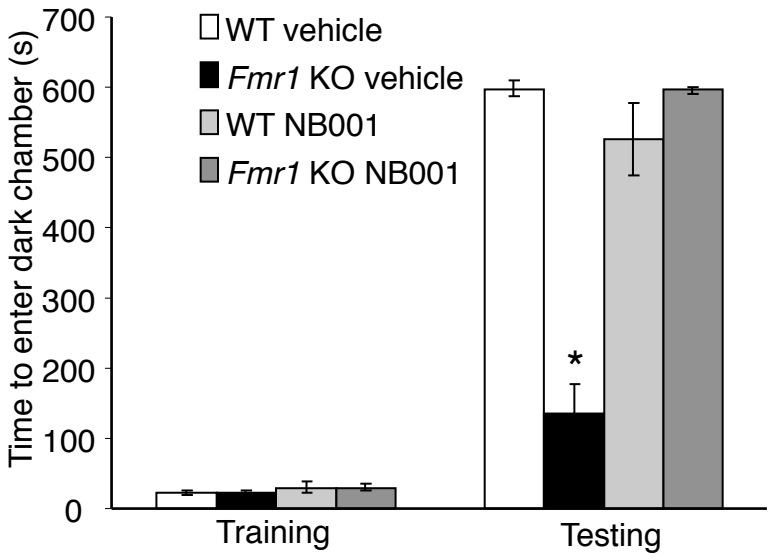

Figure 11: NB001 rescues a cognitive deficit in *Fmr1* KO mice. Passive avoidance testing was performed in 2-3 month old WT and *Fmr1* KO mice injected with vehicle (WT=12, *Fmr1* KO=12) or 1mg/kg NB001 (WT=10, *Fmr1* KO=18), latency to enter the dark chamber was measured 24 hours after shocking the mice. * $p < 0.005$ between WT and indicated group measured by Two-way ANOVA and Student's t-test.

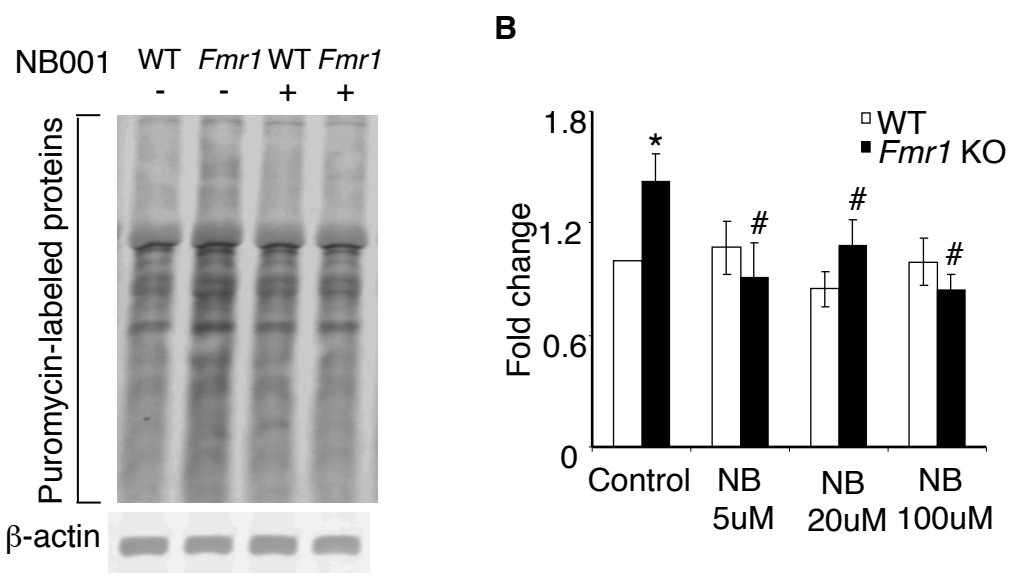

Figure 12: NB001 normalizes exaggerated protein synthesis in *Fmr1* KO neurons.

(A) Representative image of western blot. Basal protein synthesis measured in DIV8 WT and *Fmr1* KO neurons (n=6 per group) with different doses of NB001. (B) Quantification of protein bands between 150 kb and 20 kb, normalized to actin levels and expressed relative to the WT control group. Student's t-test was used to determine p-values. * shows $p < 0.05$ between indicated group and WT, # shows $p<0.05$ between indicated group and *Fmr1* KO.

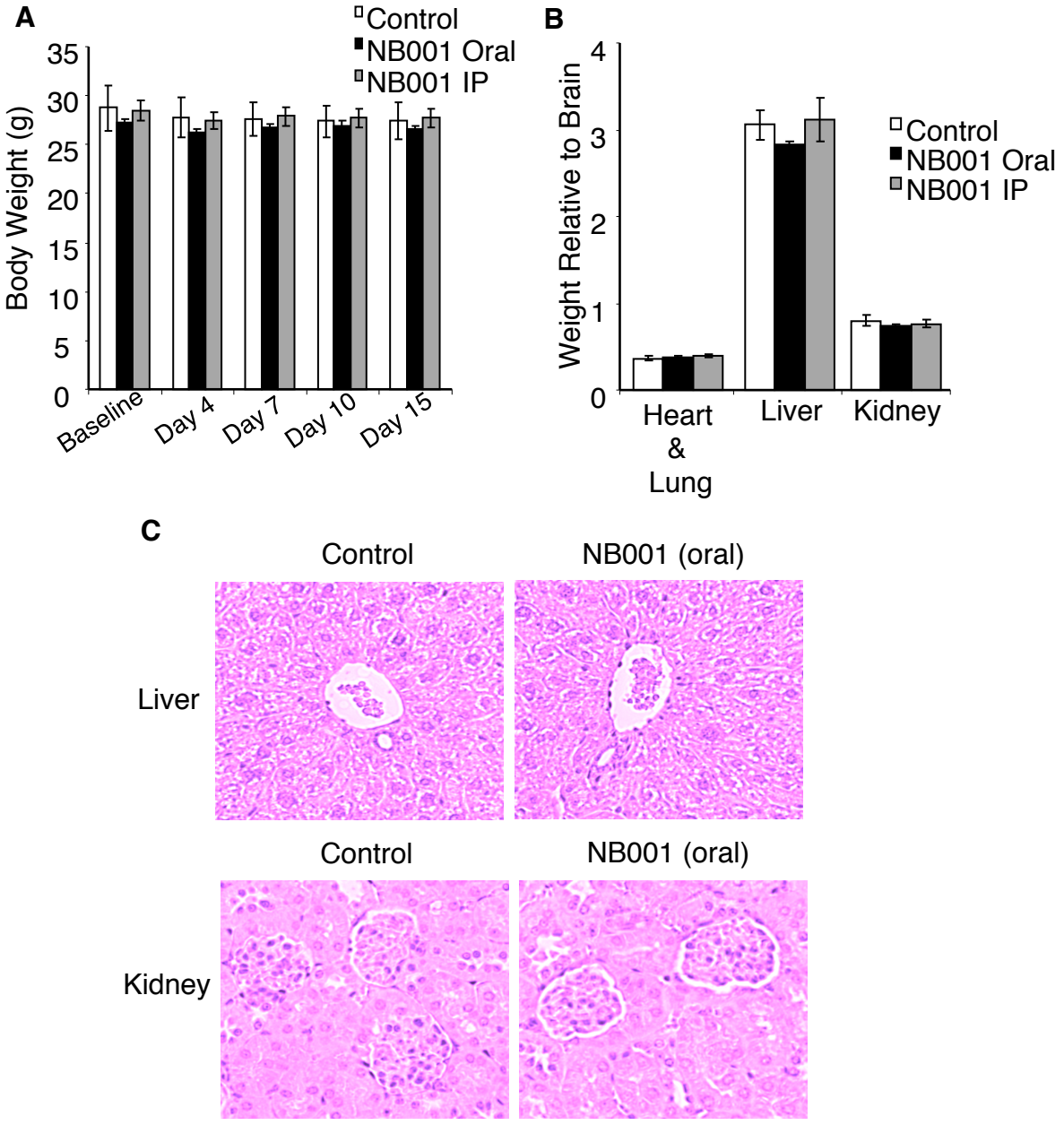

Figure 13: NB001 toxicity studies. 100mg/kg NB001 or saline was repeatedly administered orally (Saline=3, NB001=5) or intraperitoneally (Saline=3, NB001=5) to 2 month old mice for 15 days (A) Body weight at different days. (B) Heart/lung, liver and

Figure 13 (cont'd)

kidney weight normalized to brain weight after 15 days of administration. (C) H&E staining and histology of liver and kidney tissue after 15 days of oral administration.

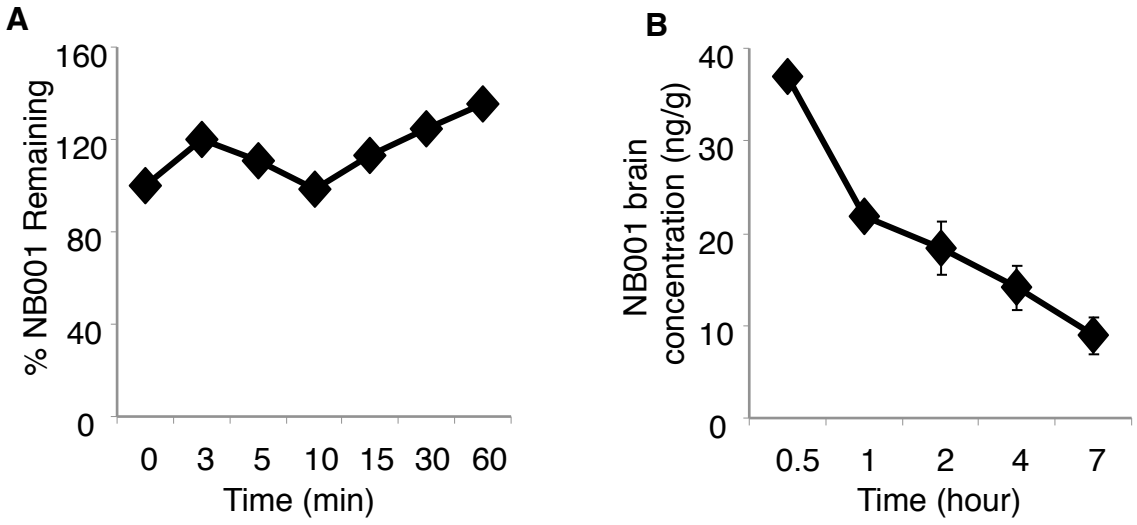

Figure 14: Pharmacokinetics of NB001. (A) Mouse liver microsome assay of NB001.

(B) Pharmacokinetic stability assay of NB001 in the brain.

Table 5: Chronic high dose NB001 administration does not alter blood chemistry in mice

	Control	NB001 oral	NB001 i.p.
Urea Nitrogen (mg/dL)	21.67 ±1.33	25.00 ±0.71	24.50 ±0.87
Sodium (mmol/L)	151.33 ±0.33	152.50 ±1.04	150.50 ±1.50
Potassium (mmol/L)	4.77 ±0.03	4.55 ±0.13	4.73 ±0.22
Chloride (mmol/L)	108.33 ±0.67	110.25 ±1.03	112.25 ±0.85
TCO2 (mmol/L)	13.00 ±0.58	13.50 ±0.29	13.50 ±1.04
Anion Gap (mmol/L)	35.00 ±0.58	33.25 ±0.75	29.50 ±2.36
Na/K Ratio	31.67 ±0.33	33.75 ±0.75	32.00 ±1.47
Osmolarity (mOs/L)	321.00 ±1.00	322.25 ±2.06	321.00 ±4.00
Glucose (mg/dL)	183.50 ±15.50	154.25 ±10.86	216.50 ±8.50
Calcium (mg/dL)	8.60 ±0.00	8.83 ±0.09	8.83 ±0.20
Phosphorus (mg/dL)	7.37 ±0.18	6.98 ±0.22	6.50 ±0.24
Magnesium (mg/dL)	3.33 ±0.12	3.13 ±0.10	2.60 ±0.11
Iron (ug/dL)	107.00 ±44.00	135.00 ±16.41	115.50 ±4.50
Albumin (g/dL)	2.80 ±0.00	2.98 ±0.05	2.65 ±0.13
ALT (U/L)	22.67 ±1.45	24.00 ±1.47	18.50 ±0.96
AST (U/L)	40.33 ±1.86	39.75 ±1.11	32.50 ±1.55
ALP (U/L)	72.00 ±2.89	66.00 ±2.27	62.75 ±4.48
Amylase (U/L)	576.67 ±12.25	613.50 ±12.01	586.50 ±29.02
Chol (mg/dL)	95.67 ±4.81	104.75 ±2.56	100.00 ±5.96
Hemolysis Chem	Normal	Normal	Normal
Lipemia Chem	Normal	Normal	Normal
Icterus Chem	Normal	Normal	Normal

Table 5: Measurement of ions, metabolites and enzymes in blood plasma of mice injected with saline (control n=3), orally fed NB001 (NB001 oral n=5) and injected with NB001 (NB001 i.p. n=5) after repeated administration of 100mg/kg NB001 twice daily for 15 days.

REFERENCES

REFERENCES

Abdel-Majid, R.M., Leong, W.L., Schalkwyk, L.C., Smallman, D.S., Wong, S.T., Storm, D.R., et al. (1998). Loss of adenylyl cyclase I activity disrupts patterning of mouse somatosensory cortex. Nat. Genet. *19*: 289–91.

Ascano, M., Mukherjee, N., Bandaru, P., Miller, J.B., Nusbaum, J.D., Corcoran, D.L., et al. (2012). FMRP targets distinct mRNA sequence elements to regulate protein expression. Nature *492*: 382–6.

Bear, M.F., Huber, K.M., and Warren, S.T. (2004). The mGluR theory of fragile X mental retardation. Trends Neurosci. *27*: 370–7.

Bhattacharya, a, Kaphzan, H., Alvarez-Dieppa, a C., Murphy, J.P., Pierre, P., and Klann, E. (2012). Genetic Removal of p70 S6 Kinase 1 Corrects Molecular, Synaptic, and Behavioral Phenotypes in Fragile X Syndrome Mice. Neuron *76*: 325–337.

Brown, V., Jin, P., Ceman, S., Darnell, J.C., O'Donnell, W.T., Tenenbaum, S. a, et al. (2001). Microarray Identification of FMRP-Associated Brain mRNAs and Altered mRNA Translational Profiles in Fragile X Syndrome. Cell *107*: 477–487.

Chen, L., and Toth, M. (2001). Fragile X mice develop sensory hyperreactivity to auditory stimuli. Neuroscience *103*: 1043–50.

Darnell, J.C., Driesche, S.J. Van, Zhang, C., Hung, K.Y.S., Mele, A., Fraser, C.E., et al. (2011). FMRP stalls ribosomal translocation on mRNAs linked to synaptic function and autism. Cell *146*: 247–61.

Darnell, J.C., Jensen, K.B., Jin, P., Brown, V., Warren, S.T., and Darnell, R.B. (2001). Fragile X mental retardation protein targets G quartet mRNAs important for neuronal function. Cell *107*: 489–99.

Darnell, J.C., and Klann, E. (2013). The translation of translational control by FMRP: therapeutic targets for FXS. Nat. Neurosci. *16*: 1–7.

Dölen, G., Osterweil, E., Rao, B.S.S., Smith, G.B., Auerbach, B.D., Chattarji, S., et al. (2007). Correction of fragile X syndrome in mice. Neuron *56*: 955–62.

Goebel-Goody, S.M., Wilson-Wallis, E.D., Royston, S., Tagliatela, S.M., Naegele, J.R., and Lombroso, P.J. (2012). Genetic manipulation of STEP reverses behavioral abnormalities in a fragile X syndrome mouse model. Genes. Brain. Behav. *11*: 586–600.

Gross, C., Nakamoto, M., Yao, X., Chan, C.B., Yim, S.Y., Ye, K., et al. (2010). Excess phosphoinositide 3-kinase subunit synthesis and activity as a novel therapeutic target in fragile x syndrome. J Neurosci *30*: 10624–10638.

Huber, K.M., Gallagher, S.M., Warren, S.T., and Bear, M.F. (2002). Altered synaptic plasticity in a mouse model of fragile X mental retardation. Proc. Natl. Acad. Sci. U. S. A. *99*: 7746–7750.

Jin, P., Zarnescu, D.C., Ceman, S., Nakamoto, M., Mowrey, J., Jongens, T. a, et al. (2004). Biochemical and genetic interaction between the fragile X mental retardation protein and the microRNA pathway. Nat. Neurosci. *7*: 113–7.

Kelley, D.J., Davidson, R.J., Elliott, J.L., Lahvis, G.P., Yin, J.C.P., and Bhattacharyya, A. (2007). The cyclic AMP cascade is altered in the fragile X nervous system. PLoS One *2*: e931.

Knight, Z. a, and Shokat, K.M. (2007). Chemical genetics: where genetics and pharmacology meet. Cell *128*: 425–30.

Krueger, D.D., and Bear, M.F. (2011). Toward fulfilling the promise of molecular medicine in fragile X syndrome. Annu. Rev. Med. *62*: 411–29.

Mines, M. a, Yuskaitis, C.J., King, M.K., Beurel, E., and Jope, R.S. (2010). GSK3 influences social preference and anxiety-related behaviors during social interaction in a mouse model of fragile X syndrome and autism. PLoS One *5*: e9706.

Park, S., Park, J.M., Kim, S., Kim, J.-A., Shepherd, J.D., Smith-Hicks, C.L., et al. (2008). Elongation factor 2 and fragile X mental retardation protein control the dynamic translation of Arc/Arg3.1 essential for mGluR-LTD. Neuron *59*: 70–83.

Pixxuti, A., Refner, O., Richards, S., Victoria, M.F., Zhang, F., Eussen, B.E., et al. (1991). Identification of a gene (FMR-1) containing a CGG repeat coincident with a breakpoint cluster region exhibiting length variation in fragile X syndrome. Cell *65*: 905–914.

Price, T., Rashid, M., Millecamps,M., Sanoja, R., Entrena, J., and Cervero, F. (2007). Decreased Nociceptive Sensitization in Mice Lacking the Fragile X Mental Retardation Protein: Role of mGluR1/5 and mTOR. J. Neurosci. *27(51)*: 13958-13967.

Ronesi, J., and Huber, K. (2008). Homer Interactions Are Necessary for Metabotropic Glutamate Receptor-Induced Long-Term Depression and Translational Activation. J. Neurosci. *28(2)*: 543-547.

Santoro, M.R., Bray, S.M., and Warren, S.T. (2012). Molecular mechanisms of fragile X syndrome: a twenty-year perspective. Annu. Rev. Pathol. *7*: 219–45.

Schmidt, E.K., Clavarino, G., Ceppi, M., and Pierre, P. (2009). SUnSET , a nonradioactive method to monitor protein synthesis. *6*: 275–277.

Sethna, F., Moon, C., and Wang, H. (2013). From FMRP Function to Potential Therapies for Fragile X Syndrome. Neurochem. Res.

Vrij, F.M.S. de, Levenga, J., Linde, H.C. van der, Koekkoek, S.K., Zeeuw, C.I. De, Nelson, D.L., et al. (2008). Rescue of behavioral phenotype and neuronal protrusion morphology in Fmr1 KO mice. Neurobiol. Dis. *31*: 127–32.

Wang, H., and Storm, D.R. (2003). Calmodulin-Regulated Adenylyl Cyclases : Cross-Talk and Plasticity in the Central Nervous System. *63*: 463–468.

Wang, H., Xu, H., Wu, L.-J., Kim, S.S., Chen, T., Koga, K., et al. (2011). Identification of an adenylyl cyclase inhibitor for treating neuropathic and inflammatory pain. Sci. Transl. Med. *3*: 65ra3.

Westmark, C.J., and Malter, J.S. (2007). FMRP mediates mGluR5-dependent translation of amyloid precursor protein. PLoS Biol. *5*: e52.

Yan, Q.J., Rammal, M., Tranfaglia, M., and Bauchwitz, R.P. (2005). Suppression of two major Fragile X Syndrome mouse model phenotypes by the mGluR5 antagonist MPEP. Neuropharmacology *49*: 1053–66.

Zalfa, F., Giorgi, M., Primerano, B., Moro, A., Penta, A. Di, Reis, S., et al. (2003). The fragile X syndrome protein FMRP associates with BC1 RNA and regulates the translation of specific mRNAs at synapses. Cell *112*: 317–27.

Zhou, X., Lin, D.S., Zheng, F., Sutton, M. a, and Wang, H. (2010). Intracellular calcium and calmodulin link brain-derived neurotrophic factor to p70S6 kinase phosphorylation and dendritic protein synthesis. J. Neurosci. Res. *88*: 1420–32.

CHAPTER 3: TRIFLUOPERAZINE INHIBITS Gq-COUPLED RECEPTOR SIGNALING AND RESCUES CELLULAR AND BEHAVIORAL ABNORMALITIES IN A MOUSE MODEL OF FRAGILE X SYNDROME

3.1 ABSTRACT

Aberrantly elevated basal protein synthesis and over-activation of the Gq-coupled glutamate and acetylcholine receptors have been considered as potential mechanisms underlying the pathophysiology in Fragile X syndrome (FXS). Identification of functional components in Gq signaling that affect protein synthesis may aid in development of novel therapeutic targets for FXS. Through pharmacological inhibition, we tested the function of calmodulin (CaM) in intracellular signaling stimulated by the activation of the Gq-coupled metabotropic glutamate receptor 1/5 (mGluR1/5) and muscarinic cholinergic receptors (Gq-mAchR). CaM inhibitors suppressed mGluR1/5- and Gq-mAchR-mediated Arc upregulation and the activation of ERK1/2, whose activity is required for protein synthesis and synaptic long-term depression (LTD). Further, we used acute injection of a known CaM inhibitor- trifluoperazine (an FDA approved drug for treating psychosis) and examined FXS-related behaviors and elevated protein synthesis in a mouse model of FXS. Low dose administration of trifluoperazine at 0.05 mg/kg

attenuated audiogenic seizures and corrected multiple FXS-related symptoms including hyperactivity, repetitive behavior, and defective passive avoidance memory in *Fmr1* knockout mice. Trifluoperazine also normalized the elevated protein synthesis in FXS neurons to the wild type level. Our data suggest CaM as a new therapeutic target. Our study also suggests a potential new application of trifluoperazine in FXS.

3.2 Introduction

Fragile X syndrome (FXS), caused by mutations in the *FMR1* (fragile X mental retardation 1) gene, is the most common form of inherited mental retardation and a leading cause of autism (Santoro et al., 2012). Most cases of FXS occur due to a significant expansion of the CGG repeats in the 5' untranslated region of the *FMR1* gene. This inhibits its transcription, thus preventing the expression of its gene product FMRP (fragile X mental retardation protein). FXS patients exhibit numerous neurological abnormalities including learning disability, higher susceptibility to seizures, hyperactivity, and perseveration (Bagni et al., 2012).

Biochemical studies have demonstrated that FMRP binds to roughly 4% of mRNAs (Brown et al., 2001; Darnell et al., 2011; Ascano et al., 2012). Neurons lacking FMRP show enhanced basal protein synthesis, supporting the idea that FMRP is a translational suppressor of its mRNA targets (Darnell and Klann, 2013). The lack of FMRP-mediated suppression of translation in FXS patients may cause alterations in synaptic functions that require activity-dependent protein synthesis. In a seminal study, Huber et al. reported that long-term depression (LTD) triggered by the activation of the Gq-coupled mGluR1/5 is enhanced in *Fmr1* knockout (KO) mice (Huber et al., 2002). Strikingly, protein synthesis inhibitors only suppress the mGluR1/5-mediated LTD in wild

type (WT) but not *Fmr1* KO mice (Hou et al., 2006; Nosyreva and Huber, 2006). As mGluR1/5 activation leads to translational upregulation, it is hypothesized that over-activation of mGluR1/5 signaling may be causal for both enhanced translation and LTD in FXS (Bear et al., 2004). In support of this idea, inhibition of mGluR5 has shown significant therapeutic effects to rescue several FXS-related symptoms in mouse models (Yan et al., 2005; de Vrij et al., 2008; Thomas et al., 2012). However, the efficacy of mGluR5 inhibitors in a human clinical trial was limited to a sub-population of FXS patients (Jacquemont et al., 2011).

mGluR5-based therapies may be enhanced when used in conjunction with strategies targeting other etiological factors. Similar to the effects of mGluR1/5 activation, activation of the Gq-mAchR (such as the M1 receptor) also triggers protein synthesis and LTD. Interestingly, the M1-mediated LTD in *Fmr1* KO mice is also enhanced and resistant to protein synthesis inhibitors (Volk et al., 2007). Inhibition of the Gq-mAchR rescues certain but not all FXS symptoms in *Fmr1* KO mice (Veeraragavan et al., 2011). Studies on the pathophysiology associated with the exaggerated mGluR1/5 and Gq-mAchR signaling in FXS raise an important question: can we achieve more robust therapeutic efficacy by simultaneously inhibiting both receptors through dampening a common downstream signaling target?

Our strategy was to block intracellular signaling following the activation of both mGluR1/5 and muscarinic receptors. We found that inhibition of calmodulin (CaM) activity suppressed signal transduction triggered by the activation of both mGluR1/5 and muscarinic receptors. Further, systemic administration of a clinically used CaM inhibitor, trifluoperazine, attenuated audiogenic seizures in *Fmr1* KO mice. Trifluoperazine also corrected hyperactivity, repetitive behavior, and defective passive avoidance memory in *Fmr1* KO mice. Moreover trifluoperazine suppressed the enhanced mRNA translation in *Fmr1* KO neurons. Our results suggest that inhibiting signal propagation of multiple Gq-coupled receptors may be considered as a new strategy to treat FXS.

3.3 Materials and Methods

3.3.1 Animals

Fmr1 KO mice on C57BL/6 background were obtained from Dr. James Malter and Dr. Cara Westmark. Animals were housed in the University Laboratory Animal Research facility. All manipulations were approved by the Institutional Animal Care and Use Committee at Michigan State University. The mice had *ad libitum* access to water and food and were housed under 12 h dark/light cycle.

3.3.2 Neuronal cell culture and Western blotting

Primary hippocampal cultures were established from neonatal rats (Sprague Dawley) or wild type (WT) and *Fmr1* KO mice as described (Zhou et al., 2010). Control and treated neurons were lysed and proteins were extracted in Laemmli buffer. Equal amounts of cell extract were separated by SDS-PAGE followed by transferring to nitrocellulose membranes. The following antibodies were used to detect the corresponding targets. Arc antibody was obtained from Synaptic Systems (Cat # 156011, 1:1000 dilution). β-actin antibody was from Sigma (Cat #A5441, 1:10,000 dilution). Anti-phospho-ERK1/2 (Cat #9101, 1:1000 dilution), anti-ERK1/2 (Cat #9102, 1:1000 dilution), anti-S6K1 (Cat #9202, 1:1000 dilution), anti-phospho-S6K1 (at Thr421/Ser424) (Cat #9204, 1:1000

dilution), and anti-phospho-S6K1 (at Thr389) (Cat # 9234, 1:1000 dilution) were from Cell Signaling.

For quantification, the level of Arc was normalized to the level of β-actin. The level of phosphorylated ERK1/2 and S6K1 was normalized to the level of total ERK1/2 and S6K1, respectively. The relative intensity of the Western blot signal in the no treatment control group, was defined as 1. The signal in the treatment samples was normalized to the control group. All bands were quantified using ImageJ (NIH, MD, USA).

3.3.3 Electrophysiology

Field excitatory postsynaptic potentials (fEPSP) in the CA1 region of the hippocampus were measured in anaesthetized mice (2- to 3-month old) (100 mg/kg Nembutal sodium solution for the initial dose, another dose of 10 mg/kg was given 30 min later) or acute brain slices (obtained from 1-month old mice) as described (Zhang et al., 2011; Bhattacharya et al., 2012). To induce LTD *in vivo*, 0.5 ul of 2.5 mM mGluR1/5 agonist DHPG ([*RS*]-3,5-Dihydroxyphenylglycine, Tocris Cat #0342) (with the infusion rate of 0.05 ul/min) was infused to the CA1 region of the anaesthetized mice. To determine the effects of calmodulin inhibition on mGluR1/5-LTD, 0.5 ul 1.75 mM W13 (*N*-[4-Aminobutyl]-5-chloro-2-naphthalenesulfonamide hydrochloride, Tocris Cat #0361) or 0.5 ul 1.75 mM W13 plus 2.5 mM DHPG (with the infusion rate of 0.05 ul/min) was delivered

to the CA1 region. To determine the mGluR1/5-LTD *in vitro*, DHPG (100 uM) or DHPG (100 uM) plus W13 (70 uM) was perfused to the recording chamber. The ratio of fEPSP after drug administration to baseline fEPSP was used to determine the degree of synaptic depression.

3.3.4 Behavioral tests

To measure audiogenic seizures (AGS), twenty one- to twenty four-day old male and female mice were placed in a box (30 cm L by 17 cm W by 12 cm H) with a flat plastic lid. A personal alarm (from Streetwise, item # SWPDAL) was taped to the lid of the box and wired to a DC power supply to keep the sound amplitude constant. The mouse was allowed to acclimatize to the box for 5 min, following which a 120 dB sound was emitted from the alarm for 2 min. The number of mice undergoing seizure within the 2-min period was counted. Audiogenic seizures were classified into different stages: wild running, clonic/tonic seizure and death.

To determine animal activity in the open field, two-month old male mice were placed in the center of an open field chamber measuring 28 cm by 28 cm with 34-cm high walls and were allowed to move freely for 2 hours. Total ambulatory movement distance, and ambulatory distance in the center area of the open field were determined every 10-min

during the 2-hour testing period by the TruScan Photo Beam Activity System (Coulbourn Instruments, Whitehall, PA).

To perform the marble burying test, two- to three-month old male mice were placed in a box (27 cm by 15 cm box with 12-cm high walls) with 7.6 cm depth of bedding for 1 hour prior to the test. The mouse was then briefly removed from the testing box and 15 marbles were evenly arranged in a 5 by 3 pattern on the surface of the bedding. The mouse was reintroduced into the testing box and was allowed to bury marbles for 10 min. At the end of the testing period, the mouse was removed from the box and the number of marbles that were fully buried, partially buried, and left on the surface was counted.

To examine animal activity in the light-dark test, three- to four-month old male mice were placed in the dark half of the light-dark chamber and the trap door was opened 1 min later. The mice were allowed to move freely between the dark and the lit chambers for 5 min. The time spent in the lit chamber and the number of crossings into the lit side were recorded.

To examine passive avoidance learning, three- to four-month old male mice were introduced into the lit half of the passive avoidance chamber (Coulbourn Instruments, Whitehall, PA) and allowed to explore for 1 min before the trap door was opened. The

trap door was closed as soon as the mouse entered the dark chamber. A mild foot shock (0.7 mA for 2 sec) was immediately delivered. The mouse was removed from the dark chamber and returned to its home cage 30 sec after the foot shock was delivered. The mice were tested 24 hours after training. During testing, the mouse was put in the lit chamber and crossover latency to the dark chamber was recorded. If mice stayed in the lit chamber for more than 600 sec, they were manually removed from the chamber, and 600 sec was used as their crossover latency.

3.3.5 Administration of Trifluoperazine

For drug administration, Trifluoperazine dihydrochloride from Sigma (Cat #T8516) was dissolved in water to give a 5 mg/ml stock solution. The stock was diluted in saline and i.p. injected into mice at 0.05 mg/kg. In all cases except for open field, the drug was administered 1 hour before testing or before training for passive avoidance. For open field analysis, the drug was administered 30 min before testing. Control mice were treated similarly but injected with vehicle.

3.3.6 Measurements of protein synthesis in cultured neurons

Protein synthesis was determined by the SUnSET method (Schmidt et al., 2009; Bhattacharya et al., 2012). DIV (days in vitro) 14 hippocampal neurons were pre-treated with trifluoperazine for 30 min followed by 5 ug/ml puromycin (Sigma, Cat #P8833)

treatment for 30 min. Cells were lysed in Buffer H (50 mM b-glycerophosphate, 1.5 mM EGTA, 0.1 mM Na_3VO_4, 1 mM DTT). The samples were sonicated and centrifuged. An aliquot of the supernatant was used to determine protein concentration, and the rest was denatured in Laemmli buffer. 20 ug protein was separated by 4-20% SDS-PAGE (Invitrogen) and transferred onto nitrocellulose membranes. The membranes were probed with anti-puromycin antibody (KeraFAST, Cat # EQ0001, 1:1000). The relative amount of loading was determined by the level of β-actin. ImageJ was used to measure the combined signal intensity of proteins with molecular weights ranging from 15 to 250 kDa.

3.3.7 Statistical analysis

For data analysis, one-way ANOVA followed by LSD (least significant difference) post-hoc test was used to compare multiple groups. Two-way repeated measures ANOVA or two-way repeated measures ANOVA followed by Student's t-test were used to analyze the electrophysiology data or the open field data. Chi-squared test was used to analyze the AGS data. Two-way ANOVA followed by pairwise comparison or Student's t-test was used to compare different groups in the light-dark, passive avoidance, marble burying tests as well as the SUnSET assay. Data were expressed as the mean ± SEM.

Differences with p values less than 0.05 were considered significant. SPSS 11.5 for Windows (IBM) was used for all data analysis.

3.4 Results

3.4.1 Calmodulin activity is required for mGluR1/5-mediated intracellular signaling

Overactivation of mGluR1/5 has been considered as a cellular mechanism underlying the pathophysiology of FXS. Thus, it is hypothesized that dampening mGluR1/5 signaling may be of therapeutic value for FXS (Bear et al., 2004). To effectively manipulate mGluR1/5-mediated signal transduction, I investigated components in the signaling cascade. By using cultured rat hippocampal neurons, I first confirmed that stimulation with the mGluR1/5 agonist DHPG caused significant phosphorylation of ERK1/2 (Figure 15A, $p < 0.05$), whose phosphorylation level is elevated in *Fmr1* KO neurons (Michalon et al., 2012). The activity of S6K1 (p70-S6 kinase 1) is positively regulated by phosphorylation and involved in regulating ribosomal biogenesis. *In vitro* studies have shown that ERK1/2 can directly phosphorylate S6K1 at Thr421/Ser424. Consistently, activation of mGluR1/5 stimulated phosphorylation of S6K1 at Thr421/Ser424 ($p < 0.05$) as well as Thr389 ($p < 0.05$) (Figure 15B), a target

site of PI3K (Zhou et al., 2010). DHPG also caused significant upregulation of Arc (Figure 15C, $p < 0.05$), whose function is implicated in mGluR1/5-mediated LTD (Park et al., 2008). DHPG-induced Arc translation is also required for mGluR1/5-mediated LTD (Waung et al., 2008).

Because increased Ca^{2+} release from the internal storage is one of the major downstream cellular events following Gq activation, we expected that inhibiting the Ca^{2+} effector molecule CaM might block the propagation of mGluR1/5 signaling. I pre-treated neurons with a CaM inhibitor W13 followed by DHPG stimulation. W13 blocked DHPG-stimulated phosphorylation of ERK1/2 (Figure 16A, $p < 0.05$) and S6K1 (Figure 16B, $p < 0.05$) as well as the upregulation of Arc (Figure 16C, $p < 0.05$). Treatment with W13 alone decreased the level of ERK1/2 phosphorylation (Figure 16A) whereas the level of Arc expression and S6K1 phosphorylation remained unchanged (Figure 16B and 16C).

3.4.2 CaM activity is required for mGluR1/5-mediated LTD

We next determined the effects of CaM inhibition on synaptic functions following the activation of mGluR1/5. After infusion of DHPG to the CA1 region of the hippocampus in anesthetized mice, we observed significant LTD (68.4 ± 4.6%); infusion of the vehicle did not change synaptic responses (97.9 ± 3.4%) (Figure 17A, $p < 0.005$).

Infusion of W13 alone (99.4 ± 7.1%) or W13 plus DHPG (111.1 ± 7.6%) caused transient synaptic depression but not LTD (Figure 17B). One-way ANOVA followed by post hoc Bonferroni test indicated that W13 suppressed mGluR1/5-mediated LTD ($p < 0.01$) (Figure 17C) (Dr. Ming Zhang).

In acute hippocampal slices, application of DHPG induced significant LTD, which was significantly suppressed by W13 ($p < 0.001$) (Figure 17D) (Dr. Hanoch Kaphzan and Dr. Eric Klann). These results implicate CaM as a functional component in the mGluR1/5 signaling cascade.

3.4.3 ERK1/2 activity is required for mGluR1/5-mediated upregulation of Arc expression

I found that CaM activity was required for both ERK1/2 activation and Arc upregulation following mGluR1/5 stimulation. To determine whether W13 inhibits Arc translation through suppressing ERK1/2 activity, I pre-treated neurons with the MEK inhibitor U0126. Because MEK directly regulates ERK1/2 phosphorylation, U0126 suppressed the level of phospho-ERK1/2 in both un-stimulated and DHPG stimulated neurons (Figure 18A, $p < 0.05$). I next found that U0126 also significantly blocked DHPG-stimulated Arc upregulation (Figure 18B, $p < 0.05$). A previous study using

hippocampal slices showed that U0126 suppresses mGluR1/5-LTD (Gallagher et al., 2004). Here, we observed that U0126 inhibited hippocampal mGluR1/5-LTD in anesthetized mice (Figure 18C, $p < 0.005$) (Dr. Ming Zhang). These data imply that the attenuation of ERK1/2 activity by CaM inhibition is relevant to the suppression of Arc upregulation and mGluR1/5-LTD.

3.4.4 Trifluoperazine attenuates audiogenic seizures and corrects hyperactivity, repetitive behavior, and defective passive avoidance memory in *Fmr1* KO mice

We reasoned that suppression of mGluR1/5 signaling through CaM inhibition might have therapeutic value for FXS treatment. As W13 is not suitable for systemic administration, we searched for available reagents that could be administered at peripheral sites and cross the blood-brain barrier. We chose trifluoperazine, because it is a well-documented CaM inhibitor and approved for clinical use by FDA to treat psychotic conditions and anxiety in humans.

FXS and autism patients show higher susceptibility to seizures. As the major FXS animal model, *Fmr1* KO mice analogously exhibit significant audiogenic seizure (AGS) (Musumeci et al., 2000; Chen and Toth, 2001). On exposing mice to a sound at 120 dB, I observed wild running, clonic/tonic seizures, and death in juvenile *Fmr1* KO but not

wild type (WT) animals (Table 6). *Fmr1* KO mice receiving intraperitoneal injection of trifluoperazine at 0.05 mg/kg had lower occurrence of AGS (Table 6, $p < 0.05$).

Hyperactivity is observed in both human FXS patients and *Fmr1* KO mice (Qin et al., 2002). During the 2-hour open field test, *Fmr1* KO mice displayed higher total travel distance (Figure 19A1, $p < 0.01$; Figure 19A2, $p < 0.01$), and higher locomotor activity in the center area of the arena (Figure 19B1, $p < 0.01$; Figure 19B2, $p < 0.01$) than the WT animals. Administration of trifluoperazine (at 0.05 mg/kg) to *Fmr1* KO mice corrected the overall hyperactivity (Figure 19 4A1, drug effect: $p < 0.01$, genotype-drug interaction: $p < 0.05$; Figure 19A2, drug effect: $p < 0.01$, genotype-drug interaction: $p < 0.01$) and the higher activity in the center area (Figure 19B1, drug effect: $p < 0.01$, genotype-drug interaction: $p < 0.01$; Figure 19B2, drug effect: $p < 0.01$, genotype-drug interaction: $p < 0.01$).

Fmr1 KO mice show significant repetitive behavior, recapitulating perseverative symptoms in FXS and autism patients. I examined animal behavior in the marble-burying test, which has been considered to measure repetitive behavior and barely involves novelty-induced anxiety (Thomas et al., 2009). I first confirmed that *Fmr1* KO mice buried more marbles than WT animals (Figure 20A, $p < 0.05$) leaving less number of marbles on the surface (Figure 20A, $p < 0.05$) (Zang et al., 2009). We further

examined *Fmr1* KO mice with the light-dark test. The mutant mice showed more transition between the light and dark chambers than WT animals, indicating both hyperactivity and repetitive behavior ($p < 0.001$) (Figure 20B1). *Fmr1* KO and WT mice spent comparable time in the light and dark chamber (Figure 20B2) (Dr. Qi Ding). Administration of trifluoperazine (at 0.05 mg/kg) corrected both marble-burying (Figure 20A, drug effect: $p < 0.05$, genotype-drug interaction: $p < 0.05$ for the fully buried marbles; drug effect: $p < 0.05$, genotype-drug interaction: $p < 0.05$ for the surface marbles) and light-dark test (Figure 20B1, drug effect: $p = 0.26$, genotype-drug interaction: $p < 0.005$) phenotypes in *Fmr1* KO mice, without affecting the behavior of WT mice.

We next trained *Fmr1* KO and WT mice with passive avoidance test following intraperitoneal injection of trifluoperazine (0.05 mg/kg) or vehicle. All groups of animals showed similar crossover latency during training. When tested 24 hours later, the vehicle-treated WT mice showed significantly longer crossover latency than the vehicle-treated *Fmr1* KO mice (Figure 21, $p < 0.005$). This confirms the impaired passive avoidance memory in the FXS mice (Qin et al., 2002). Although trifluoperazine did not have an effect on WT animals, the crossover latency in the trifluoperazine-treated *Fmr1* KO mice increased to WT levels (Figure 21, drug effect: $p < 0.01$, genotype-drug

interaction: $p < 0.05$) (Dr. Qi Ding). Thus, trifluoperazine corrected this cognitive deficit in FXS mice.

3.4.5 Trifluoperazine blocks intracellular signaling triggered by the activation of Gq-coupled receptors

Although previous studies have demonstrated that trifluoperazine inhibits CaM activity, it is important to examine its effects on mGluR1/5 signaling. I found that trifluoperazine blocked DHPG-induced phosphorylation of ERK1/2 (Figure 22A, $p < 0.05$) and Arc upregulation (Figure 22B, $p < 0.05$). Similar to the effects of W13 (Figure 16A and C), trifluoperazine also suppressed the basal level of ERK1/2 activity (Figure 22A) in non-stimulated neurons.

A previous study reported that activation of Gq-coupled muscarinic cholinergic receptors (i.e., M1, M3, and M5) by carbachol (CCh) induces translation-dependent LTD, which is also enhanced in *Fmr1* KO mice (Volk et al., 2007). Since the activation of either mGluR1/5 or M1/3/5 leads to the activation of Gq signaling, it is not surprising that mGluR1/5- and M1/3/5-mediated LTD share similar mechanisms. Here, I confirmed that carbachol stimulates ERK1/2 phosphorylation in hippocampal neurons (Figure 22C and D). Neurons co-treated with W13 and carbachol did not show upregulation of ERK1/2

phosphorylation (Figure 22C, $p < 0.05$). Trifluoperazine also blocked ERK1/2 phosphorylation in carbachol-treated neurons (Figure 22D, $p < 0.05$). These results demonstrate that CaM is a common downstream target of both mGluR1/5 and Gq-coupled muscarinic cholinergic receptors, and pharmacological inhibition of CaM is effective in dampening the signaling triggered by activation of multiple Gq-coupled receptors.

3.4.6 Trifluoperazine corrects the enhanced protein synthesis in *Fmr1* KO neurons

Enhanced basal protein synthesis in neurons is thought to be the core molecular abnormality associated with FXS and manipulations that correct the enhanced protein synthesis are potential strategies to treat FXS (Darnell and Klann, 2013). Here, I labeled newly synthesized proteins in neurons with puromycin using the SUnSET method (Schmidt et al., 2009; Bhattacharya et al., 2012). I observed enhanced protein synthesis in *Fmr1* KO neurons compared to WT neurons (Figure 23A and B, genotype effect: $p < 0.05$). Treatment with different concentrations of trifluoperazine specifically reduced the level of puromycin-labeled proteins in *Fmr1* KO neurons to the WT level (Figure 23B) while it did not affect protein synthesis in WT neurons (Figure 23B).

In summary, this study suggests CaM as a new potential therapeutic target. Administration of a known CaM inhibitor, trifluoperazine, blocked Gq-coupled receptor signaling and attenuated both cellular and behavioral symptoms associated with FXS.

3.5 Discussion

Due to lack of effective medical treatments for FXS, there is a significant need for novel therapeutics. Following the discovery that showed enhanced mGluR1/5-mediated LTD in *Fmr1* KO mice, mGluR1/5 has been considered the most viable target for FXS therapy. By using the FXS mouse model, several studies have demonstrated therapeutic effects of mGluR5 antagonists. For example, the mGluR5 antagonist MPEP reduces AGS and hyperactivity in the center area of the open field arena (Yan et al., 2005). A negative allosteric mGluR5 modulator fenobam improves associative motor learning in *Fmr1* KO mice, but has significant negative effects on WT controls (Veloz et al., 2012). In a recent study, Thomas et al. reported that MPEP and JNJ16259685 (an mGluR1 antagonist) both reduced AGS in *Fmr1* KO (Thomas et al., 2012). Considering that FXS is a complex neurological disorder, it is not surprising that inhibition of mGluR5 alone is not effective to rescue many of the FXS-related behavioral and synaptic abnormalities in mice (Suvrathan et al., 2010; Thomas et al., 2012; Franklin et al., 2014)

as well as in human patients. In a small open-label single dose trial that involved 12 FXS patients, fenobam improved pre-pulse inhibition but showed no obvious effects on the continuous performance test (Berry-Kravis et al., 2009). Disclosure of a recent placebo-controlled phase II clinical trial using the mGluR5 antagonist AFQ056 revealed therapeutic effects only on patients with full promoter methylation (Jacquemont et al., 2011). It is important to note that these human studies only involved a single dosing regime for a fairly short period of time. Further trials using multiple doses and longer treatment durations should be seriously considered. Nevertheless, these results indicate the possibility that inhibition of mGluR5 alone may not be robust enough to correct multiple symptoms associated with FXS. Other drug targets should be considered in conjunction with mGluR1/5.

One interesting mGluR1/5-independent pathophysiology in FXS is mediated by the overactivation of the Gq-coupled muscarinic acetylcholine receptors (Gq-mAchRs consisting of M1, M3, and M5). Volk et al. showed that the mAchR agonist carbachol induced translation-dependent LTD that is mainly mediated through the activation of the Gq-mAchR M1 (Volk et al., 2007). Because both mGluR1/5 and M1 are coupled to Gq, it is not surprising that enhanced LTD in *Fmr1* KO mice is observed following the stimulation with either DHPG or carbachol. Further, Veeraragavan et al. demonstrated

that administration of the M1 antagonist dicyclomine rescued AGS in *Fmr1* KO mice (Veeraragavan et al., 2011). However, it is evident that suppression of Gq-coupled M1 receptor alone is not robust enough to correct the multiple FXS symptoms. For instance, dicyclomine non-specifically reduces marble-burying behavior in both WT and *Fmr1* KO animals, and does not correct some core behavioral abnormalities such as hyperactivity (Veeraragavan et al., 2011).

In this study, we demonstrated that blocking CaM activity with two different known inhibitors dampened signal transduction triggered by both mGluR1/5 and muscarinic cholinergic receptors. We hypothesized that inhibiting CaM activity, would offer therapeutic effects that are more robust than blocking a single type of Gq-coupled receptor. In support of this hypothesis, acute administration of trifluoperazine attenuated multiple FXS-related phenotypes ranging from audiogenic seizures to hyperactivity, repetitive behavior, and certain aspect of cognitive defects. Interestingly, trifluoperazine suppressed the basal level of ERK1/2 phosphorylation, which is enhanced in the brains of FXS patients (Wang et al., 2012) and *Fmr1* KO mice (Michalon et al., 2012). Such a pharmacological effect may represent a possible mechanism underlying its therapeutic efficacy, as it has been reported that lovastatin indirectly dampens ERK1/2 phosphorylation and corrects several cellular and behavioral FXS phenotypes

(Osterweil et al., 2013). It has also been reported that either direct or indirect inhibition of ERK1/2 suppresses the enhanced mRNA translation in FXS (Osterweil et al., 2010; Osterweil et al., 2013). Although the causal role of enhanced protein synthesis in FXS is not clear, we found that trifluoperazine specifically dampened protein synthesis and affected behavioral phenotypes in *Fmr1* KO mice without showing major effects on WT mice, except for the locomotor activity in the open field test (Figure 19A2 and 19B2).

Trifluoperazine belongs to the phenothiazine group, and has been primarily used to treat schizophrenia and severe anxiety. Due to its extrapyramidal effects such as akathisia, dystonia, and Parkinsonism (Marques et al., 2004), adjustment in the dosing regime should be seriously considered for any treatment of FXS patients. Several pre-clinical studies suggested new applications of trifluoperazine and other phenothiazines in treating allodynia (Luo et al., 2008; Shirahama et al., 2012), addiction (Ye et al., 2004; Tang et al., 2006), and cancer (Gutierrez et al., 2014). Luo et al. showed that, possibly through inhibition of CaM and its down-stream target CaM-dependent protein kinase II, trifluoperazine at 0.25 to 0.5 mg/kg attenuated inflammatory pain in mice (Shirahama et al., 2012). Another study found that trifluoperazine at 0.1 mg/kg and 0.3 mg/kg reduced oxaliplatin-induced mechanical allodynia (Shirahama et al., 2012). It was reported that the anti-allodynia doses (ranging from 0.1 mg/kg to 0.5 mg/kg) did not have significant

effects on rotarod performance (Chen et al., 2009) and spontaneous locomotion (Ye et al., 2004) in rodents. Encouraged by these animal studies, an open-label human phase I study was performed with trifluoperazine (Molokie et al., 2013). Compared to the recommended dose used for Schizophrenia (i.e., 15-20 mg/day), lower trifluoperazine (ranging from 0.5 to 10 mg/day) was given to adults with sickle cell disease. Patients reported no adverse effects, as judged by the Extrapyramidal Symptom Rating Scale, after receiving trifluoperazine at < 5 mg/day. Promisingly, dose at as low as 1 mg/day had analgesic effects in 2 out of 3 patients. Considering that the pre-clinical dose to attenuate FXS (0.05 mg/kg in this study) is lower than the pre-clinical doses used for allodynia (i.e. > 0.1 mg/kg), daily administration of less than 1 mg/day of trifluoperazine in human FXS may show therapeutic efficacy without extrapyramidal effects.

Because all available small molecule drugs have multiple pharmacological effects, it is difficult to conclude that the therapeutic effects of trifluoperazine are mediated exclusively through CaM inhibition. The primary application of trifluoperazine in Schizophrenia shows strong effects on correcting the positive symptoms possibly through its inhibition on dopamine receptors. It is known that the anti-dopamine effect of trifluoperazine decreases locomotor activity but does not improve cognitive function. I found that while trifluoperazine at 0.05 mg/kg dampened locomotor activity in WT mice

in the open field test, it reduced the hyperactivity in *Fmr1* KO mice to the WT level. Notably, 0.05 mg/kg trifluoperazine rescued the cognitive impairment in *Fmr1* KO mice, and did not affect locomotion activity of the WT mice in the light/dark test. Furthermore, a previous study showed hypo-dopaminergic function in FXS and that a dopamine receptor agonist rescued hyperactivity in *Fmr1* KO mice (Wang et al., 2008). These lines of evidence suggest that the therapeutic effects of trifluoperazine may not be mainly mediated through its anti-dopamine functions. However, molecular and genetic manipulations of CaM are needed for future studies to further examine the significance of CaM inhibition in FXS therapy. Considering that CaM activity may be essential to regulate many cellular targets and neuronal functions, the degree of pharmacological inhibition and the dose of CaM inhibitors should be carefully considered.

In summary, our study identifies new pharmacological effects of trifluoperazine on mGluR1/5- and muscarinic cholinergic receptor-mediated intracellular signaling, and suggests targeting CaM as a novel strategy to treat FXS. Repurposing existing FDA-approved drugs may offer benefits to FXS patients without involving the lengthy and expensive process of de novo drug development. Our study suggests a potential new application of trifluoperazine in FXS, and encourages future human studies using low dose trifluoperazine.

APPENDIX

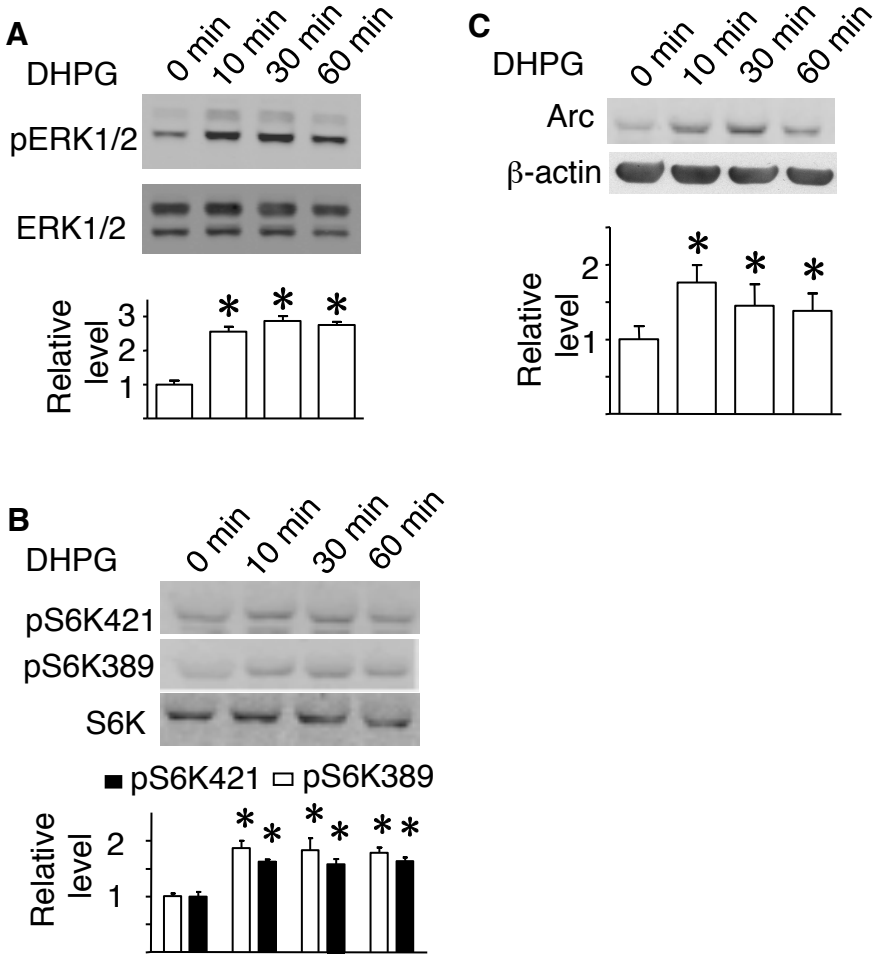

Figure 15: mGluR5 stimulation leads to phosphorylation of ERK1/2 and S6 kinase and Arc translation. (A-C), DIV (days in vitro) 8 rat hippocampal neurons were treated with 100 μM DHPG for 10, 30 and 60 min. The levels of pERK1/2 (A), pS6K (at Thr421/Ser424 and Thr389) (B), and Arc (C) were determined by Western blot. Representative images are shown in the upper panels and quantifications are shown in

Figure 15 (cont'd)

the lower panels. The level of pERK1/2 and pS6K was normalized to the level of total ERK1/2 and total S6K, respectively. The level of Arc was normalized to the level of β-actin. The relative protein level in the no treatment control group was defined as 1, and all samples were normalized to the control group. All data were collected from 6 independent samples. *: $p < 0.05$ between control and the DHPG-treated samples determined by One-way ANOVA and LSD test.

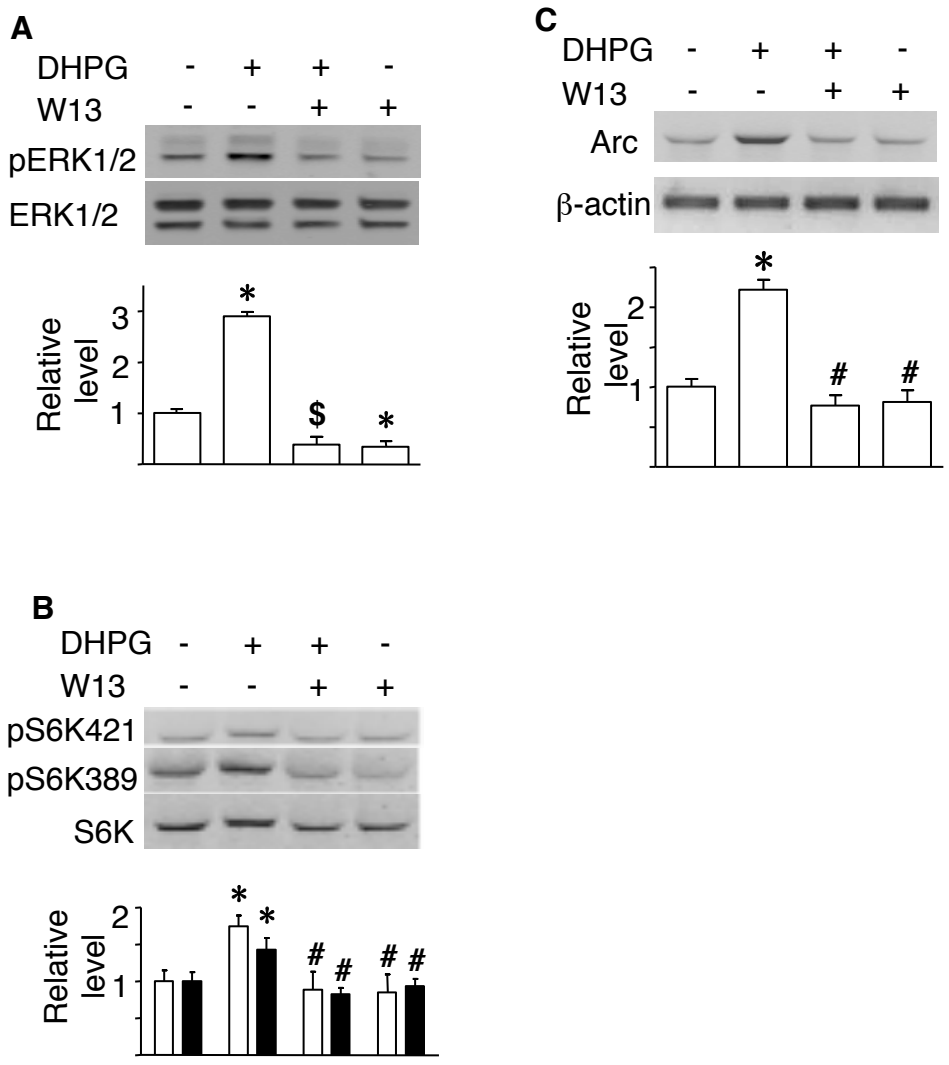

Figure 16: Calmodulin activity is required for mGluR1/5 signaling. (A-C) DIV8 rat hippocampal neurons were pre-treated with 75 μM W13 or vehicle control for 30 min, after which the cells were treated with 100 μM DHPG or vehicle for 30 min. The levels of pERK1/2 (A), pS6K (at Thr421/Ser424 and Thr389) (B), and Arc (C) were determined

Figure 16 (cont'd)

by Western blot. Representative images are shown in the upper panels and quantifications are shown in the lower panels. The level of pERK1/2 and pS6K was normalized to the level of total ERK1/2 and total S6K, respectively. The level of Arc was normalized to the level of β-actin. The relative protein level in the no treatment control group was defined as 1, and all samples were normalized to the control group. All data were collected from 6 independent samples. *: $p < 0.05$ between control and the DHPG-treated samples. $: $p < 0.05$ between the indicated group and the control group as well as the DHPG-treated group. #: $p < 0.05$ between the indicated group and the DHPG-treated group. The *p* value was determined by one-way ANOVA and post hoc LSD test.

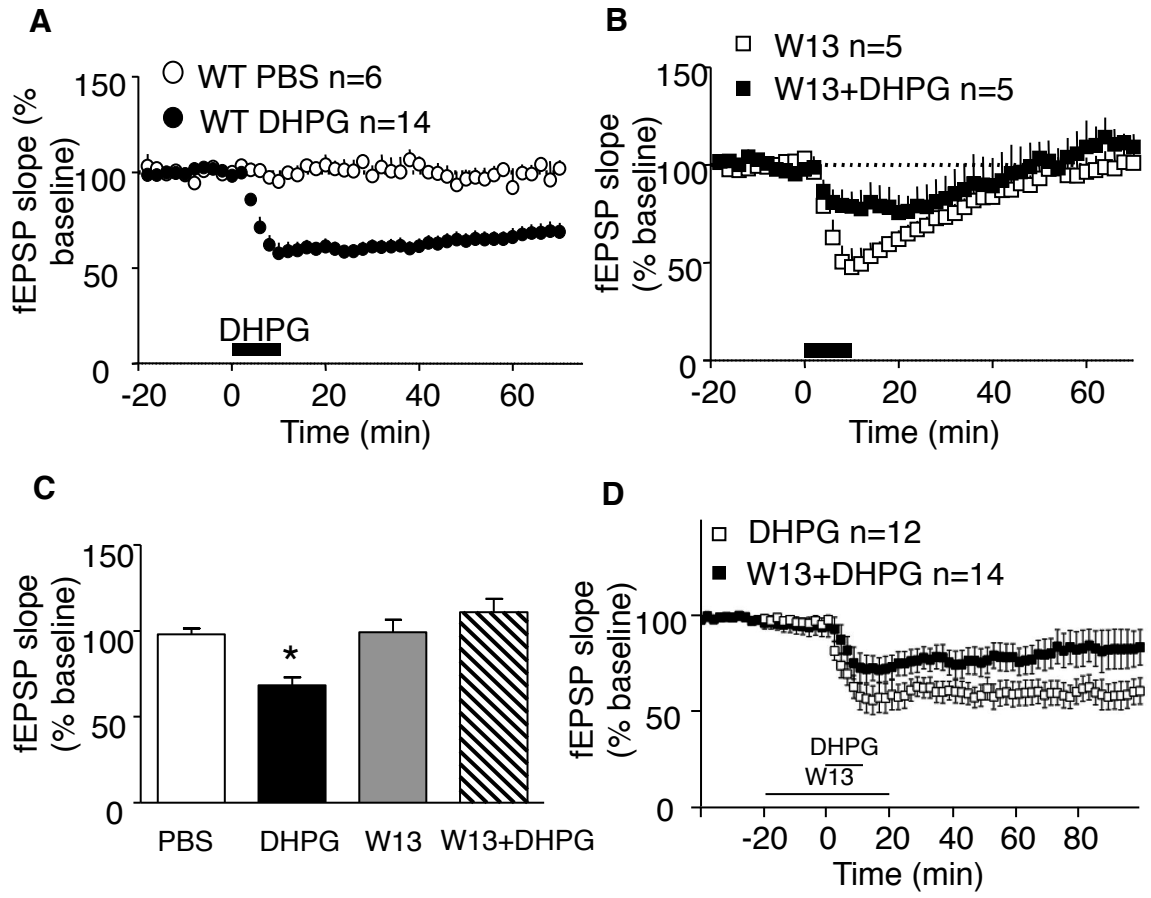

Figure 17: Calmodulin activity is required for mGluR1/5-mediated synaptic LTD. (A-C), DHPG, vehicle, W13, or W13 plus DHPG was infused to the CA1 region of the anesthetized mice. The changes of fEPSP during the whole recording period (A and B), and the averages during the last 5 min of recording **(C)** are presented as mean +/- SEM. **(D)** DHPG or W13 plus DHPG was applied to acute hippocampal slices, and changes of fEPSP were recorded and presented as mean +/- SEM. *: significantly different ($p < 0.05$) from other three groups.

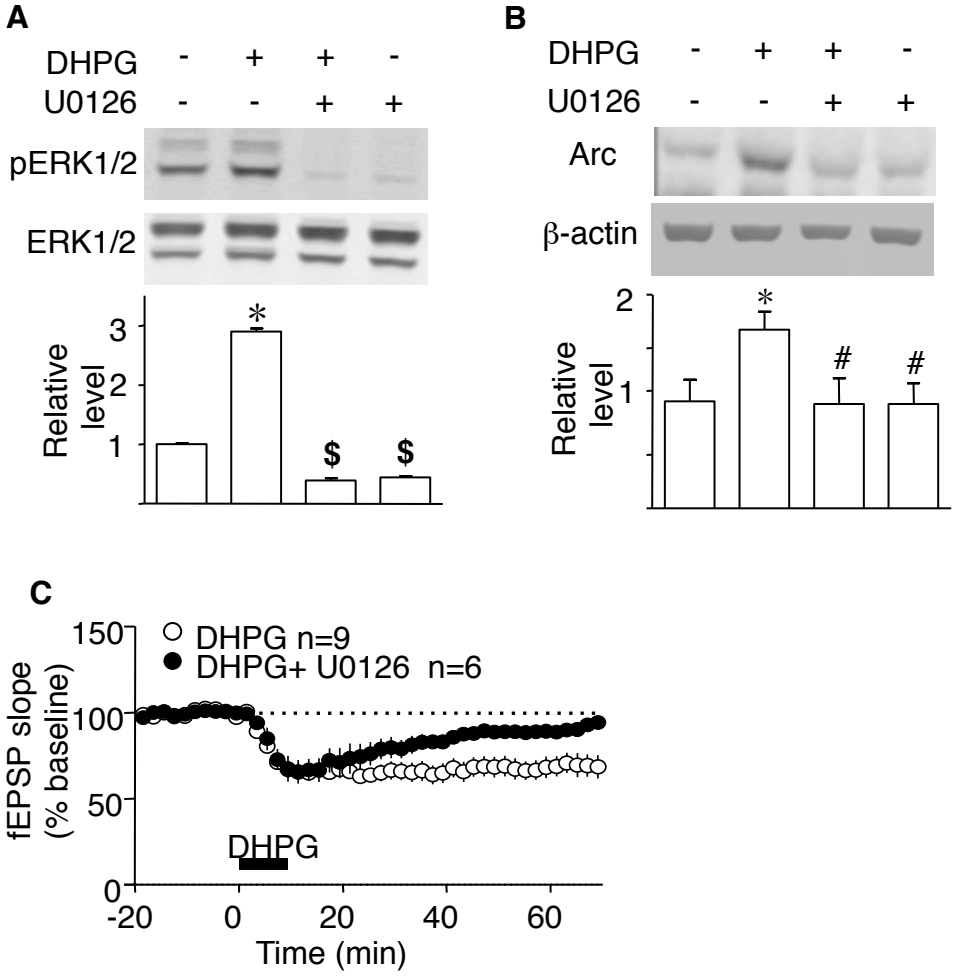

Figure 18: Inhibition of ERK1/2 suppresses mGluR1/5-mediated Arc upregulation and LTD. DIV 8 rat hippocampal neurons were treated with 10 μM MEK inhibitor U0126 for 30 min, following which the cells were stimulated with 100 μM DHPG for 30min. Protein samples were analyzed by Western blot and are presented as normalized protein levels relative to the no treatment control. (A) U0126 suppressed ERK1/2 phosphorylation in both control and DHPG-stimulated neurons. (B). U0126 inhibited

Figure 18 (cont'd)

DHPG-stimulated Arc upregulation. Representative results are shown in the upper panels, and quantification (n = 6 for each group) is shown in the lower panels. *: $p <$ 0.05 between control and DHPG-treated samples. $: $p < 0.05$ between the indicated group and the control group as well as the DHPG-treated group. #: $p < 0.05$ between the indicated group and the DHPG-treated group. The p value was determined by one-way ANOVA and post hoc LSD test. (C) U0126 suppressed DHPG-induced LTD in anesthetized mice. 0.5 ul DHPG (2.5 mM) or 0.5 ul DHPG (2.5 mM) plus U0126 (2 mM) was infused to the CA1 region. The relative fEPSP value was normalized to the baseline level.

Table 6: TFP rescues audiogenic seizure in *Fmr1* KO mice

	n	%Wild running	% seizures	%Death
WT	5	0	0	0
Fmr1	27	55.5	29.6	3.7
WT+TFP	5	0	0	0
Fmr1+TFP	29	34.5	17.2	3.4

Table 6: Audiogenic seizures were tested with 21- to 24-day old mice. The percentage of animals showing wild running, seizures, and death is presented for WT and *Fmr1* KO mice receiving vehicle or trifluoperazine. Chi-square test was used to determine significance between *Fmr1* KO vehicle and TFP groups.

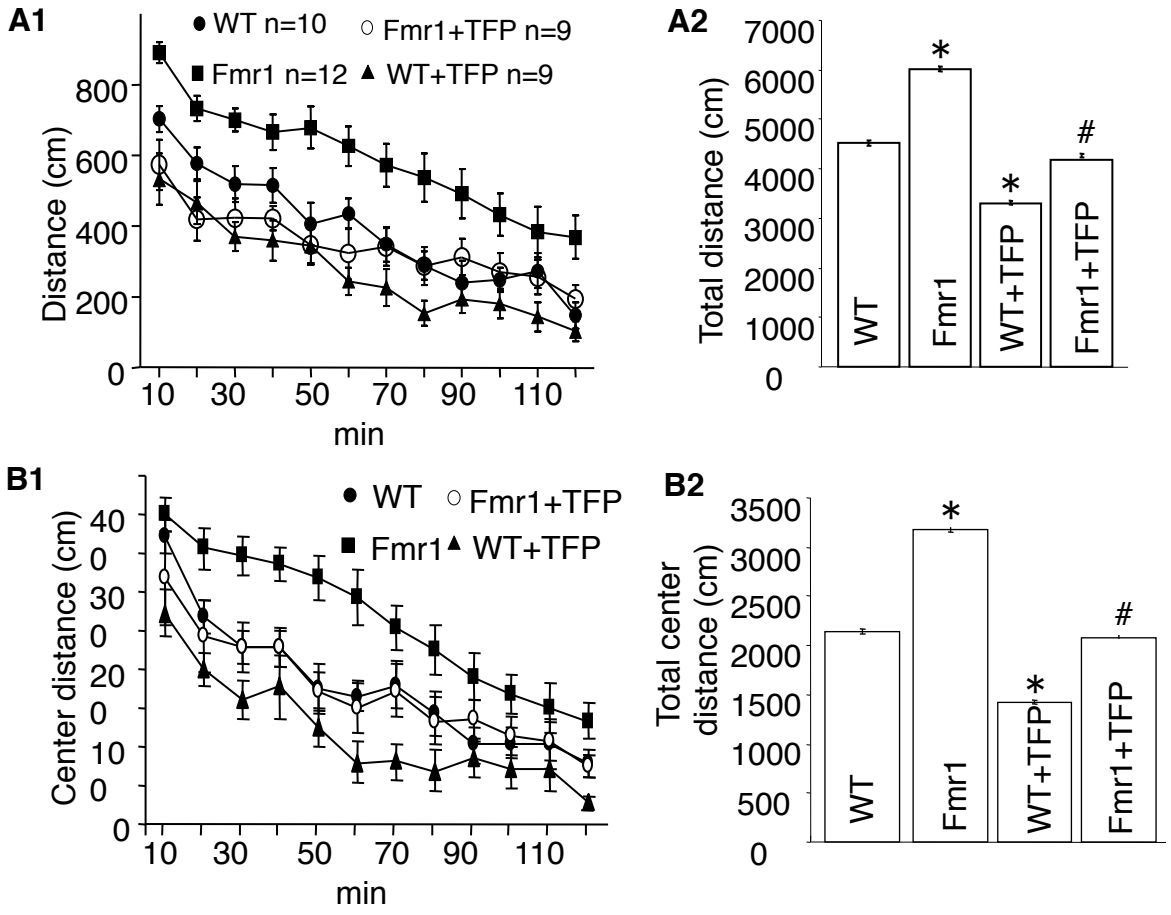

Figure 19: Trifluoperazine attenuates the hyperactivity phenotype in *Fmr1* KO mice. Two- three-month old WT and *Fmr1* KO mice receiving vehicle or trifluoperazine were subjected to a 2-hour open filed test. The total travel distance (A1 and A2) and center distance (B1 and B2) are presented. The activity for each 10-min bin is presented in A1 and B1. Cumulative activity during the whole 2-hour testing is presented in A2 and B2. Two-way ANOVA followed by Student's t-test were used to

Figure 19 (cont'd)

determine the *p* values. *: $p < 0.05$ between the indicated group and vehicle-treated WT mice. #: $p < 0.05$ between vehicle- and trifluoperazine-treated *Fmr1* KO mice.

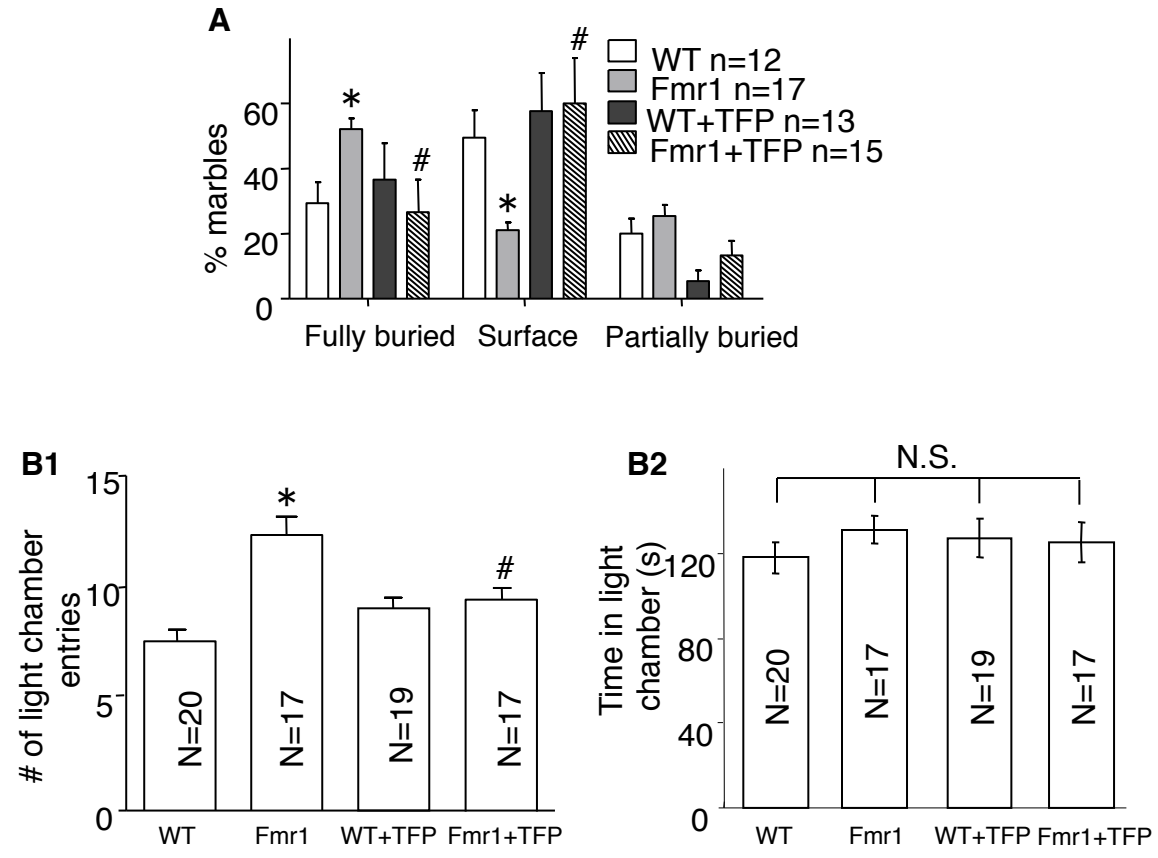

Figure 20: Trifluoperazine rescues repetitive behavior in *Fmr1* KO mice. 2-3 month old WT and *Fmr1* KO mice were injected with vehicle or trifluoperazine 60 min before testing. (A) The percentage of marbles fully buried, on the surface and partially buried was determined. (B) WT and *Fmr1* KO mice (2 to 3 months of age) receiving vehicle or trifluoperazine were subjected to the light/dark test. The total number of entries to the lit chamber (B1) and time spent in the lit chamber (B2) were scored. Two-way ANOVA followed by Student's t-test or pairwise comparison was used to determine the *p* value.

Figure 20 (cont'd)

*: $p < 0.05$ between the indicated group and vehicle treated WT mice. #: $p < 0.05$ between indicated group and vehicle-treated *Fmr1* KO mice. N.S.: not significant.

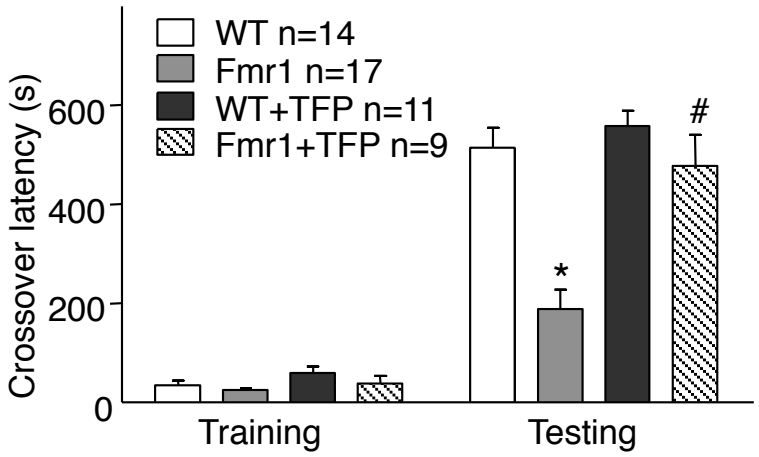

Figure 21: Trifluoperazine rescues the impaired passive avoidance memory in *Fmr1* KO mice. Two- to three-month old WT and *Fmr1* knockout mice were injected with vehicle or trifluoperazine 60 min before passive avoidance training. Mice were tested 24 hours after training, and crossover latency was scored. Two-way ANOVA followed by pairwise comparison was used to determine the p value. *: $p < 0.05$ between the indicated group and the vehicle-treated WT mice, #: $p < 0.05$ between indicated group and vehicle-treated *Fmr1* KO mice.

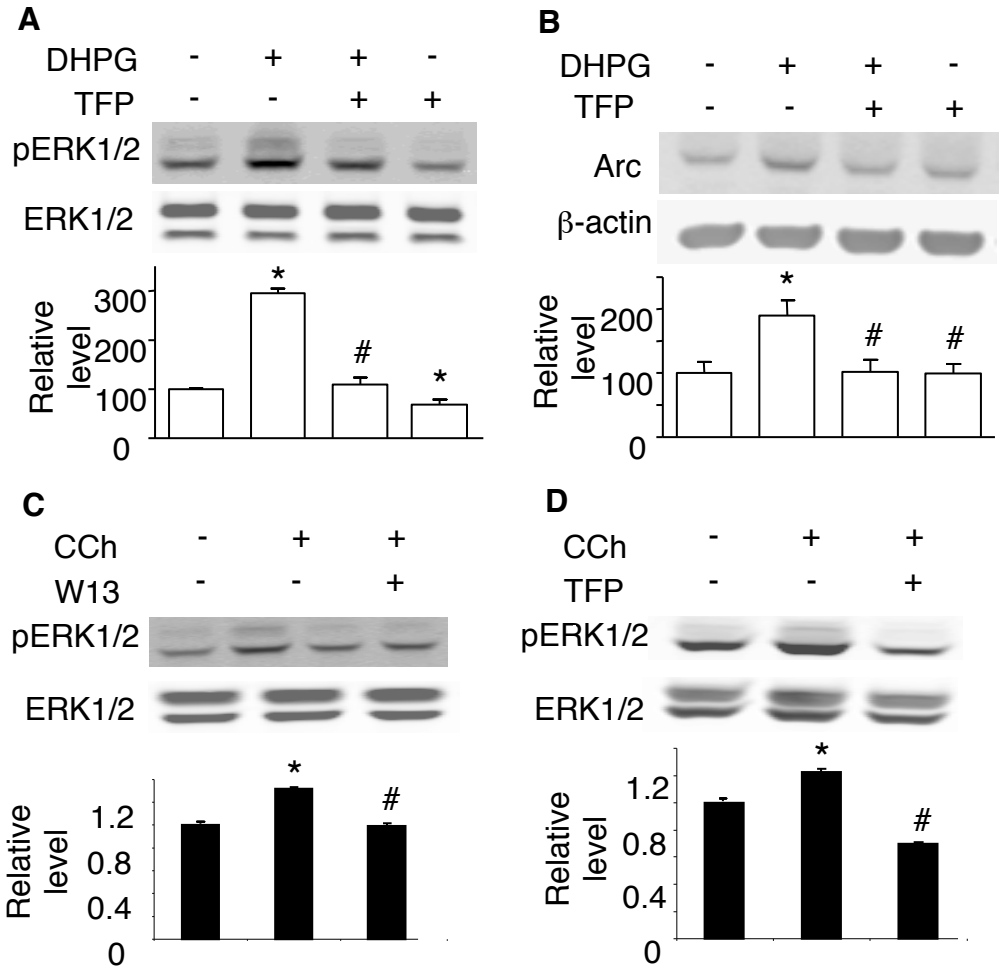

Figure 22: Trifluoperazine suppresses mGluR1/5- and muscarinic receptor-mediated intracellular signaling. DIV 8 rat hippocampal neurons were treated with 20 μM trifluoperazine (A, B and D) or 75 uM W13 (C) for 30 min before the 30-min treatment with 100 μM DHPG (A and B) or 100 μM carbachol (C and D). Samples harvested immediately after the stimulation were analyzed by Western blot. The representative results showing the levels of p-ERK1/2, total ERK1/2, Arc, and b-actin

Figure 22 (cont'd)

are presented in the upper panels. Quantification (n = 6 from 2 independent experiments for each treatment) is presented in the lower panels, all samples are normalized to the control. One-way ANOVA and post hoc LSD test were used to determine the *p* value. *: $p < 0.05$ between the indicated group and the non-treated control group. #: $p < 0.05$ between the indicated group and the DHPG- or carbachol-treated group.

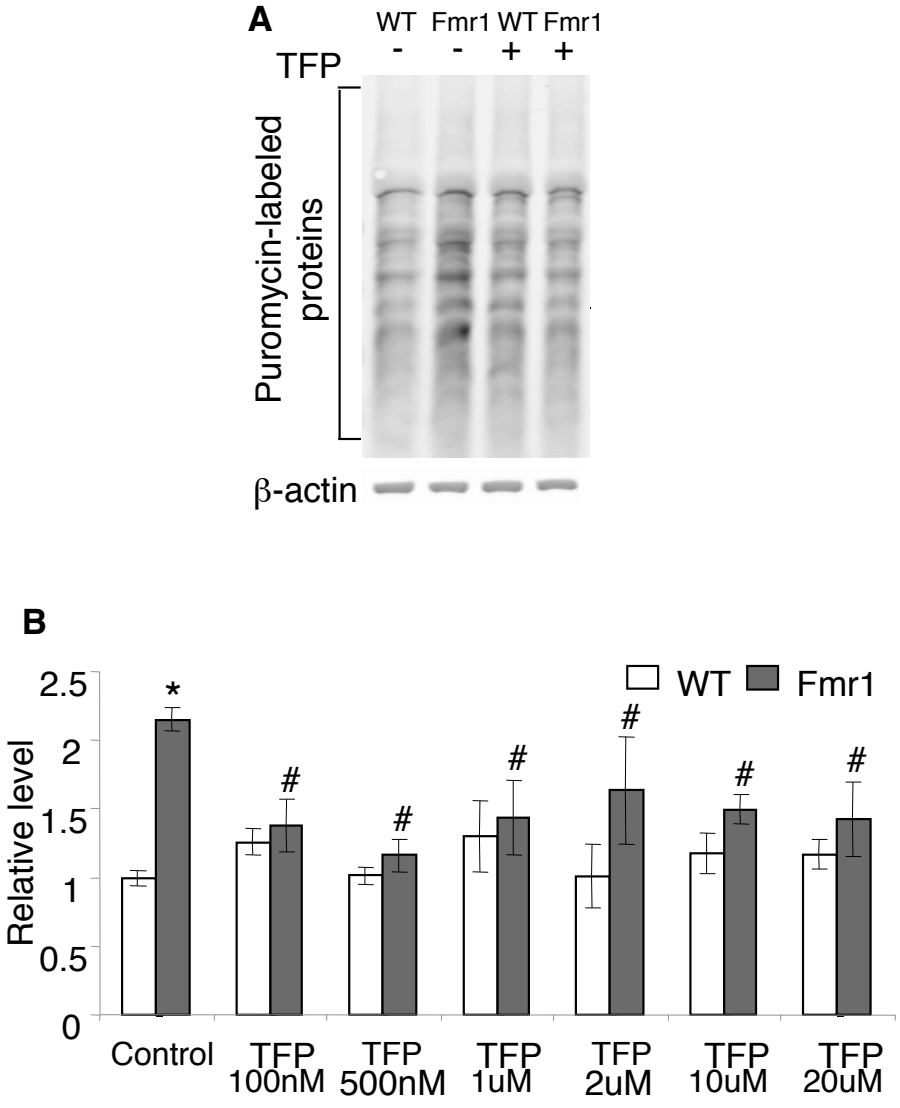

Figure 23: Trifluoperazine suppresses enhanced basal protein translation in *Fmr1* KO neurons. Basal protein synthesis was determined in DIV 14 WT and *Fmr1* KO mouse neurons by the SUnSET method. Cells were pre-incubated with vehicle or trifluoperazine for 60 min before the addition of puromycin into the culture media. Equal amounts of protein were loaded on the gel for Western blot analysis. (A) Representative

Figure 23 (cont'd)

image shows the level of puromycin-labeled proteins is higher in *Fmr1* KO than WT neurons, and 100 nM trifluoperazine dampens protein synthesis in *Fmr1* KO but not WT neurons. (B) Quantification (n = 6 from 2 independent experiments for each treatment) shows that the enhanced protein synthesis in *Fmr1* KO but not WT neurons was suppressed by different concentrations of trifluoperazine. All the samples are relative to control WT levels. Student's t-test were used to determine the p value. *: $p < 0.05$ between *Fmr1* KO and WT neurons. #: $p < 0.05$ between the treated and non-treated *Fmr1* KO neurons.

REFERENCES

REFERENCES

Ascano M, Jr., Mukherjee N, Bandaru P, Miller JB, Nusbaum JD, Corcoran DL, Langlois C, Munschauer M, Dewell S, Hafner M, Williams Z, Ohler U, Tuschl T (2012) FMRP targets distinct mRNA sequence elements to regulate protein expression. Nature 492:382-386.

Bagni C, Tassone F, Neri G, Hagerman R (2012) Fragile X syndrome: causes, diagnosis, mechanisms, and therapeutics. J Clin Invest 122:4314-4322.

Bear MF, Huber KM, Warren ST (2004) The mGluR theory of fragile X mental retardation. Trends Neurosci 27:370-377.

Berry-Kravis E, Hessl D, Coffey S, Hervey C, Schneider A, Yuhas J, Hutchison J, Snape M, Tranfaglia M, Nguyen DV, Hagerman R (2009) A pilot open label, single dose trial of fenobam in adults with fragile X syndrome. J Med Genet 46:266-271.

Bhattacharya A, Kaphzan H, Alvarez-Dieppa AC, Murphy JP, Pierre P, Klann E (2012) Genetic removal of p70 S6 kinase 1 corrects molecular, synaptic, and behavioral phenotypes in fragile X syndrome mice. Neuron 76:325-337.

Brown V, Jin P, Ceman S, Darnell JC, O'Donnell WT, Tenenbaum SA, Jin X, Feng Y, Wilkinson KD, Keene JD, Darnell RB, Warren ST (2001) Microarray identification of FMRP-associated brain mRNAs and altered mRNA translational profiles in fragile X syndrome. Cell 107:477-487.

Chen L, Toth M (2001) Fragile X mice develop sensory hyperreactivity to auditory stimuli. Neuroscience 103:1043-1050.

Chen Y, Luo F, Yang C, Kirkmire CM, Wang ZJ (2009) Acute inhibition of Ca2+/calmodulin-dependent protein kinase II reverses experimental neuropathic pain in mice. J Pharmacol Exp Ther 330:650-659.

Darnell JC, Klann E (2013) The translation of translational control by FMRP: therapeutic targets for FXS. Nat Neurosci.

Darnell JC, Van Driesche SJ, Zhang C, Hung KY, Mele A, Fraser CE, Stone EF, Chen C, Fak JJ, Chi SW, Licatalosi DD, Richter JD, Darnell RB (2011) FMRP stalls ribosomal translocation on mRNAs linked to synaptic function and autism. Cell 146:247-261.

de Vrij FM, Levenga J, van der Linde HC, Koekkoek SK, De Zeeuw CI, Nelson DL, Oostra BA, Willemsen R (2008) Rescue of behavioral phenotype and neuronal protrusion morphology in Fmr1 KO mice. Neurobiol Dis 31:127-132.

Franklin AV, King MK, Palomo V, Martinez A, McMahon LL, Jope RS (2014) Glycogen synthase kinase-3 inhibitors reverse deficits in long-term potentiation and cognition in fragile X mice. Biol Psychiatry 75:198-206.

Gallagher SM, Daly CA, Bear MF, Huber KM (2004) Extracellular signal-regulated protein kinase activation is required for metabotropic glutamate receptor-dependent long-term depression in hippocampal area CA1. J Neurosci 24:4859-4864.

Gutierrez A, Pan L, Groen RW, Baleydier F, Kentsis A, Marineau J, Grebliunaite R, Kozakewich E, Reed C, Pflumio F, Poglio S, Uzan B, Clemons P, Verplank L, An F, Burbank J, Norton S, Tolliday N, Steen H, Weng AP, Yuan H, Bradner JE, Mitsiades C, Look AT, Aster JC (2014) Phenothiazines induce PP2A-mediated apoptosis in T cell acute lymphoblastic leukemia. J Clin Invest.

Hou L, Antion MD, Hu D, Spencer CM, Paylor R, Klann E (2006) Dynamic translational and proteasomal regulation of fragile X mental retardation protein controls mGluR-dependent long-term depression. Neuron 51:441-454.

Huber KM, Gallagher SM, Warren ST, Bear MF (2002) Altered synaptic plasticity in a mouse model of fragile X mental retardation. Proc Natl Acad Sci U S A 99:7746-7750.

Jacquemont S, Curie A, des Portes V, Torrioli MG, Berry-Kravis E, Hagerman RJ, Ramos FJ, Cornish K, He Y, Paulding C, Neri G, Chen F, Hadjikhani N, Martinet D, Meyer J, Beckmann JS, Delange K, Brun A, Bussy G, Gasparini F, Hilse T, Floesser A, Branson J, Bilbe G, Johns D, Gomez-Mancilla B (2011) Epigenetic modification of the FMR1 gene in fragile X syndrome is associated with differential response to the mGluR5 antagonist AFQ056. Sci Transl Med 3:64ra61.

Luo F, Yang C, Chen Y, Shukla P, Tang L, Wang LX, Wang ZJ (2008) Reversal of chronic inflammatory pain by acute inhibition of Ca2+/calmodulin-dependent protein kinase II. J Pharmacol Exp Ther 325:267-275.

Marques LO, Lima MS, Soares BG (2004) Trifluoperazine for schizophrenia. Cochrane Database Syst Rev:CD003545.

Michalon A, Sidorov M, Ballard TM, Ozmen L, Spooren W, Wettstein JG, Jaeschke G, Bear MF, Lindemann L (2012) Chronic pharmacological mGlu5 inhibition corrects fragile X in adult mice. Neuron 74:49-56.

Molokie RE, Wilkie DJ, Wittert H, Suarez ML, Yao Y, Zhao Z, He Y, Wang ZJ (2013) Mechanism-driven phase I translational study of trifluoperazine in adults with sickle cell disease. Eur J Pharmacol.

Musumeci SA, Bosco P, Calabrese G, Bakker C, De Sarro GB, Elia M, Ferri R, Oostra BA (2000) Audiogenic seizures susceptibility in transgenic mice with fragile X syndrome. Epilepsia 41:19-23.

Nosyreva ED, Huber KM (2006) Metabotropic receptor-dependent long-term depression persists in the absence of protein synthesis in the mouse model of fragile X syndrome. J Neurophysiol 95:3291-3295.

Osterweil EK, Krueger DD, Reinhold K, Bear MF (2010) Hypersensitivity to mGluR5 and ERK1/2 leads to excessive protein synthesis in the hippocampus of a mouse model of fragile X syndrome. J Neurosci 30:15616-15627.

Osterweil EK, Chuang SC, Chubykin AA, Sidorov M, Bianchi R, Wong RK, Bear MF (2013) Lovastatin corrects excess protein synthesis and prevents epileptogenesis in a mouse model of fragile X syndrome. Neuron 77:243-250.

Park S, Park JM, Kim S, Kim JA, Shepherd JD, Smith-Hicks CL, Chowdhury S, Kaufmann W, Kuhl D, Ryazanov AG, Huganir RL, Linden DJ, Worley PF (2008) Elongation factor 2 and fragile X mental retardation protein control the dynamic translation of Arc/Arg3.1 essential for mGluR-LTD. Neuron 59:70-83.

Qin M, Kang J, Smith CB (2002) Increased rates of cerebral glucose metabolism in a mouse model of fragile X mental retardation. Proc Natl Acad Sci U S A 99:15758-15763.

Santoro MR, Bray SM, Warren ST (2012) Molecular mechanisms of fragile X syndrome: a twenty-year perspective. Annu Rev Pathol 7:219-245.

Schmidt EK, Clavarino G, Ceppi M, Pierre P (2009) SUnSET, a nonradioactive method to monitor protein synthesis. Nat Methods 6:275-277.

Shirahama M, Ushio S, Egashira N, Yamamoto S, Sada H, Masuguchi K, Kawashiri T, Oishi R (2012) Inhibition of Ca2+/calmodulin-dependent protein kinase II reverses oxaliplatin-induced mechanical allodynia in rats. Mol Pain 8:26.

Suvrathan A, Hoeffer CA, Wong H, Klann E, Chattarji S (2010) Characterization and reversal of synaptic defects in the amygdala in a mouse model of fragile X syndrome. Proc Natl Acad Sci U S A 107:11591-11596.

Tang L, Shukla PK, Wang ZJ (2006) Trifluoperazine, an orally available clinically used drug, disrupts opioid antinociceptive tolerance. Neurosci Lett 397:1-4.

Thomas A, Burant A, Bui N, Graham D, Yuva-Paylor LA, Paylor R (2009) Marble burying reflects a repetitive and perseverative behavior more than novelty-induced anxiety. Psychopharmacology (Berl) 204:361-373.

Thomas AM, Bui N, Perkins JR, Yuva-Paylor LA, Paylor R (2012) Group I metabotropic glutamate receptor antagonists alter select behaviors in a mouse model for fragile X syndrome. Psychopharmacology (Berl) 219:47-58.

Veeraragavan S, Bui N, Perkins JR, Yuva-Paylor LA, Carpenter RL, Paylor R (2011) Modulation of behavioral phenotypes by a muscarinic M1 antagonist in a mouse model of fragile X syndrome. Psychopharmacology (Berl) 217:143-151.

Veloz MF, Buijsen R, Willemsen R, Cupido A, Bosman LW, Koekkoek SK, Potters JW, Oostra BA, De Zeeuw CI (2012) The effect of an mGluR5 inhibitor on procedural memory and avoidance discrimination impairments in Fmr1 KO mice. Genes Brain Behav.

Volk LJ, Pfeiffer BE, Gibson JR, Huber KM (2007) Multiple Gq-coupled receptors converge on a common protein synthesis-dependent long-term depression that is affected in fragile X syndrome mental retardation. J Neurosci 27:11624-11634.

Wang H, Wu LJ, Kim SS, Lee FJ, Gong B, Toyoda H, Ren M, Shang YZ, Xu H, Liu F, Zhao MG, Zhuo M (2008) FMRP acts as a key messenger for dopamine modulation in the forebrain. Neuron 59:634-647.

Wang X, Snape M, Klann E, Stone JG, Singh A, Petersen RB, Castellani RJ, Casadesus G, Smith MA, Zhu X (2012) Activation of the extracellular signal-regulated kinase pathway contributes to the behavioral deficit of fragile x-syndrome. J Neurochem 121:672-679.

Waung MW, Pfeiffer BE, Nosyreva ED, Ronesi JA, Huber KM (2008) Rapid translation of Arc/Arg3.1 selectively mediates mGluR-dependent LTD through persistent increases in AMPAR endocytosis rate. Neuron 59:84-97.

Yan QJ, Rammal M, Tranfaglia M, Bauchwitz RP (2005) Suppression of two major Fragile X Syndrome mouse model phenotypes by the mGluR5 antagonist MPEP. Neuropharmacology 49:1053-1066.

Ye XF, Lu Y, Zhang P, Liang JH (2004) Calmodulin inhibitor trifluoperazine attenuates the development and expression of morphine-induced conditioned place preference in rats. Eur J Pharmacol 486:265-271.

Zang JB, Nosyreva ED, Spencer CM, Volk LJ, Musunuru K, Zhong R, Stone EF, Yuva-Paylor LA, Huber KM, Paylor R, Darnell JC, Darnell RB (2009) A mouse model of the human Fragile X syndrome I304N mutation. PLoS Genet 5:e1000758.

Zhang M, Storm DR, Wang H (2011) Bidirectional synaptic plasticity and spatial memory flexibility require Ca2+-stimulated adenylyl cyclases. J Neurosci 31:10174-10183.

Zhou X, Lin DS, Zheng F, Sutton MA, Wang H (2010) Intracellular calcium and calmodulin link brain-derived neurotrophic factor to p70S6 kinase phosphorylation and dendritic protein synthesis. J Neurosci Res 88:1420-1432.

CHAPTER 4: CONCLUDING REMARKS AND FUTURE DIRECTIONS

This research identifies two novel therapeutic targets for fragile X syndrome, using the *Fmr1* KO mouse model.

The results in *Chapter 2* show that type-1 adenylyl cycalse (AC1) mRNA translation is repressed by FMRP. This results in AC1 protein overexpression in the absence of FMRP. Further AC1 protein is rapidly translated in response to mGluR5 stimulation and this response is lost in the absence of FMRP. Using a genetic knockout and pharmacological inhibition, this study shows that abolishing or reducing AC1 activity in *Fmr1* KO mice rescues cellular, synaptic and behavioral phenotypes related to mental retardation and autism. We currently do not understand the cellular mechanisms that result in AC1 translation upon mGluR5 stimulation and whether mGluR5 stimulated translation of AC1 is regulated by FMRP. One possible mechanism worth investigating would be to check whether the status of FMRP phosphorylation can control AC1 mRNA translation via microRNA mediated mechanisms. Muddhashetty et al., demonstrated that FMRP phosphorylation promotes the formation of an AGO2-miR125a inhibitory complex on PSD-95 mRNA, further mGluR5 stimulation leads to dephosphorylation of FMRP which results in release of the complex from the mRNA and rapid translation of PSD-95. These studies could be performed using phosphomimic and phosphodeficient

FMRP and the luciferase assays described in *Chapter 2*. FMRP may also regulate AC1 via other mechanisms that we did not test. Co-immunoprecipitation of AC1 mRNA with FMRP would aid in identifying its binding sites on the mRNA. Since mouse AC1 mRNA is 12.26 kb long, this could be challenging. Bioinformatically identifying potential binding sites such as G-quartet forming structures or the proposed RNA recognition elements of FMRP: ACUK and WGGA (where K is G or U and W is A or U), may aid in this search.

Another aspect that needs to be studied is the mechanistic contribution of AC1 in mGluR or other Gq signaling pathways that are altered in the absence of FMRP. Interestingly, previous work from our lab shows that mGluR5 induced LTD is absent in AC1 KO mice (Dr. Ming Zhang). Given our current findings, and the knowledge that *Fmr1* KO mice show enhanced mGluR5 LTD, it would be interesting to study how DHPG would affect LTD in the DKO mice. We tested ERK1/2 (phosphorylation) activation by AC1 as one plausible mechanism that could link AC1 to mGluR5 LTD. Since AC1 is a Ca^{2+}/Calmodulin stimulated protein, and mGluR5 is a Gq coupled protein which can activate Ca^{2+}/Calmodulin signaling, we hypothesized that AC1 may indirecly phosphorylate ERK1/2 by activating Rap1 upon mGluR5 stimulation. However, I observed increased ERK1/2 phosphorylation upon mGluR5 stimulation in AC1 KO neurons, making this conclusion difficult. It is possible that AC1 could indeed modulate

ERK1/2 singaling in this pathway, but our preliminary studies could not reveal this mechanism. Further studies into these mechanisms are warranted.

Finally, our experiments show that an acute single dose of NB001 can rescue various phenotypes in the *Fmr1* KO mouse. This is indeed encouraging, and the next critical step would be to check how a repeated dose and preferably orally administered regimen will affect these phenotypes. Since FXS is also a developmental disorder, it would be interesting to study whether prenatal exposure to NB001 could ameliorate FXS phenotypes.

Chapter 3 demonstrates that calmodulin is a signaling component in the mGluR5 pathway and is crucial for mGluR5 induced LTD. It is important to note that these studies were performed using a pharmacological inhibitor of calmodulin and studies using genetic inhibition are important for confirming these results. Since there are no available inhibitors of calmodulin that can be systemically administered and cross the blood-brain barrier, we used trifluoperazine which is a known calmodulin inhibitor. Trifluoperazine is a 'typical' antipsychotic used for treatment of schizophrenia. Its use is often associated with extrapyrimidal side effects in patients and with the development of better antipsychotics, it is no longer extensively used in the clinic. However we used a low dose of this drug in our studies and demonstrated that this FDA approved drug can

rectify cellular and behavioral phenotypes associated with FXS in the *Fmr1* KO mouse. It is important to note that trifluoperazine is not a specific calmodulin inhibitor and like many other drugs used clinically; the mechanistic basis of this phenotypic rescue is not known. To aid in understanding whether calmodulin is a good target for FXS, we need to investigate whether a highly specific calmodulin inhibitor and/or acute genetic inhibition of calmodulin can cause phenotypic rescue in *Fmr1* KO mice. Towards this, we can inject W13 (a high specificity calmodulin inhibitor), express dominant- negative calmodulin or deliver siRNA to the mouse brain and observe the phenotypes in *Fmr1* KO mice. If calmodulin is indeed a good therapeutic target for FXS, these studies would further the development of better and safer calmodulin inhibitors and aid in drug development. Our study using this FDA approved drug is nonetheless important because there is currently no cure for FXS and often a cocktail of various drugs are administered to manage the symptoms, antipsychotics being one of them. Thus low doses of trifluoperazine may benefit current FXS patients without them having to wait for the process of the lengthy clinical trials which are associated with the development of new drugs.